Present State of Knowledge of the Upper Atmosphere 1990: An Assessment Report

Report to Congress

R. T. Watson,
M. J. Kurylo,
M. J. Prather,
and F. M. Ormond

NASA

Present State of Knowledge of the Upper Atmosphere 1990: An Assessment Report

Report to Congress

R. T. Watson,
M. J. Kurylo,
M. J. Prather,
and F. M. Ormond
NASA Office of Space Science and Applications
Washington, D.C.

R. T. Watson and D. L. Albritton, Co-Chairs, *International Scientific Assessment of Stratospheric Ozone: 1989*

M. J. Prather and R. T. Watson, *Transient Scenarios for Atmospheric Chlorine and Bromine*

M. J. Kurylo, R. F. Hampson, and the NASA Panel for Data Evaluation, *Chemical Kinetics and Photochemical Data for Use in Stratospheric Modeling*

M. J. Prather et al., *An Assessment of the Impact on Stratospheric Chemistry and Ozone Caused by the Launch of the Space Shuttle and Titan IV*

High Speed Research Program Atmospheric Advisory Committee, *The Atmospheric Effects of Stratospheric Aircraft*

Preface

NASA has relied heavily on the entire scientific community, national and international, in its effort to provide a better understanding of the upper atmosphere and its perturbation in response to natural phenomenon and human activities. The lists of contributors to the individual sections in this report are given in Section G. We are indebted to those who gave their time and knowledge.

Robert T. Watson

Michael J. Kurylo

Michael J. Prather

TABLE OF CONTENTS

List of Figures

List of Tables

SECTION A

INTRODUCTION

In compliance with the Clean Air Act Amendments of 1977, Public Law 95-95, the National Aeronautics and Space Administration (NASA) has prepared this Report on the state of our knowledge of the Earth's upper atmosphere, and particularly, of stratospheric ozone. The Report for the year 1990 presents new findings since the last Report in 1988 and is printed in two parts. Part I (Research Summaries) was issued earlier in this year and summarized the objectives, status, and accomplishments of the research tasks supported under NASA's Upper Atmosphere Research Program (UARP). Part II (this document) presents several scientific assessments of our current understanding of the chemical composition and physical structure of the stratosphere, in particular how the abundance and distribution of ozone is predicted to change in the future. These reviews include: (Section B) a summary of the most recent international assessment of stratospheric ozone; (Section C) a study of future chlorine and bromine loading of the atmosphere; (Section D) a review of the photochemical and chemical kinetics data that are used as input parameters for the atmospheric models; (Section E) a new assessment of the impact of Space Shuttle launches on the stratosphere; (Section F) a summary of the environmental issues and needed research to evaluate the impact of the newly re-proposed fleet of stratospheric supersonic civil aircraft; and (Section G) a list of the contributors to this Report.

For two decades scientists have postulated that certain pollutants directly associated with human activity could cause harmful effects by reducing the amount of stratospheric ozone. Initial concerns focussed on supersonic aircraft emissions of NO and NO_2, and then shifted to the issue of chlorine loading of the stratosphere from chlorofluorocarbons (CFCs). In recognition of the importance of understanding such perturbations, Congress directed NASA in June 1975 to "develop and carry out a comprehensive program of research, technology, and monitoring of the phenomena of the upper atmosphere so as to provide for an understanding of and to maintain the chemical and physical integrity of the Earth's upper atmosphere".

Responding to this Congressional mandate, NASA implemented a long-range scientific research program, the UARP, aimed at developing a comprehensive understanding of processes in the upper atmosphere. In the near-term NASA has the responsibility of providing biennial reports to the Congress and concerned regulatory agencies on the status of upper atmospheric research, including scientific assessments of potential effects of human activities on the atmosphere, and particularly, on stratospheric ozone.

Many governments around the world, including the United States, have recognized that the ozone layer must be protected in order to protect human health and aquatic and terrestrial ecosystems from damage due to enhanced levels of ultraviolet radiation. In particular, it was recognized that the use of chemicals containing chlorine (in the form of chlorofluorocarbons, CFCs) and bromine (in the form of halons) constitute a potential threat to the stability of the ozone layer. More than twenty nations, including the United States, signed the Vienna Convention for the Protection of the Ozone Layer in Vienna, Austria, in March 1985, and the Montreal Protocol on Substances that Deplete the Ozone Layer, in Montreal, Canada, in September 1987. The United States and 46 other nations (as of November 1989) have subsequently ratified both the Vienna Convention and the Montreal Protocol. The Vienna Convention and the Montreal Protocol both call for all regulatory decisions to be based on a scientific understanding of the issues, and specifically the Montreal Protocol called for an international scientific assessment in 1989 in preparation for the 1990 policy review.

The 1989 scientific assessment was coordinated by NASA, the National Oceanic and Atmospheric Administration (NOAA), the United Kingdom Department of the Environment (DOE), the United Nations Environment Program (UNEP), and the World Meteorological Organization (WMO). This report was written and peer reviewed by more than 75 scientists from 23 countries, who are regarded as experts in their respective fields. During this period, fifteen CFC-producing companies from around the world organized and sponsored the Alternative Fluorocarbon Environmental Acceptability Study (AFEAS). The AFEAS work similarly involved the international scientific community and was extensively peer reviewed; its results contributed to the ozone assessment and became a companion volume. The "Scientific Assessment of Stratospheric Ozone: 1989" was published this year as WMO Report No. 20. The executive summaries of the 4 assessment chapters (Volume I) and of the AFEAS report (Volume II) are reproduced here in Section B.

During the process of re-evaluating and amending the Montreal Protocol at UNEP meetings in Nairobi (August 1989) and Geneva (November 1989), the need to compare the impact of different policy options arose. The relative atmospheric response over the next 10 to 100 years had to be evaluated, considering a large range of political options to limit production of CFCs, other chlorocarbons, and halons. Drs. Watson and Prather used the results of the international assessment (Section B) to prepare a criteria document that demonstrated the time-dependent growth and decay of atmospheric chlorine and bromine in response to different controls over halocarbons. This document clarified approaches to achieving environmental goals (i.e., limit peak chlorine, removing the Antarctic ozone hole) and was incorporated into the UNEP proceedings as Annex II. It is reproduced here as Section C. The biennial review of the status of kinetics and photochemistry by the NASA Panel for Data Evaluation is an important document for the atmospheric sciences community. It provides a regular focus that brings together the laboratory measurements and the theoretical studies and establishes a reference standard for atmospheric modelling. The most recent recommendations of this panel are published as JPL 90-1 "Chemical Kinetics and Photochemical Data for use in Stratospheric Modeling," and reproduced as Section D in this Report.

The impact of chlorine from the Space Shuttle exhaust has been reexamined because of the clear evidence that atmospheric chlorine increases have led to the formation of the Antarctic ozone hole as well as the much smaller decline over northern mid-latitudes (see Section B). Data on the emissions from the solid rocket motors was supplied by the Thiokol Corporation and three modelling groups simulated the magnitude of the perturbation to stratospheric chlorine levels. Results from all models show that individual launches, or a launch frequency of about one per month, would lead to small (<1 %) perturbations to the background stratospheric chlorine. Larger uncertainty exists regarding the impact of the added burden of stratospheric aerosols from the launch of all types of space vehicles. This study was peer reviewed and is presented in Section E.

Renewed commercial interest in a fleet of supersonic civil aircraft has led to the formation of a research program within NASA to evaluate the environmental and technical issues of supersonic aircraft. A key component of this High Speed Research Program (HSRP) involves evaluation of the atmospheric effects of these stratospheric aircraft, particularly the potential depletion of ozone caused by engine exhaust. The Upper Atmosphere Research Program is working with the HSRP and is overseeing the atmospheric assessment of supersonic civil aircraft. An international scientific advisory panel has been convened by the UARP to provide the scientific guidance that will be needed for a full evaluation of the effects of stratospheric pollution by aircraft. That panel drafted a statement of research needs that formed the basis of the NASA Research Announcement (NRA-89-OSSA-16) that initiated this study in 1989. The research plan is summarized in Section F. Contributors are listed in Section G.

SECTION B

Scientific Assessment of Stratospheric Ozone: 1989

VOLUME I

VOLUME II - THE AFEAS REPORT

SECTION B

SCIENTIFIC ASSESSMENT OF STRATOSPHERIC OZONE: 1989
Volume I

I. SUMMARY

The *Scientific Assessment of Stratospheric Ozone: 1989* is a scientific review of the current understanding of stratospheric ozone, prepared by international scientific experts who are leaders in their respective fields. This is a summary of its major points.

The aims of this summary section are threefold. The Executive Summary (Sec. II) is a digest of the key points of the *Assessment* and is directed at government officials, the private sector, and the general public. The Scientific Summaries (Sec. III) of each of the four chapters contain the major research findings of the *Assessment* and are directed to the scientific community.

In Section G, the numerous contributors to the preparation of the *Assessment* are identified. The success of the *Assessment* rests on the prodigious efforts and dedication of these people.

This introductory section briefly gives the background to the *Assessment*, its scientific scope, and its place in the current discussions of public policies regarding the protection of the stratospheric ozone layer.

1. Background

The goals, scope, contents, authors, and timetable of the *Assessment* were planned at two international meetings:

- The first was part of a two-day meeting, "Scientific Review of Ozone Layer Modification and Its Impact," which was held at The Hague, The Netherlands, 17-18 October 1988. There were about 70 international scientific attendees at this first of a series of meetings sponsored by the United Nations Environment Program (UNEP). About half of these attendees were involved in the subgroup that focused on defining the scope of the *Assessment* and establishing a scientific steering group.

- The second meeting occurred on 29 November 1988 at the U. K. Department of the Environment in London. Fourteen scientists attended, coming from eight countries, as well as representation from UNEP and the World Meteorological Organization (WMO). The focus of this Steering Committee was on establishing the structure, authors, and timetable of the *Assessment*.

The preparation of the *Assessment* document occurred over the period from January to June, 1989. Numerous scientists from 25 countries were involved either as authors, contributors, or reviewers (see Appendix). Their professional institutions included universities, government laboratories, and the private sector. A review draft was available on 15 June 1989 and was circulated worldwide for comment. This draft was discussed and evaluated at a review meeting at

Les Diablerets, Switzerland on 10-14 July 1989, sponsored by WMO. Forty-three scientists from 14 countries were in attendance and many others participated via mail reviews. Those suggestions and comments have been incorporated into the present final version.

2. Scientific Scope

The focus of the *Assessment* is on four major current aspects of stratospheric ozone: (1) polar ozone, (2) global trends, (3) theoretical predictions, and (4) halocarbon ozone depleting potentials and global warming potentials. Other ozone-related topics are also included: (i) the trends of stratospheric temperature, stratospheric aerosols, source gases, and surface ultraviolet radiation and (ii) the oxidizing capacity of the troposphere as it pertains to the lifetimes of ozone-related chemicals (e.g., the partially halogenated compounds that can serve as shorter-lived substitutes for the long-lived, fully halogenated ozone-depleting gases).

The *Assessment* is an update of the comprehensive "Atmospheric Ozone: 1985" (WMO Report No. 16, 1986) and builds upon the recent "International Ozone Trends Panel Report: 1988" (WMO Report No. 18, in press). It focuses on the results of subsequent recent research and the implications for the stratosphere. The ozone research of the past few years has been remarkable. Several major ground-based and airborne field campaigns have explored the recently discovered Antarctic ozone "hole," as well as the Arctic ozone layer. New laboratory studies of gas-phase and surface-induced chemical processes have provided a better characterization of the polar phenomena. Statistical analyses of hemispheric data sets have revealed significant ozone trends for the first time. Theoretical investigations have aided the interpretation of all of these findings. The picture contained in the *Assessment* reveals a new and deeper understanding of the influence of human activities on the Earth's protective ozone layer.

3. Relation to Public Policy

While the *Assessment* is a scientific document, it also will be useful as essential scientific input to policy decisions regarding the safeguarding of the ozone layer, just as was its predecessor documents (e.g., "Atmospheric Ozone: 1985"). In that regard, one of the most noteworthy applications of the *Assessment* will be the forthcoming international review of the Montreal Protocol on Substances that Deplete the Ozone Layer. Indeed, the above timetable was planned such that the international ozone scientific community can provide that service in the form of the *Assessment*. The Executive Summary of the present document has been written with this need to communicate the state of ozone science in mind.

At the meeting in October 1988 at The Hague, UNEP established four panels to review the current scientific, environmental, technical, and economic information relative to possible amendments to the Montreal Protocol. The *Scientific Assessment of Stratospheric Ozone: 1989* is the report of the first of these panels. There are corresponding reports from the three other panels. The main findings of all four reports were presented to a Working Group meeting in Nairobi, Kenya, on 28 August - 5 September 1989, where the reports were reviewed. Their integration into a single document will be completed, and the resulting integrated report will serve as key input for considerations of possible draft amendments to the Montreal Protocol.

II. EXECUTIVE SUMMARY

1. Recent Findings

The past few years have been remarkable insofar as stratospheric ozone science is concerned. There have been highly significant advances in the understanding of the impact of human activities on the Earth's protective ozone layer. Since the last international scientific review (1985), there are four major findings that each heighten the concern that chlorine- and bromine-containing chemicals can lead to a significant depletion of stratospheric ozone:

- Antarctic Ozone Hole: The weight of scientific evidence strongly indicates that chlorinated (largely man-made) and brominated chemicals are primarily responsible for the recently discovered substantial decreases of stratospheric ozone over Antarctica in springtime.

- Perturbed Arctic Chemistry: While at present there is no ozone loss over the Arctic comparable to that over the Antarctic, the same potentially ozone-destroying processes have been identified in the Arctic stratosphere. The degree of any future ozone depletion will likely depend on the particular meteorology of each Arctic winter and future atmospheric levels of chlorine and bromine.

- Long-Term Ozone Decreases: The analysis of the total-column ozone data from ground-based Dobson instruments show measurable downward trends from 1969 to 1988 of 3 to 5% (i.e., 1.8-2.7% per decade) in the Northern Hemisphere (30 to 64°N latitudes) in the winter months that cannot be attributed to known natural processes.

- Model Limitations: These findings have led to the recognition of major gaps in theoretical models used for assessment studies. Assessment models do not simulate adequately polar stratospheric cloud (PSC) chemistry or polar meteorology. The impact of these shortcomings for the prediction of ozone depletion at lower latitudes is uncertain.

2. Supporting Evidence and Other Results

These and other findings are based upon the results from several major ground-based and aircraft field campaigns in the polar regions, a reanalysis of ground-based ozone data from the past thirty-one years, a reanalysis of satellite ozone and PSC data, laboratory studies of gas-phase and surface-induced chemical processes, and model simulations incorporating these new laboratory data and observations. The highlights and conclusions from these activities in four research areas are summarized below.

Polar Ozone

- *There has been a large, rapid, and unexpected decrease in the abundance of springtime Antarctic ozone over the last decade.*

Beginning in the late 1970s, total column ozone decreases (lately reaching 50%) have been observed by both ground-based and satellite techniques, the latter showing that the loss is a continental-scale phenomenon. Ozonesondes at several stations have shown that the ozone loss occurs between 12 and 24 km, reaching as much as 95% at some altitudes.

- *The weight of scientific evidence strongly indicates that man-made chlorine and bromine compounds are primarily responsible for the ozone loss in Antarctica.*

  The ozone loss over Antarctica is initiated by chemical reactions that occur on the surfaces of PSCs and that convert the long-lived chlorine into chemically more-reactive forms. Laboratory studies have provided important evidence that such chemical reactions can occur on PSC surfaces. Furthermore, reactions can also remove reactive nitrogen species, thereby slowing the reformation of the less reactive chlorine compounds. Satellite data show that the frequency of occurrence of PSCs is the highest in the Antarctic stratosphere. Indeed, the abundance of the reactive chlorine compounds is observed to be elevated by 50 to 100 times in springtime. The observed reactive chlorine and bromine abundances explain a substantial fraction (60 to 100%) of the rapid ozone loss observed following the return of sunlight to Antarctica in September, 1987.

- *While the onset of the Antarctic ozone hole is linked to the recent growth in the atmospheric abundance of chlorofluorocarbons (CFCs) and to a lesser extent bromine compounds, many of its features are influenced by meteorological conditions.*

  Within the strong circumpolar vortex over Antarctica, temperatures are very low during the winter and spring and there is abundant production of PSCs. These special meteorological conditions set the stage for the occurrence of the ozone hole.

  The year-by-year variability in the depth of the ozone hole appears to be related, in part, to the Quasi-Biennial Oscillation (QBO), which is a natural oscillation of equatorial stratospheric winds. For example, there was a very deep ozone hole in 1987, but it was substantially less deep in 1988, possibly influenced by the observed temperature extremes between the years, which modulated the abundance of PSCs. Tropospheric weather systems can also influence stratospheric temperatures and water vapor on regional scales, which would in turn influence PSC abundance and ozone changes.

- *The chemical composition of the Arctic stratosphere was found to be highly perturbed.*

  The chemical perturbations in the Arctic were similar to those found in Antarctica, namely, an increase in the abundance of the ozone depleting forms of chlorine in association with PSCs. The studies conducted in January and February in 1989 found that the reactive chlorine abundances were enhanced by a factor of 50 to 100. No unambiguous evidence for ozone loss has yet been identified for the winter of 1988/1989. Readily detectable ozone reductions would be expected during January and February only if high concentrations of reactive chlorine species were maintained for sufficiently long periods in cold, illuminated air. The degree of Arctic ozone depletion will be influenced by the year-by-year timing of the warming of the polar vortex relative to the arrival of sunlight, as well as future chlorine and bromine abundances. In the Antarctic, the warming of the polar vortex always occurs after the arrival of sunlight (hence, ozone depletion), which contrasts with the Arctic, where warming generally occurs prior to the arrival of sunlight, as in 1989.

Global Trends

- *Several recent analyses of total column ozone data support the conclusion of the 1988 International Ozone Trends Panel (OTP) that there is a downward trend in ozone during winter at mid-to-high latitudes in the Northern Hemisphere over the past two decades.*

  The OTP analyzed the re-evaluated data from the ground-based Dobson instruments for the effects of known natural geophysical processes (seasonal variability, the approximately 28-month QBO, and the 11-year solar cycle) and possible human perturbations. After

allowing for natural variability, the analysis showed measurable decreases in the range of 2.3 to 6.2% between 30 and 64°N latitude for the winter months (December - March) between 1969 and 1986, with the larger decreases being at the higher latitudes. This was the first analysis that showed statistically significant downward trends.

The results of model calculations of chlorine-induced ozone loss are broadly consistent with these observed latitudinal and seasonal changes in column ozone, except that the mean values of the observed decreases at mid- and high latitudes in winter are a factor of two to three larger than the mean values of the predicted decreases. This finding suggested that the observed ozone changes may be due, in part, to the increased atmospheric abundances of the CFCs.

Subsequent to the OTP, the results from five new reanalyses of the same OTP data set by three independent analyses, using a variety of statistical models and assumptions, were generally consistent with the earlier result. Zonal mean ozone decreases derived for winter lie in the range 3.2 to 4.0% over 17 years, when averaged over the latitudes 30 to 64°N, compared to the value of 4.4% from the OTP analysis. The conclusions were found to be insensitive to the representations used for the QBO and solar cycle, strengthening the belief that the observed trends cannot be attributed to known natural processes.

The extension of the data set beyond that used by the OTP to include 1987 and 1988 does not alter the basic conclusions regarding trends in winter. In addition, no statistically significant zonal trends were found for the summer period (May - August) through 1988. Lastly, within longitudinal sectors, regional differences in the ozone trends were indicated in the Northern Hemisphere, i.e., with the largest changes being observed over North America and Europe and the smallest over Japan.

The present Dobson network and data are inadequate to determine total column ozone changes in the Arctic, tropics, subtropics, or Southern Hemisphere outside of Antarctica. Satellite data can provide the desired global coverage, but the current record is too short to differentiate the effects of natural and human-influenced processes on ozone.

- *Substantial uncertainties remain in defining changes in the vertical distribution of ozone.*

Since the chlorine/ozone theory had predicted that the greatest percentage ozone depletion should occur near 40 km altitude, the OTP looked for indications of such changes in a variety of reanalyzed data sets. The Panel reported that, based on the SAGE satellite data averaged over 20 to 50°N and S latitudes, ozone near 40 km had decreased by $3 \pm 2\%$ between February 1979-November 1981 and October 1984-September 1987. The SAGE data also indicated a percentage decrease in ozone near 25 km that is comparable in magnitude to that at 40 km. Furthermore, the Panel reported that, based on the Umkehr data from five northern mid-latitude stations, the ozone between 38 and 43 km had decreased by $9 \pm 4\%$ between 1979 and 1986, but this uncertainty range did not account for possible systematic errors. Because the SAGE and Umkehr data records were so short (i.e., less than one solar cycle), no attempt was made to distinguish between solar-induced and human-influenced contributions to these changes.

Adding 15 months of new SAGE data does not change the picture appreciably. Again, no attempt was made to separate the contributions from natural and human-influenced processes. Additionally, a more thorough analysis of data from 10 Umkehr stations in the Northern Hemisphere for the period 1977 to 1987 reports a statistically significant decrease in ozone between 30 and 43 km. The decrease near 40 km being $4.8 \pm 3.1\%$, after allowing for seasonal and solar-cycle effects and correcting the data for aerosol

interferences. These losses are somewhat less than those predicted by the chlorine/ozone theory.

Based on SAGE, Umkehr, and ozonesonde data, there are continuing indications of a stratospheric ozone decrease at 25 km and below. Changes at these altitudes are not predicted by global models based only on gas-phase processes. It is not clear whether this points to missing processes in the models or that these sparse measurements are not representative of the global atmosphere. However, such changes are qualitatively consistent with those required for compatibility with the total column measurements.

• *Recent measurements suggest that the rate of growth in atmospheric methane has slowed somewhat.*

It would appear that the rate of methane increase has been slowing down over the last decade, namely, from 16 to 20 ppbv per year in the early 1980s to 12 to 16 ppbv per year in the late 1980s. For the other trace gases that influence stratospheric ozone and climate (CFCs, nitrous oxide, and carbon dioxide), the observed rates of increase have not changed significantly since the time of the OTP report.

Theoretical Predictions

• *Theoretical models do explain many of the general features of the atmosphere, but new limitations have been recognized.*

Many processes control the distribution of trace gases in the atmosphere. To adequately simulate the atmosphere, models must include representations of numerous radiative, chemical, and small- and large-scale dynamical processes. Current models do indeed reproduce many of the patterns observed, for example, in the ozone column: a minimum in the tropics and maxima at high latitudes in the spring of both hemispheres. Furthermore, the north - south and vertical distributions of the ozone concentration are in general agreement with satellite observations, except for Antarctica. On the other hand, a long-standing discrepancy has been the systematic underestimation of ozone concentrations near 40 km.

Several major shortcomings have been identified recently. None of the assessment models adequately represent polar meteorology or attempt to include heterogeneous processes, i.e., chemical reactions on PSCs. The failure to include these processes would likely lead to an underprediction of ozone loss, both directly at polar latitudes and possibly indirectly at midlatitudes due to dilution arising from large polar ozone losses.

Furthermore, only a few models include the influence of increasing carbon dioxide abundances and decreasing ozone abundances on temperature, which, in turn, leads to a decrease in the destruction of ozone through lower temperatures in the stratosphere. Hence, while there are still open questions regarding the quantitative treatment of the influence of CO_2 (temperature feedback), the predicted ozone depletions from chlorine- and bromine-containing chemicals are less for those global assessment models used in this report (gas-phase chemistry only) that account for CO_2 increases than the predicted ozone depletions from those models that keep temperatures fixed.

• *Current understanding predicts that, if substantial emissions of halocarbons continue, the atmospheric abundances of chlorine and bromine will increase and, as a result, significant ozone decreases, even outside of Antarctica, are highly likely in the future.*

Several scenarios, which represent a spectrum of possible choices regarding man-made emissions of chlorine- and bromine-containing chemicals, have been used to examine the response of stratospheric ozone to atmospheric chlorine and bromine abundances. The predictions for the year 2060 relative to the year 1980 are discussed below for some of those scenarios. In each scenario, it was assumed that the recent trends continue in the atmospheric abundances of methane, nitrous oxide, and carbon dioxide of 15 ppbv, 0.25%, and 0.4% per year, respectively. The scenarios examined and the results predicted are the following:

SCENARIO (1)   A freeze of CFCs 11, 12, 113, 114, 115, halons 1211, 1301 and 2402 at 1985 production levels; CCl_4, CH_3CCl_3, Hydrochlorofluorocarbon (HCFC) 22 abundances increase at approximately 1 part per trillion by volume (pptv) (1% of today's level), 4 pptv (3% of today's level), and 6 pptv (7.5% of today's level) per year, respectively.

The chlorine loading of the atmosphere is predicted to reach 9.2 ppbv by the year 2060, about three times today's level, and the bromine loading 31 pptv, about two and one half times today's level . For models that did not include the effect of carbon dioxide (i.e., temperature feedback), predicted column ozone reductions were 1 to 4% in the tropics, and from 8 to 12% at high latitudes in late winter. For models that did include the effect of carbon dioxide, predicted column ozone reductions were 0 to 1.5% in the tropics and from 4 to 8% at high latitudes in late winter. These predictions do not include the effects of heterogeneous processes, which would increase the predicted ozone depletions, at least in polar regions. Ozone is predicted to decrease by 35-50% at 40 km in models with no temperature feedback, and about 25-40% in models with temperature feedback, and results in stratospheric temperature decreases of 10 to 20 K.

SCENARIO (2)   A 50% cut in emissions of CFCs 11, 12, 113, 114, 115, halons 1211, 1301 and 2402 from 1985 production levels by the year 2000; CCl_4, CH_3CCl_3, HCFC 22 increase at approximately 1 pptv, 4 pptv, and 6 pptv per year, respectively, plus a 50% substitution of CFC reductions augmenting HCFC 22 fluxes (used as a surrogate for other HCFCs).

The chlorine loading of the atmosphere is predicted to reach 7.2 ppbv by the year 2060, and the bromine loading 22 pptv. Only models that did not include the effect of carbon dioxide were used to calculate ozone depletions for this scenario. Predicted column ozone reductions were 1.5 to 3.0% in the tropics, and from 5 to 8% at high latitudes in late winter. These predictions do not include the effects of heterogeneous processes, which would increase the predicted ozone depletions, at least in polar regions. Ozone is predicted to decrease by 25-40% at 40 km (without temperature feedback). Temperature feedbacks are expected to reduce the predicted ozone depletions as in scenario 1.

SCENARIO (3)   A 95% cut in emissions of CFCs 11, 12, 113, 114, 115, halons 1211, 1301 and 2402 from 1985 production levels by the year 2000; CCl_4, CH_3CCl_3, HCFC 22 increase at approximately 1 pptv, 4 pptv, and 6 pptv per year, respectively, plus a 50% substitution of CFC reductions augmenting HCFC 22 fluxes.

The chlorine loading of the atmosphere is predicted to reach 5.4 ppbv by the year 2060, and the bromine loading 14 pptv. For models that did not include the effect of carbon dioxide, there was little change in column ozone in the tropics, and a decrease from 2 to 4%

11

at mid-latitudes. For the one model that did include the effect of carbon dioxide, column ozone was predicted to increase by 0 to 2% at most latitudes. These predictions do not include the effects of heterogeneous processes, which would increase the predicted ozone depletions, at least in polar regions. Ozone is predicted to decrease by 20-30% at 40 km.

SCENARIO (4)   95% cut in emissions of CFCs 11, 12, 113, 114, 115; halons 1211, 1301, 2402; freeze of CCl_4 and CH_3CCl_3 atmospheric levels constant at 1985; HCFC 22 increase at approximately 6 pptv per year, but no substitution of CFCs with HCFC 22.

The chlorine loading of the atmosphere is predicted to be about 3.6 ppbv by the year 2060, comparable to that of today, and the bromine loading 14 pptv. One model that did not include the effect of carbon dioxide predicted little change of ozone in the tropics and a decrease of up to to 4% at high latitudes. These predictions do not include the effects of heterogeneous processes, which would increase the predicted ozone depletions, at least in polar regions.

SCENARIO (5)   100% cut in emissions of CFCs 11, 12, 113, 114, 115; halons 1211, 1301, 2402; and CCl_4, CH_3CCl_3, and HCFC 22 by the year 2000.

This calculation was performed to examine the chlorine loading of the atmosphere with time. By the year 2060, the chlorine loading is predicted to be about 1.9 ppbv, significantly less than that of today and approximately the level required to return the Antarctic ozone layer to levels approaching its natural state, assuming that current meteorological conditions continue. Although no model calculations were performed using this scenario, it is likely that all models would predict an increase in global ozone due to the effects of carbon dioxide and methane.

Halocarbon Ozone Depletion and Global Warming Potentials (ODPs and GWPs)

• *The impact on stratospheric ozone of the halocarbons (HCFCs and HFCs) that are proposed as substitutes for the CFCs depends upon their chemical removal processes in the lower atmosphere (troposphere).*

Because they contain hydrogen atoms, the HCFCs and HFCs are primarily removed in the troposphere by reaction with the hydroxyl radicals (OH). Although the photochemical theory of tropospheric OH is well developed, it has not been validated experimentally, and the global OH distributions are based on models. Furthermore, the global abundance of OH is influenced by tropospheric composition, which is changing.

The various estimates of the lifetimes of HCFCs and HFCs in the troposphere have an uncertainty of ± 50%. This contributes an important source of uncertainty in the prediction of the ODPs and GWPs of the HCFCs and HFCs. The fate of the degradation products of the HCFCs and HFCs and their environmental consequences are inferred from data on analogous compounds and hence the specific degradation processes require further study.

• *The values of the ODPs for the HCFCs are significantly lower than those for the CFCs.*

Theoretical predictions performed by different groups using a variety of models have calculated similar, but not identical, values for the ODPs of the HCFCs, as indicated in Table 1 below.

None of the models used for calculating the ODPs are able to simulate the chemical and dynamical processes causing the Antarctic ozone hole. However, relative to CFC 11, the local Antarctic ODPs of HCFCs 22, 142b, and 124 will be larger, perhaps as much as a

factor of two or three times greater than those derived from model calculations that do not include heterogeneous chemistry and that cannot simulate polar dynamical processes. The ramifications of polar ozone depletion for ODPs is not currently clear.

The HCFCs all have much larger relative ozone depletion potentials during the first 30 to 50 years after their emission into the atmosphere compared to their steady-state ODP values. The transient values depend upon the atmospheric lifetime and their transport time to the region of destruction of the gas. This transient affect is implicitly taken into account by all models calculating atmospheric chlorine abundances and ozone depletion.

- *The steady state values of the halocarbon GWPs of the HCFCs and HFCs are lower than those of the CFCs.*

The key factors that establish the halocarbon GWP of a HCFC or HFC are its lifetime in the troposphere and its ability to absorb atmospheric infrared radiation. Halocarbon GWP values differ between species due primarily to differences in their lifetimes, since their abilities to absorb infrared radiation are similar. Hence, one of the the largest sources of uncertainty in the calculation of the halocarbon GWPs of the HCFCs and HFCs is quantifying their rate of removal in the troposphere. Calculations by three groups using different models for the halocarbon GWPs of the CFCs, HCFCs, and HFCs yield similar, but not identical, values, as indicated in Table 1.

The HCFCs all have much larger relative global warming potentials during the first 30 to 50 years after their emission into the atmosphere compared to their steady-state halocarbon GWP values.

Table 1. Range of Ozone Depletion Potentials (ODPs) and halocarbon Global Warming Potentials (GWPs) determined by one-dimensional and two-dimensional models, assuming scaling for HCFC ODPs and GWPs by CH_3CCl_3 derived lifetime (6.3 years).

Species	ODPs 1-D Models	ODPs 2-D Models	GWP 1-D Models
CFC-11	1.0	1.0	1.0
CFC-12	0.9 - 1.0	0.9	2.8 - 3.4
CFC-113	0.8 - 0.9	0.8 - 0.9	1.3 - 1.4
CFC-114	0.6 - 0.8	0.6 - 0.8	3.7 - 4.1
CFC-115	0.4 - 0.5	0.3 - 0.4	7.4 - 7.6
HCFC-22	0.04 - 0.05	0.04 - 0.06	0.32 - 0.37
HCFC-123	0.013 - 0.016	0.013 - 0.022	0.017 - 0.020
HCFC-124	0.016 - 0.018	0.018 - 0.024	0.092 - 0.10
HFC-125	0	0	0.51 - 0.65
HFC-134a	0	0	0.24 - 0.29
HCFC-141b	0.07 - 0.08	0.09 - 0.11	0.084 - 0.097
HCFC-142b	0.05 - 0.06	0.05 - 0.06	0.34 - 0.39
HFC-143a	0	0	0.72 - 0.76
HFC-152a	0	0	0.026 - 0.033
CCl_4	1.0 - 1.2	1.0 - 1.2	0.34 - 0.35
CH_3CCl_3	0.10 - 0.12	0.13 - 0.16	0.022 - 0.026

3. Implications

The findings and conclusions from the intensive and extensive ozone research over the past few years have several major implications as input to public policy regarding restrictions on man-made substances that lead to stratospheric ozone depletion:

• The scientific basis for the 1987 Montreal Protocol on Substances that Deplete the Ozone Layer was the theoretical prediction that, should CFC and halon abundances continue to grow, there would eventually be substantial ozone depletion. *The research of the last few years has demonstrated that actual ozone loss due to the CFCs has already occurred, i.e., the Antarctic ozone hole.*

• Even if the control measures of the Montreal Protocol were to be implemented by all nations, today's atmospheric abundance of chlorine (about 3 ppbv) will at least double to triple during the next century. *Assuming that the atmospheric abundance of chlorine reaches about 9 ppbv by 2060, ozone depletions of 0 - 4% ozone in the tropics and 4 - 12% at high latitudes would be predicted, even without including the effects of heterogeneous processes.*

• The heterogeneous, PSC-induced chemical reactions that cause the ozone depletion in Antarctica and that also occur in the Arctic represent additional ozone-depleting processes that were not included in the stratospheric ozone assessment models on which the Montreal Protocol was based. Recent laboratory studies suggest that similar reactions involving chlorine compounds may occur on sulfate particles present at lower latitudes, which could be particularly important immediately after a volcanic eruption. *Hence, even with the Montreal Protocol, future global ozone depletions could well be larger than originally predicted.*

• Large-scale ozone depletions in Antarctica appeared to have started in the late 1970s and were initiated by atmospheric chlorine abundances of about 1.5 - 2 ppbv, compared to today's level of about 3 ppbv. *To return the Antarctic ozone layer to levels approaching its natural state, and hence to avoid the possible ozone dilution effect that the Antarctic ozone hole could have at other latitudes, one of a limited number of approaches is a complete phase out of all fully halogenated CFCs, halons, carbon tetrachloride, and methyl chloroform, as well as careful considerations of the HCFC substitutes. Otherwise, the Antarctic ozone "hole" is expected to remain, provided the present meteorological conditions continue.*

III. SCIENTIFIC SUMMARIES

Chapter 1. Polar Ozone

1.1 Polar Ozone Trends

The observation of substantial springtime reductions in Antarctic ozone, the Antarctic ozone "hole," focused world attention on the polar regions. In the few years since the discovery of this phenomenon, a great deal of field and laboratory data have been gathered. Theoretical studies have kept pace with the experimental investigations. This chapter provides a detailed review of the current understanding of the science of polar ozone depletion.

Differences in atmospheric dynamics of the hemispheres cause naturally lower ozone abundances in the Antarctic early spring as compared with the Arctic which should not be confused with the Antarctic ozone hole. Planetary waves are generally weaker in the Southern Hemisphere than in the Northern Hemisphere. The Southern Hemisphere polar winter stratosphere is colder and the westerly vortex is stronger and more persistent than in the Northern Hemisphere. These factors strongly influence the seasonal and latitudinal variations in ozone in the two hemispheres. The ozone hole is identified not merely with the difference in ozone abundances between the hemispheres nor with the latitude gradients, but with a decrease in the ozone abundances found in September and October over the past decade. It is now clear that these decadal trends result from a dramatic drop in total ozone that occurs each September. This unexpected ozone removal results in about a 50% decrease in column abundance by the end of September in recent years, as demonstrated by ground-based measurements from Halley Bay, Syowa, and the South Pole. Ozonesonde and satellite data reveal comparable total column changes, and show that the decreases occur primarily in the height region from about 12 to 24 km, the heart of the polar ozone layer. Further, the satellites demonstrate that the ozone hole extends over broad horizontal scales, at times covering the entire Antarctic continent.

Observed ozone trends in the warmer, winter Northern Hemisphere stratosphere are far smaller than those of Antarctica. Recent analyses suggest that the sub-polar column ozone decreases are largest in the winter and spring, on the order of 5% over the period from 1969 to 1988.

The trend in Antarctic ozone has not been monotonic, but this is not surprising. Inter-annual variations in total ozone occur at all latitudes. One cause of inter-annual variability is the Quasi-Biennial Oscillation (QBO), which is a natural fluctuation of equatorial stratospheric zonal winds and circulation. The mechanisms connecting polar latitude phenomena with the tropical QBO wind oscillation are not well understood.

1.2 Polar Stratospheric Chemistry

Hypotheses to explain the ozone hole included halocarbon chemistry, nitrogen chemistry associated with the solar cycle, and dynamical effects. Observations have ruled out the dynamical and solar cycle theories, while a broad range of measurements have been shown to be consistent with the general concepts of the halocarbon theory. The halocarbon theory is based on observations of the widespread occurrence of polar stratospheric clouds (PSCs) in the extremely cold Antarctic lower stratosphere. These provide surfaces on which heterogeneous chemical reactions can take place.

Satellite data from 1978 to the present provide information regarding the vertical, geographical and seasonal extent of the PSCs. Their frequency in the Antarctic stratosphere is about 10 to 100 times greater than in the Arctic. There is an apparent QBO variation in the occurrence of PSCs during both September and October, as well as increasing numbers of PSC sightings during the Octobers of 1985 and 1987 (years of westerly QBO phase). PSCs may also influence the radiative budget of the polar lower stratosphere, hence affecting the mean circulation and ozone distributions.

Laboratory studies suggest that some PSCs are composed of nitric acid and water, condensing at temperatures considerably warmer than the frost point. As the stratosphere cools, these will be the first type of clouds to form, while water ice clouds will form only at colder temperatures. Field studies have demonstrated that the former contain a substantial amount of nitrate. Laboratory studies have also shown that reactions involving nitrogen oxides and relatively long-lived chlorine species (such as $ClONO_2$ and HCl) can occur on cloud surfaces. These reactions convert relatively inert chlorine reservoirs to reactive species that photolyze readily, releasing chlorine free radicals which can then destroy ozone. The reactions also tie up nitrogen oxides in the long-lived species, HNO_3, thereby slowing the reformation of chlorine reservoirs such as $ClONO_2$. This maintains elevated abundances of chlorine free radicals and the associated rapid ozone destruction over notably longer periods than would be possible if the heterogeneous reactions affected only the composition of chlorine species. Both sunlight and extremely cold temperatures are necessary for accelerated ozone loss.

Once liberated, the chlorine rapidly forms chlorine monoxide (ClO), which can then participate in several ozone-destroying catalytic cycles. These involve formation of the dimer of chlorine monoxide as well as reactions of ClO with bromine monoxide (BrO), hydroperoxyl radicals, and atomic oxygen. Laboratory studies have provided most of the rate coefficients and photochemical parameters needed to characterize these cycles, although there are still significant uncertainties in both homogeneous and heterogeneous chemistry.

1.3 Field Observations

Observations of ClO and BrO in Antarctica have provided a critical test of the halocarbon theory of ozone depletion. In situ and remote measurements using two independent techniques have demonstrated that the ClO abundances near 20 km are typically about 1 ppbv in the Antarctic vortex during September, about one hundred times greater than theoretical predictions that do not include heterogeneous chemistry. However, these elevated ClO abundances are broadly consistent with modeling studies considering the likely PSC chemistry, frequency and duration. While there are differences in detail among these studies, all show that a substantial fraction of the observed ozone loss (60 to 100%) can be explained by the observed ClO and BrO abundances using current measurements of kinetic rates. The Antarctic ozone loss is at present believed to be dominated by the dimer cycle during years when depletion is largest, with bromine reactions contributing about 15 to 35% and reactive hydrogen contributing about 10 to 15% to the total chemical loss rate. During years of lower Antarctic ozone depletion (e.g., 1988) and in the Arctic, the bromine chemistry is calculated to be more important. Uncertainties in measurements, model formulation and the potential importance of transport processes currently preclude a fully quantitative evaluation of the consistency between observed rates of ozone change and photochemical mechanisms.

A broad range of ancillary measurements in Antarctica supports and extends our confidence in the understanding of changes in gas-phase composition caused by PSCs. These include: in situ measurements of H_2O, NO_y (total reactive nitrogen), NO, particle sizes, and particulate nitrate, as well as long-path measurements of $OClO$, HCl, HF, $ClONO_2$, NO_2 and HNO_3. Of particular importance are the observations of NO_y and H_2O, which show extensive denitrification and dehydration in the Antarctic vortex, believed to result from sedimentation of cloud particles.

Denitrification is of particular importance since it controls the amount of nitrogen oxides remaining after PSCs have disappeared, and hence, as mentioned earlier, may strongly affect the rate of reformation of chlorine reservoirs.

Similar chemical measurements have been obtained in the Arctic stratosphere. Satellite and ground-based measurements of steep latitudinal gradients in Arctic NO_2 abundances (the Noxon "cliff") suggest the presence of mechanisms depleting NO_2 in north polar regions. The decrease in NO_2 is qualitatively related to increases in HNO_3 abundances, indicating mechanisms for nitrogen oxides suppression without denitrification (different from that observed in Antarctica). Such an increase could occur, for example, through heterogeneous reactions followed by cloud evaporation. Concentrations of ClO as high as 1 ppbv were observed inside the Arctic polar vortex in the winter of 1989. Enhanced column abundances of $ClONO_2$ and reduced abundances of HCl and NO_2 also indicated the importance of heterogeneous chemistry similar to that of Antarctica. No unambiguous evidence for ozone loss has yet been identified for the winter of 1989. Readily detectable ozone reductions would be expected to occur only if high concentrations of ClO were maintained for sufficiently long periods in cold, illuminated air. Vortex dynamics during the 1989 winter probably limited these conditions, and are likely to do so in most Northern Hemisphere winter/spring seasons. Thus the Northern Hemisphere ozone trends cannot be unambiguously identified with PSC chemistry, although the observations are qualitatively consistent with such an explanation.

1.4 Dynamics

The role of dynamical coupling has been examined in many different studies. Synoptic scale disturbances (tropospheric weather systems) can affect total ozone amounts locally, and may lead to the formation of PSCs. Air may flow through such systems and become chemically perturbed. If there is significant flow of air into and out of the stratospheric polar vortex, ozone amounts may be reduced well outside of the region where heterogeneous chemical reactions on PSCs can occur. Further, some PSCs may be found outside of the denitrified and dehydrated region and may induce chemical perturbations at sub-polar latitudes during winter. Quantitative details are uncertain. Export of air that has undergone ozone depletion may dilute ozone concentrations at lower latitudes when the polar vortex breaks down in the spring. Numerical models indicate that about a 2% change might occur in ozone amounts at mid-latitudes of the Southern Hemisphere due to dilution, and suggest that some fraction of the dilution may remain from one year to the next.

Measurements of the vertical profiles of long-lived tracers such as N_2O and the chlorofluorocarbons in the polar vortices reveal low values compared to those at other latitudes. These apparently result from downward motion and have important implications not only for representations of vortex dynamics but also for chlorine chemical perturbations. For example, measurements indicate only about 0.3 ppbv of total chlorine in the form of chlorofluorocarbons near 20 km at 70°S as compared to 1.0 ppbv at 45°S in about 1987; these imply that the corresponding abundances of reactive chlorine are on the order of 2.2 and 1.5 ppbv, respectively. Thus, the amount of reactive chlorine available for reactions on PSC surfaces in the polar regions is likely to be significantly enhanced compared to lower latitudes.

The stratospheric circulation exhibits variability on a range of time scales. In particular, there is substantial inter-annual variability in the two hemispheres, especially in the Northern Hemisphere. A very deep ozone hole occurred over Antarctica in spring, 1987. The hole was not as deep in 1988, perhaps because dynamics and transport were more vigorous in 1988 than in 1987. Temperatures were also warmer during September 1988 as compared to 1987, which is likely to be the primary cause for a corresponding decrease in PSC cloud frequencies in the regions sampled by the SAM II satellite between the two years. These factors may yield important differences in

heterogeneous chemical perturbations and hence may explain qualitatively the difference in the depth of the ozone hole obtained (with 1988 being much less depleted than 1987). The observed behavior fits general expectations based on QBO behavior since the equatorial winds were strongly westerly near 25 km during October 1987, whereas 1988 was characterized by a transition from westerly to easterly winds. If the current QBO cycle has the average period of about 28 months, winds will remain easterly through October 1989, but change to westerly before September 1990. If the past correlation between the QBO and the ozone hole continues and if the current QBO cycle exhibits a period close to the average, then the ozone depletion should be expected to be relatively modest in 1989 and quite deep in 1990 (note, however, that the QBO period can vary by as much as 8 months so that the measured equatorial winds must be examined before any firm comparisons can be made). The next few years should therefore provide an excellent test of the relationship between the QBO and the Antarctic ozone hole.

Minimum temperatures in the high latitude Northern Hemisphere stratosphere were unusually low in late-January/early-February, 1989. PSCs were observed as far equatorward as 50°N. A strong, dynamically induced warming occurred at polar latitudes in mid-February and temperatures rose above the threshold values required for PSC formation. Poleward transport of air rich in ozone and nitrogen oxides is likely to have occurred. This warming of the Arctic vortex probably played an important role in limiting ozone loss during 1989.

On the basis of radiosondes and satellite data, a downward trend in lower stratospheric temperatures has been deduced at high southern latitudes from 1979 through 1987 (note, however, that in 1988 temperatures were much warmer than they would have been if this trend had continued monotonically). The largest changes, about 1K/year, were found in the means for October and for November, while no trend was found in September, when most of the Antarctic ozone loss is observed. The observed time lag between the temperature change and the ozone loss, as well as radiative studies with 1-D, 2-D, and 3-D models suggest that the temperature trend is the result of the ozone trend rather than its cause (i.e., reduced ozone abundances are predicted to yield smaller solar ultraviolet heating rates and hence colder temperatures).

1.5   Future of Polar Ozone

The future depletion of polar ozone depends in large part on mankind's use of halocarbons, although other factors may also contribute. In contrast to its behavior at ground level, increased concentrations of carbon dioxide may cool the stratosphere, perhaps affecting the duration and spatial extent of the PSCs in both hemispheres. Possible changes in climate and in the concentrations of atmospheric methane and nitrous oxide may also affect the processes related to the Antarctic ozone hole. The bulk of the chlorine currently in the stratosphere comes from chlorofluorocarbons that have atmospheric removal times on the order of 50 to 100 years, and hence the ozone hole will likely remain over Antarctica for many decades, even if all production were immediately halted. An examination of the Antarctic springtime column ozone record at several locations permits a rough estimate of the atmospheric chlorine content when the Antarctic ozone hole first became apparent. Assuming no changes in temperature, atmospheric dynamics, or photochemical processes, this provides an indication of the total chlorine abundances required to return the Antarctic ozone layer to levels approaching its natural state. A preliminary analysis of trace gas samples indicates an average age of polar lower stratospheric air of about five years. Coupled with the onset of detectable ozone reductions in the late 1970s, this suggests that organic chlorine mixing ratios of roughly the mid-1970s are necessary (corresponding to tropospheric total chlorine mixing ratios of about 1.5-2.0 ppbv, including the 0.6-0.7 ppbv of methyl chloride, which is believed to be of natural origin).

Chapter 2.   Global Trends

2.1   Introduction

This chapter largely builds upon the Ozone Trends Panel report by adding new analyses and updating the database.

Since the 1920s, numerous techniques have been developed and applied to determine total ozone and its vertical distribution. Initially, these measurements were not made for the purpose of determining long-term trends. Fortunately, some of these systems, and only the Dobson spectrophotometer for the last 30 years, have the requisite stability to provide data from which such changes may be detected and quantitatively measured.

For trend determination, short-term random noise is not usually a significant factor, since large amounts of data are averaged. The most important characteristic is stability, i.e. the absence of time-dependent systematic errors. Accuracy is desirable, but continuing systematic errors will not obscure the detection of change.

Determination of the global trends in stratospheric ozone have been based on complementary measurements, from the ground and from satellites. Ground-based instruments can be checked and recalibrated as necessary; they are regarded as capable of long-term stable operation, although this depends on some non-technical factors. Their disadvantages are that they are local systems, and provide few observations in oceanic or remote areas. Satellite-borne instruments obtain global data, but, once launched, are not available to checking and are subject to drift. It is thus desirable to have these complementary measurements to provide checks on each other.

2.2   Trends in Total Ozone

Existing data on total ozone relies heavily on the Dobson instruments and M83/M124 instruments in the Northern Hemisphere mid-latitudes (30-64°N) so that trends can only be determined in this latitude range. Dobson instruments are referenced to the World Standard instrument, whose calibration is reported to have been maintained within ± 0.5% over the past 15 years.

Satellite data are provided by the TOMS/SBUV instruments. They have proven to be very useful to verify consistency and identify erroneous readings in ground-based instruments and to confirm the reliability of the World Standard instrument. An important recent result is the development of a method for using the TOMS/SBUV data themselves to remove the effects of long-term instrumental drift. Although such new data are not used in the following analysis, results of initial testing suggest this has been successful, and that the TOMS data can provide in the future a second, independent source of data on global trends.

The main conclusions of the study of total ozone trends are as follows (± 2 standard error limits are shown):

- *New analyses of the total ozone data set used by OTP produces negative trends whose latitudinal and seasonal patterns are consistent with the earlier results (over the 17-year period from December 1969 through 1986).*

19

Zonal mean decadal changes derived using various statistical assumptions lie in the following ranges during winter (December-March): for 30-39°N or 35°N, -0.9 ± 0.9% to -1.7 ± 0.9%; for 40-52°N or 45°N, -2.0 ± 0.8% to -3.0 ± 1.7%; and for 53-64°N or 55°N, -2.5 ± 1.9% to -3.7 ± 1.8%. Analogous changes during summer (May-August) are: for 30-39°N, -0.4 ± 0.9% to -1.1 ± 0.9%; for 40-52°N, -0.7 ± 0.6% to -1.1 ± 0.8%, and for 53-64°N, -0.1 ± 0.9% to -0.7 ± 0.9%. Results of an independent study performed in the USSR lie within the ranges quoted above.

- *The trends are sensitive to data obtained after October 1982 during periods of anomalies in the ozone patterns.*

If the data are analyzed up to and including October 1982, the summertime trend moves closer to zero by 0.8 to 1.0% per decade. Depending on the details of the statistical model, the analogous change in the wintertime trend is 0.3 to 0.9% per decade less negative.

- *Derived trends for the 17-year period between 1969 and 1986 are insensitive to the statistical treatment of the quasibiennial oscillation and solar cycle relationships.*

Since the Dobson ozone record approaches 30 years, the trend estimates should be nearly independent of the 11-year solar cycle effect as represented by the F10.7-cm solar flux and the quasi-biennial effect represented by equatorial 50 hPa winds. This is important in that the derived long-term trends are robust to these known natural causes of ozone variability.

- *Extension of the data set into 1988 does not alter the nature of conclusions based on measurements through 1986, although differences in detail exist.*

During winter, derived statistically significant trends are -1.8 ± 1.1%/decade, -2.3 ± 0.9%/decade, and -2.7 ± 1.2%/decade at latitudes 35°N, 45°N, and 55°N respectively. Trends derived for summer at 35°N, 45°N, and 55°N are -0.5 ± 1.1%/decade, -0.3 ± 1.0%/decade, and -0.2 ± 1.2%/decade, respectively. None of the summertime trends are statistically significant.

- *Analyses of Dobson measurements from different geographic regions reveal differences in trends.*

Over the period 1969 to 1988, European and North American stations indicate statistically significant wintertime trends of -2.9 ± 0.7%/decade. Japanese stations indicate a non-significant wintertime trend of -0.6 ± 1.0% per decade. Summertime trends vary from -1.2 ± 0.7% per decade over North America to +0.8 ± 1.2% per decade over Japan.

- *The regional differences in trends derived from the Dobson network are consistent with geographic patterns of ozone change contained in the TOMS/SBUV data sets.*

Data sets now available from satellites are useful in identifying geographic patterns in total ozone changes. However, present satellite data sets have insufficient length for definitive studies of long-term trends.

- *The observed total ozone trends for the winter are more negative than model predictions for the period 1969 through 1986 although there is close agreement between observation and prediction in the summer.*

The observed winter total ozone trends over the latitudes 30° to 60°N ranged from -1.9 ± 0.7% per decade -2.6 ± 1.2% per decade among the study groups. Based on the observed trend uncertainty limits, these changes exceed the theoretical model calculated winter changes of -0.5 to -1.2% per decade given in the OTP report. The observed summer trends ranged from -0.6 ± 0.6% per decade to -0.8 ± 0.6% per decade and were consistent within the uncertainty limits with the summer theoretical model calculations of -0.3 to-0.6% per decade.

2.3 Trends in Ozone Vertical Distribution

The situation with regard to measurements of the vertical distribution is less satisfactory. Presently, most ground-based observations have been of the Umkehr type, with extensive records at only about 10 stations, distributed very non-uniformly over the globe. The observations have a vertical resolution of 11 to 15 km, and are subject to aerosol interference, which can now be corrected for by physical-theoretical methods. The only reliable satellite data are obtained by the SAGE instruments above 25 km. It uses a ratio technique which renders the measurement insensitive to drift. The sampling is 900 profiles a month (two per orbit) with time varying non-uniform geographical distribution.

The emphasis in the current analysis is first given to the altitude range in the upper stratosphere where the percentage change in ozone concentrations at mid-latitude due to anthropogenic chlorine perturbations is expected to be the largest. The major problem for such an analysis is the scarcity in time and space of the available data base for both satellite and ground-based measurements which precludes any true global evaluation of trends in ozone vertical distributions.

- *Over the regions of maximum density of coincidences (SAGE II minus SAGE I), i.e. 20-50°N and 20-50°S, the comparisons indicate for a 6 years average time period (1980-1986):*

  - *an ozone decrease between 35 and 44 km with the maximum ozone change of -3 ± 2% occuring at 40 km.*

  - *an ozone decrease of -3 ± 2% at 25 km and an essentially zero ozone change at 28-33 km and at 45-48 km.*

The only satellite observations that can be used currently for the determination of upper-stratospheric ozone changes are based on the comparison of 33 months (1979-1981) of SAGE I and 3 years (October 1984-December 1988) of SAGE II operations. This analysis constitutes an update of the OTP report by including two more years of SAGE II data, and confirms the previous results. These values represent the changes that occur over this time period and no attempt has been made to correct for solar cycle or any other.

- *Statistically significant negative trends are observed in Umkehr layers 6-7-8 (30-43 km) that corresponds to an average ozone change of -0.4% ± 0.3 per year at 40 km.*

A trend analysis of Umkehr observations performed at 10 stations in the Northern Hemisphere for the period 1977-1987 has been made on a station-by-station basis using an autoregressive statistical model which accounts for seasonal, solar-cycle and aerosol induced effects. The latter is of particular importance when considering the high aerosol load in the stratosphere during the year 1982-1983 following the El Chichon volcano eruption.

21

• *Within the uncertainty limits of SAGE and Umkehr trend results near 40 km, these two independent results are not inconsistent.*

When corrected for the solar effect on ozone over 6 years, the change in ozone from SAGE observations near 40 km is estimated to be -0.2 ± 0.4% per year that is not explained by natural and instrumental variation. When compared to the Umkehr trend of -0.4 ± 0.3% per year there is no inconsistency within the margins of error.

• *In the lower stratosphere (15-24 km), the estimated change from a limited network of Northern Hemisphere ozonesonde stations is -0.5% per year ± 0.4%.*

Analysis of ozonesonde data at nine stations (Canada, Europe, and Japan) with records extending for the three longest ones from 1966 to 1986 has been performed to detect possible trends in ozone concentrations in the lower stratosphere. This analysis leads to some differences in the results for the various stations which probably reflect the differences in the system operation and extent of the data bases as well as varying regional effects.

• *Although at the lower edge, the simulation results are within the error bars of the observed changes in the ozone vertical distributions.*

Calculation of changes in the ozone vertical distribution have been performed in the OTP report using 2-D models for the period 1979-1985. The calculated changes decreases peak at about -6% at mid-latitudes near 40 km.

• *The ozone decrease observed by SAGE instruments and suggested by Umkehr results in the 40 km region contribute very little to explaining the Dobson year-round total ozone trend of -1.1% per decade.*

The SAGE change of -3% ± 0.2% at 25 km over 6 years when considered together with the negative Umkehr trend in this height range and the statistically significant, but not globally representative trend of nearly -0.5% per year observed by ozonesondes between 17 and 24 km, seems to suggest that the stratosphere below 25 km is the prime contributor to the observed total ozone trend at mid-latitude.

2.4 Trends in Stratospheric Temperature

The update of the previous temperature trend report (OTP) is based on the stratospheric temperature data set already considered, and updated when possible, and the new Rayleigh lidar data. These lidar data have been compared with the SSU (Stratospheric Sounding Unit) data and the NMC (National Meteorological Center) analyses from 1981 to 1987. Substantial differences are observed, accountable in part by changes in the NOAA satellites series.

The recent finding of a statistical relationship between the stratospheric temperature, the QBO and the 11-year solar cycle has a potential implication for trend determination. The zonal asymmetry of the 11-year solar signal, clearly shown by the radiosonde data up to 30 hPa (24 km), and confirmed by the lidar and rocket data at higher altitudes, leads locally to much larger temperature dependence than the one observed on zonal or global means. Caution must be taken when using local or regional data (for T and O_3 as well) unless the data extend over a long enough period to separate trends from solar activity effects.

In the stratosphere, long-term trends can only be obtained from radiosondes at present. Satellite observations are available for less than a solar cycle:

• *In the lower stratosphere (100-30 hPa), the temperature data over the last twenty years suggest a maximum change of -0.4 K/decade at mid- and low latitudes with larger changes occuring at higher latitudes.*

• *In the upper stratosphere, the satellite data for the period (1985/1986) - (1979/1980) indicate a global temperature change of -1.5 ± 1 K. It is compatible with the -3 ±4% change in ozone concentration around 40 km as observed by SAGE instruments.*

More work is clearly needed to bring data of different sources into agreement and to understand the causes of the large spatial variability, whether or not it is related to solar activity.

2.5 Trends in Tropospheric Source Gases and Ozone

• *For most of the tropospheric trace gases, the observed rates of increase up to the end of 1987 have not changed significantly compared to those in the OTP report, which analyzed data up to the end of 1986.*

• *It would appear that the rate of methane increase has been slowing over the last decade, from 16-20 ppbv per year in the 1980s to approximately 12-16 ppbv per year in the late 1980s.*

• *Trend analysis of surface ozone measurements from ozonesonde and ground-based instruments show variable results.*

The 16 Northern Hemispheric sites show a range of trends from -1.1 to +3.1% per year. Ten of the Northern Hemispheric sites show statistically significant positive trends, one site shows a statistically significant negative trend. The remaining sites show trends that are not significant. The seven European sites all show statistically significant positive trends, ranging from +1.1 to +3.1% per year. All four Canadian sites show negative trends, from -0.1 to -1.1% per year, only one of which is statistically significant. All three Japanese sites show positive trends, ranging from +0.9 to +2.5% per year, two of which are significant. The four Southern Hemispheric sites show trends ranging from -0.5 to +0.6% per year, only one of which is significant.

2.6 Trends in Stratospheric Aerosols

• *Stratospheric aerosols can produce artifacts in ozone measurements by remote sensing instruments and, in the case of Antarctic PSCs, have been shown to impact ozone destruction through heterogeneous chemistry. In addition, laboratory studies suggest that heterogeneous processes may occur on the surface of sulfuric acid/H_2O aerosols, which are greatly enhanced after volcanic eruptions. The latter effect could be important in providing a mechanism for ozone destruction on a global scale.*

• *From the standpoint of global trends, global stratospheric aerosol loading which peaked after the eruption of El Chichon, has generally decreased. Although low in 1989, it has not yet reached the lowest values observed in 1978-1979. The 1989 values have little or no effect on ozone measurements.*

2.7 Trends in Surface UV Radiation

The Robertson-Berger meters located in the United States showed no increase in surface ultraviolet radiation over the period 1974 through 1985. The measurements do not contradict the

23

observed downward trend in total ozone. The meter is not sensitive to small changes in ozone, and in addition, the system is strongly influenced by cloudiness and sources of pollution.

Chapter 3.   Model Predictions

3.1   Stratospheric Models

In order to estimate the impact of man-made chemicals on atmospheric ozone, it is essential to develop models that perform long-term predictions. Current models that are used for these predictions include rather detailed schemes for homogeneous chemistry and, to some extent, account for radiative and dynamical feedbacks. Two-dimensional models predict the latitudinal and seasonal changes in ozone and other trace gases. Among the available models for calculating ozone globally, these 2-D models currently include the best representation of homogeneous physical and chemical processes in the middle atmosphere and have been compared extensively with observations of many stratospheric chemical species. However, none of these models properly account for heterogeneous chemistry and polar dynamics. Because of computational requirements and development time, the recently available three-dimensional models have had only limited applications in assessment studies, but are important in resolving some issues of model formulation and dynamical feedbacks.

An important prerequisite for prediction models is that they represent with sufficient accuracy the present distributions of trace gases. The 2-D models involved in the present assessment generally reproduce the patterns observed in the ozone column, with a minimum in the tropics and maxima at high latitudes in the spring of both hemispheres. The meridional distribution of local ozone is also in good agreement with the satellite observations. However, important discrepancies have also been noted: in particular, the models systematically underestimate ozone concentrations near 40 km, where they should accurately represent the physical and chemical processes controlling ozone. Calculated and observed distributions and seasonal variations of species such as nitrous oxide, methane, nitric acid, nitrogen oxides and chlorine monoxide are in qualitative agreement, although substantial quantitative differences are found in certain cases.

The recent intercomparison of stratospheric models (1988, Virginia Beach) has highlighted many specific differences in the models, but did not yet resolve their causes. For example, the photodissociation rates were compared using specified ozone and temperature fields and found to differ among models by a factor of 2 or more in many instances. Follow-up studies examining the detailed radiative transfer in the models are continuing. Tests of the model circulation using synthetic tracers with specified chemistry has revealed substantial differences in the rate of upward motion in the tropical stratosphere. In spite of these individual differences, the calculated distribution of ozone is in good agreement between the models, and may demonstrate the robustness of the ozone photochemistry in these models.

3.2   Important Issues in Ozone Modeling

Modeling the polar regions is an especially challenging task because of the difficulty both in simulating the physics and chemistry of polar stratospheric clouds (PSCs) and in modeling the dynamical processes controlling the distribution of tracers and temperature of the high-latitude lower stratosphere in winter. The model predictions in this assessment do not include the effects of heterogeneous processes involving chlorine and nitrogen-containing chemicals on the surface of particles in PSCs. These processes are known to increase the abundance of the chlorine radical, ClO, which plays an important role in reducing ozone in the Antarctic atmosphere. In several

models, exploratory studies including these effects were performed, and showed substantially enhanced ozone depletion at high latitudes during winter and smaller changes in neighboring midlatitudes for much of the year. Additional studies, including some of these 2-D models and other 3-D models, have shown that the transport of ozone-depleted air from the Antarctic region today can account for ozone reductions at mid-latitudes of several per cent.

Laboratory studies suggest that heterogeneous processes on the natural background aerosols (Junge layer, which can be perturbed by volcanic eruptions) could also contribute to enhanced chlorine-catalyzed ozone destruction over much of the globe. Several model studies have examined the effects of parameterized heterogeneous reactions on sulfuric acid aerosols and have shown the possibility for additional ozone depletion. Because of uncertainties in the laboratory data on rate constants for these reactions under stratospheric conditions, only sensitivity studies can be made at present.

Stratospheric temperature perturbations resulting from changes in CO_2 or tropospheric climate will in turn affect the photochemistry of ozone. In the upper stratosphere for the scenarios described below, increased CO_2 and reduced ozone both lead to temperature reductions near the stratopause of 10-20 K by the year 2060. This significant cooling is a robust feature of simulations; it leads to a reduced rate of ozone photochemical loss and hence moderates the ozone depletion due to chlorine. In the lower stratosphere, a particularly difficult region to model, smaller temperature changes are predicted. If the lower stratosphere cools significantly (2-4 K) in the future, then reduced chemical loss predicted by the models with homogeneous chemistry would lead to an increase in ozone concentrations that must be considered along with other perturbations. Such changes in stratospheric temperatures could be accompanied by changes in the circulation. A number of the models used in this assessment include radiative feedbacks, and some attempt to account for circulation feedbacks.

3.3   Atmospheric Scenarios and Calculated Ozone Depletion

The composition of the atmosphere will depend on the rate at which halocarbons and other trace gases will be emitted in the future. Several scenarios have been considered in this assessment in order to examine the impact of possible control policies. Their details are specified in Table 3.1. None of the individual scenarios is intended to be a prediction of the future atmospheric composition; the range is only illustrative of different strategies for halocarbon control. They are used to define a range of chlorine and bromine loadings to the atmosphere and to study the consequent response of stratospheric ozone.

The predictions given here should be interpreted with caution in the light of the models' successes and limitations discussed above. Thus, given that the broad features of the present atmosphere are in general reproduced satisfactorily, it is then the broad features of the predictions that should be given most credence. For example, predictions of ozone and temperature changes near 40 km, as well as that of global chlorine loading, are probably more robust than detailed latitudinal behavior, especially in view of the models' lack of PSC chemistry.

(1) Reference Scenario. In the reference scenario (A1), the fluxes of the CFCs (11, 12, 113, 114, 115) and halons (1211, 1301, 2402) controlled under the Montreal Protocol were held constant at their estimated 1985 production levels. The concentration of additional halocarbons and other chemically and radiatively important gases were assumed to increase at rates consistent with presently observed trends: CCl_4 at +1 pptv/yr (+1%/yr in 1985); CH_3CCl_3 at +4 pptv/yr (+3%/yr in 1985); CH_4 at +15 ppbv/yr (+0.9%/yr in 1985); N_2O at +0.25%/yr; CO_2 at +0.4%/yr. For HCFC-22 the current estimated emissions (140 Gg/yr in 1985) and growth rate in emissions (5%/yr of the 1985 emission rate) were chosen to be consistent with the limited atmospheric

Table 3.1. Scenarios for Halocarbon Abundances

(a) 1985 Conditions

Gas	Mixing Ratio (pptv)	Flux (Gg/yr)	Gas	Mixing Ratio
CFC-11	220	350	CCl_4	100 pptv
CFC-12	375	450	CH_3CCl_3	130 pptv
CFC-113	30	150	CH_3Cl	600 pptv
CFC-114	5	15	CH_3Br	10 pptv
CFC-115	4	5		
halon 1211	1.5	5	N_2O	306 ppbv
halon 1301	1.7	8	CH_4	1600 ppbv
HCFC-22	80	140	CO_2	345 ppmv

(b) Scenario Definitions

Scenario	CFC cut (1996-2000)	CFC-22 Surrogate	CFC-22 Growth	CCl_4 Growth	CH_3CCl_3 Growth
A1	0 %	---	+7 Gg/yr/yr	+1 pptv/yr	+4 pptv/yr
B1	50 %	50 %	+7 Gg/yr/yr	+1 pptv/yr	+4 pptv/yr
C1	85 %	50 %	+7 Gg/yr/yr	+1 pptv/yr	+4 pptv/yr
D1	95 %	50 %	+7 Gg/yr/yr	+1 pptv/yr	+4 pptv/yr
D2	95 %	50 %	+7 Gg/yr/yr	fix (1985)	fix (1985)
D3	95 %	0 %	+7 Gg/yr/yr	fix (1985)	fix (1985)
E1	100 %	50 %	+7 Gg/yr/yr	+1 pptv/yr	+4 pptv/yr
E2	100 %	50 %	+7 Gg/yr/yr	fix (2000)	fix (2000)
E3	100 %	50 %	+7 Gg/yr/yr	cut (2000)	fix (2000)
E4	100 %	50 %	+7 Gg/yr/yr	cut (2000)	cut (2000)
E5	100 %	0 %	+7 Gg/yr/yr	cut (2000)	cut (2000)
E6	100 %	0 %	fix (2000)	cut (2000)	cut (2000)
E7	100 %	0 %	cut (2000)	cut (2000)	cut (2000)
E8	95 %	0 %	cut (2000)	cut (2000)	cut (2000)
E9	85 %	0 %	cut (2000)	cut (2000)	cut (2000)
E10	100 %	50 % cut (2030)	cut (2030)	cut (2000)	cut (2000)

(c) Total Chlorine Abundance, Summed Over All Halocarbons (ppbv)

Year	A1	B1	C1	D1	D2	D3	E1	E2	E3	E4	E5	E6	E7	E8	E9	E10
1985	2.98	2.98	2.98	2.98	2.98	2.98	2.98	2.98	2.98	2.98	2.98	2.98	2.98	2.98	2.98	2.98
2000	4.52	4.41	4.33	4.31	4.07	3.98	4.30	4.30	4.30	4.30	4.21	4.21	4.21	4.22	4.26	4.30
2030	7.09	5.93	5.12	4.89	4.17	3.66	4.77	4.29	4.09	3.52	2.98	2.84	2.58	2.72	3.01	3.38
2060	9.16	7.15	5.75	5.35	4.15	3.55	5.15	4.19	3.87	3.30	2.67	2.27	1.95	2.18	2.64	2.13
2090	10.72	8.09	6.25	5.73	4.05	3.42	5.47	4.03	3.64	3.07	2.41	1.88	1.55	1.84	2.43	1.59

observations (+6 pptv/yr in 1985). Many of the models used in the assessment had specified temperature distributions and were therefore unable to include the radiative impact on stratospheric temperatures of CO_2 increases or ozone changes.

In this reference scenario (A1), the chlorine loading of the atmosphere increases from 3.0 ppbv in 1985 to 4.5 ppbv in the year 2000, to 7.1 in the year 2030, and to 9.2 in the year 2060. The bromine loading increases from 13 pptv in 1985 (10 pptv CH_3Br; 1.5 pptv halon 1211; 1.7 pptv halon 1301) to 31 pptv in the year 2060 (10 pptv CH_3Br; 3 pptv halon 1211; 18 pptv halon 1301). For models that did not contain the carbon dioxide effect, reductions in column ozone from 1980 to 2060 ranged from 1% to 4% in the tropics and from 8% to 12% at high latitudes in late winter. For models that included the carbon dioxide effect, the corresponding ozone reductions were less: 0% to 1.5% in the tropics and 4% to 8% in high latitudes in late winter. Ozone reductions at 40 km were about 35-50% in models with no temperature feedback and about 25-40% in models with temperature feedback, resulting in temperature decreases of 10-20 K. No heterogeneous chemistry was included in these models. When methane increases are suspended in 1985, ozone column reductions are larger in all latitudes and seasons by about 3%. Methane increases lead to increases in ozone by conversion of active chlorine (Cl, ClO) into inactive chlorine (HCl) and further by contributing to the direct production of ozone by "smog chemistry" in the lower stratosphere and troposphere. Many of the differences in the model results occur in the lower stratosphere where it is more difficult to predict the impacts of radiative and chemical forcing.

(2) <u>Scenarios with CFC Reductions</u>. Several scenarios were considered in which emissions of CFCs and halons were reduced between 1995 and the year 2000, with 50% of the total CFC reduction augmenting the HCFC-22 budget. The increase in carbon tetrachloride and methyl chloroform are taken from the reference scenario. When CFC emissions are cut by 50% (B1), the chlorine loading in the year 2060 reaches 7.2 ppbv and the bromine loading is 22 pptv. The corresponding reductions in column ozone by 2060 are about 65% of those calculated for the reference scenario: 1-3% in the tropics and 5-8% at high latitudes in late winter for models without temperature feedback. Ozone reductions at 40 km are also less than in A1, 25-40% (without temperature feedback). No heterogeneous chemistry was included in these models.

When the CFC emissions are reduced by 85% (C1), the chlorine and bromine loadings in 2060 are 5.5 ppbv and 16 pptv, respectively. The reductions in column ozone are approximately 50% of those calculated in the reference scenario. No heterogeneous chemistry was included in these models.

When the CFC emissions are reduced by 95% (D1), the chlorine and bromine loadings in 2060 are 5.4 ppbv and 14 pptv, respectively. The reductions in column ozone at mid- to high latitudes are approximately 40 to 50% of those calculated in the reference scenario: very little change in the tropics and 2-4% at mid-latitudes for models without temperature feedback. Ozone reductions at 40 km are 20-30%. In the one model that includes the CO_2 effect, modest ozone column increases, 0-2%, are found at most latitudes. No heterogeneous chemistry was included in these models.

Further reductions in chlorine loading were considered by freezing concentrations of methyl chloroform and carbon tetrachloride (D2). When CFC emissions were also cut by 95%, the chlorine loading at 2060 was reduced to 4.2 ppbv. The reductions in column ozone were about 30% of that in the reference scenario, corresponding to about 60% of those calculated in the similar case when CCl_4 and CH_3CCl_3 were assumed to increase. If in addition, the 95% cut back in CFC emissions is not compensated for by increased emission of HCFC-22 (D3), the chlorine loading at 2060 is reduced further to 3.6 ppbv, but the calculated ozone columns are not significantly different: little change in the tropics and a decrease of up to 4% at high latitudes. This change in

chlorine loading, from 4.2 to 3.6 ppbv, has little effect on column ozone because it is associated with changes in HCFC-22 abundance. In these current assessment models, HCFC-22 does not release a large fraction of its chlorine in the middle stratosphere where chlorine catalyzed loss of ozone is most important. No heterogeneous chemistry was included in these models.

(3) Examination of chlorine loading. Thus far, in all of the scenarios (A-D) the tropospheric mixing ratio of chlorine, when summed over all halocarbons (i.e., chlorine loading), is well above the 1985 levels of 3 ppbv by the end of the scenarios in 2060. It is interesting to note what different combination of halocarbon reductions could possibly yield a chlorine loading of less than 3 ppbv by 2060, and also whether chlorine levels prior to the onset of the Antarctic ozone hole (at most 2 ppbv) could be achieved by 2060 with any combination of freezes or cuts in halocarbon emissions in the year 2000. Additional scenarios (E) in the Table 3.1 explore the range of chlorine loading assuming that emissions of all halocarbons by 2000 can be completely eliminated by 2000, except for CH_3Cl. Only a complete cut in emissions of CFCs, HCFC-22, CCl_4, and CH_3CCl_3 results in chlorine loading less than 2 ppbv by 2060, although a combination of cuts and reductions in emissions (including low levels of CFC emissions) can give values below 3 ppbv. If the time frame is extended to 2090, there is a slightly greater range of emission restrictions that will result in 2 ppbv of atmospheric chlorine. Model assessments of these scenarios were not performed since the ozone perturbations would be dominated by the increases in CH_4, N_2O, and CO_2 rather than the chlorine abundances.

3.4   Changes in Ultraviolet Radiation at the Surface

The changes in UV radiation at the surface have been calculated both for the observed changes in ozone column over the past decade and for the predicted changes in the future. The ultraviolet spectrum has been averaged to account for DNA damage, for plant damage, and for the Robertson-Berger meter's response. The TOMS data normalized to Dobson was used to define the change in the column over the past decade (0 to -4% in the tropics, -4 to -8% in northern high-latitude winter, and -8 to -30% at high southern latitudes from March through December). The calculated UV doses for DNA and plant damage increased by 2-5% in the Northern Hemisphere, by 2-10% between 30°S and 60°S, and by 10-60% under the Antarctic ozone hole. Predictions for 2060 from a model with fixed temperatures and circulation, neglecting heterogeneous chemistry, were used to illustrate future ozone perturbations (reference scenario A1 yielding a chlorine loading of 9.2 ppbv in 2060, 1-4% reduction in tropical total ozone, and 8-12% reduction at high latitudes). The largest absolute increase in average UV dose for the 1960-2060 period is predicted to occur in the springtime at mid-latitudes, and values may be sensitive to systematic latitudinal differences in cloud cover. The greatest relative increase, 20-40%, occurs at high latitudes in early spring. For the scenario in which CFC emissions are cut by 95% in year 2000 (chlorine loading of 5.4 ppbv), the calculated increases in UV dose are half as large.

Chapter 4.   Halocarbon Ozone Depletion and Global Warming Potentials

Concern over global environmental consequences of fully halogenated chlorofluorocarbons (CFCs) has sparked interest in the determination of the potential impacts on stratospheric ozone and climate of halocarbons, both chlorinated and brominated. In particular, the recent search for replacement compounds for the CFCs has primarily focused on several hydrogen-containing halocarbons (HCFCs, HFCs) which need to be closely examined. The kinetics and degradation mechanisms of many of these compounds (CFCs, HCFCs, HFCs, and halons) in the troposphere,

their potential relative effects on stratospheric ozone, and their potential relative effects on global climate have been evaluated.

4.1 Halocarbon Oxidation in the Atmosphere

The halocarbons containing hydrogen atoms (HFCs and HCFCs), which have been proposed for substitutes for CFCs, react with the OH radical and are primarily removed in the troposphere by this process. The rate constants for attack of OH on these compounds are well defined ($\pm 20\%$ at relevant temperatures) and this reaction is the major loss process for these molecules in the atmosphere.

There are virtually no experimental data available concerning the subsequent reactions occurring in the atmospheric degradation of HFCs and HCFCs. By analogy with similar chemical species it is predicted that the major products formed from the reactions of the OH radical with HFCs and HCFCs under tropospheric conditions are halogen substituted carbonyl compounds and hydrogen halides. Based on the available knowledge of gas phase chemistry only four of the possible products appear to be potentially significant carriers of chlorine to the stratosphere: $CClFO$, CF_3CClO, $CClF_2CO_3NO_2$ and $CCl_2FCO_3NO_2$. Physical removal processes (to the liquid phase) will probably reduce this potential, but tropospheric removal pathways for the carbonyl compounds, especially the physical processes, are not well understood and require further study.

The oxidizing efficiency of the troposphere is determined by the abundance of OH radicals. However, quantitative validation of photochemical models by direct experimental measurement of the tropospheric OH concentrations has not been satisfactorily achieved. Global budgets and distributions of methyl chloroform and ^{14}CO have been used to estimate a volume-averaged global OH concentration of 6 (± 2) x 10^5 molecule cm^{-3}. The budget and lifetime of methyl chloroform calculated using OH fields predicted by models is in general agreement with these results.

The calculated lifetimes of HFCs and HCFCs range from 0.25-40 years with an uncertainty of $\pm 50\%$. These are shorter than the lifetimes for the fully halogenated CFCs.

Ozone and ozone precursors (CH_4, CO, NO_x, and non-methane hydrocarbons) can influence OH concentrations in the troposphere and hence could indirectly influence the lifetime of halocarbons. Model calculations indicate that, if manmade emissions of ozone precursors continue to increase, ozone concentrations are anticipated to grow throughout the Northern Hemisphere. The magnitude of the predicted ozone increase will depend on the detailed assumptions made concerning future emissions of ozone precursors. Model calculations indicating future ozone increases as large as 50% also indicate future OH concentrations could decrease by as much as 25%. This would lead to increased lifetimes for many molecules removed by hydroxyl radical chemistry.

4.2 Ozone Depletion Potentials

Ozone Depletion Potentials (ODPs) have been defined as the ratio of steady-state calculated ozone column changes for each unit mass of a gas emitted into the atmosphere relative to the depletion for a mass unit emission of CFC-11. This definition provides a single-valued estimate of the cumulative ozone depletion for a gas, relative to CFC-11 on an equal mass basis.

One-dimensional and two-dimensional global atmospheric models have determined ODPs for a number of halocarbons, including CFCs, other chlorinated compounds, several potential

replacement hydrohalocarbons and several brominated compounds. Table 4.1 gives the range of calculated ODPs from one-dimensional and two-dimensional models for the CFCs, HCFCs, HFCs, plus CCl4 and CH3CCl3. Although 2-D models have generally a sounder physical basis, there are no real differences between the 1-D and 2-D results. In general, the ODPs for fully halogenated compounds, such as the CFCs, are much larger than those for the hydrogenated halocarbons, which include the potential replacement compounds considered.

Table 4.2 gives the ODPs determined for several brominated halocarbons from calculations by two models. These compounds should be compared to each other, because of the strong dependence of bromine effects on ozone to background chlorine levels. Bromine Ozone Depletion Potential (BODPs) are used for relative comparisons with Halon-1301, which has the longest lifetime and largest ODP, as the reference.

Although the calculated ODPs agree reasonably well among models, many uncertainties still exist. None of the models used for calculating ODPs include the chemical and dynamical processes causing the seasonal ozone losses over Antarctica. Another uncertainty lies in the model-calculated OH, which is a major source of uncertainty for both lifetimes and ODPs of the HCFCs.

Because of the apparent special chlorine processing and dynamics within the polar winter vortex, local Antarctic ODPs are expected to be larger than those shown in Table 4.1. Insofar as the observed long-lived tracer distributions, such as CFC-11 in the polar vortex, suggest that much of the total chlorine may be available there, then an upper limit on Antarctic ODPs can be determined by calculating the relative amounts of chlorine transported through the tropopause by the different gases. These chlorine loading potentials (CLPs) determined using assumed reference lifetimes (which generally agree with those in the models used here) can be as large as a factor of two to three times the derived ODP values (c.f., Tables 4.1 and 4.3). The ramifications of polar ozone depletion for global ozone depletion potentials (ODPs) are not currently clear.

The time-dependent relative ozone depletion values differ from the steady-state ODP values. The time-dependent values depend on the atmospheric lifetime and the transport time to the region of destruction of the gas. The shorter the stratospheric lifetime, the sooner the gas will impact stratospheric ozone and hence the higher the transient relative ozone depletion. An example of this behavior is shown by the HCFC-123 curve in Figure 4.1. It has a shorter lifetime than CFC-11; its relative ozone depletion is largest soon after emission. Other gases in this category include HCFC-141b and CH3CCl3. Species such as HCFC-22, HCFC-124, and HCFC-142b have somewhat longer time constants in the stratosphere. Their relative ozone depletions build slowly to values (based on their time constants) as large as 0.2 and then decay slowly with time to the derived ODP value. Relative ozone depletion values for HCFCs are greater than ODP values even after 30 to 50 years. Time-dependent relative ozone depletions for CFCs with lifetimes longer than CFC-11 show a monotonic increase to the ODP value. As shown for a pulse injection in Figure 4.2, the ratio of the cumulative calculated depletion of HCFC-22 or HCFC-123 to the cumulative depletion of CFC-11 is equal to the ODP for these species. Therefore, the ODP is the cumulative response; as discussed above, the transient response of relative ozone depletion may be larger that the ODP value at early times after emission.

Several of the halocarbons indicate a strong latitude dependence in their ODP values and a generally weaker seasonal variation. In particular, ODPs for species such as CFC-12, HCFC-22, HCFC-124, and HCFC-142b, which have greatly different stratospheric loss patterns than CFC-11, produce strong latitudinal gradients in ODPs, with the largest ODPs near summer poles and smallest values in the tropics. The effects of heterogeneous chemistry and polar dynamical effects could modify these findings.

Table 4.1. Range of Ozone Depletion Potentials (ODP) determined by one-dimensional and two-dimensional models, assuming scaling for HCFC ODPs by CH_3CCl_3 observed lifetime (6.3 years).

Species	1-D Models*	2-D Models**
CFC-11	1.0	1.0
CFC-12	0.9 - 1.0	0.9
CFC-113	0.8 - 0.9	0.8 - 0.9
CFC-114	0.6 - 0.8	0.6 - 0.8
CFC-115	0.4 - 0.5	0.3 - 0.4
HCFC-22	0.04 - 0.05	0.04 - 0.06
HCFC-123	0.013 - 0.016	0.013 - 0.022
HCFC-124	0.016 - 0.018	0.018 - 0.024
HFC-125	0	0
HFC-134a	0	0
HCFC-141b	0.07 - 0.08	0.09 - 0.11
HCFC-142b	0.05 - 0.06	0.05 - 0.06
HFC-134a	0	0
HFC-152a	0	0
CCl_4	1.0 - 1.2	1.0 - 1.2
CH_3CCl_3	0.10 - 0.12	0.13 - 0.16

*   1-D models from AER, LLNL, DuPont, and IAS
**   2-D models from AER, LLNL, University of Oslo, and DuPont

Table 4.2. Ozone Depletion Potentials for brominated compounds as calculated in the LLNL one-dimensional model and University of Oslo two-dimensional model.

Species	ODP*		BODP**	
	LLNL	Oslo	LLNL	Oslo
Halon-1301	13.2	7.8	1.0	1.0
Halon-1211	2.2	3.0	0.17	0.38
Halon-1202	0.3		0.02	
Halon-2402	6.2	5.0	0.5	0.64

*   Relative to CFC-11, shown for historical purposes. Values will be underestimates if account is taken of polar effects. Assumed upper stratospheric Cl_x mixing ratio is 3 ppbv in the LLNL model and 4.5 ppbv in the Oslo model.

**   Bromine Ozone Depletion Potentials (BODPs) defined relative to Halon-1301, the longest lived brominated gas.

Table 4.3. Maximum relative Chlorine Loading Potential (CLP) for examined CFCs, HCFCs, HFCs, and other chlorinated halocarbons based on reference species lifetimes chosen to be compatible with available atmospheric measurements and modeling studies.

Species	Reference * Lifetime (yrs)	Chlorine Loading Potentials**
CFC-11	60.0	1.0
CFC-12	120.0	1.5
CFC-113	90.0	1.11
CFC-114	200.0	1.8
CFC-115	400.0	2.0
HCFC-22	15.3	0.14
HCFC-123	1.6	0.016
HCFC-124	6.6	0.04
HFC-125	28.1	0
HFC-134a	15.5	0
HCFC-141b	7.8	0.10
HCFC-142b	19.1	0.14
HFC-143a	41.0	0
HFC-152a	1.7	0
CCl_4	50.0	1.0
CH_3CCl_3	6.3	0.11

*   Lifetimes (e-folding time) are based on estimates used in scenario development in Section 3.3.1 for the CFCs and from the analysis in Section 4.2 for the HCFCs and HFCs.

**   Chlorine Loading Potential is defined as the maximum chlorine transported across the tropopause per mass emitted relative to the same for CFC-11. It is proportional to lifetime and the number of chlorine atoms per molecule. It is inversely proportional to molecular weight.
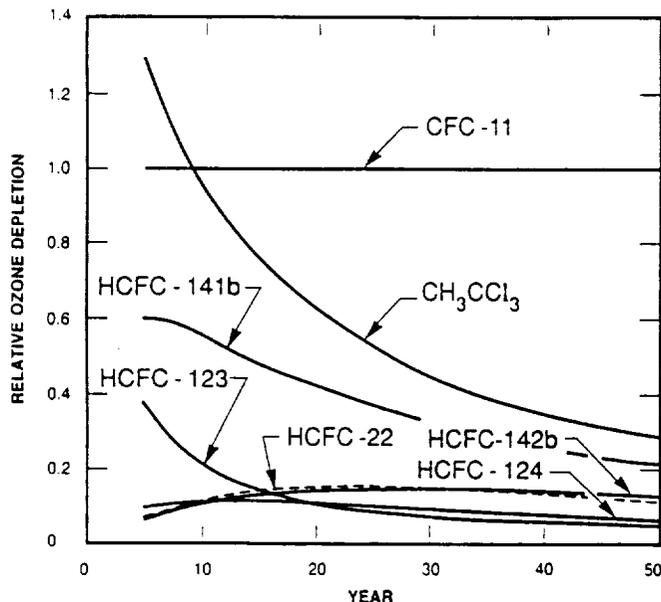
Figure 4.1. Calculated time-dependent change in relative ozone column depletion following a step change in emission of halocarbons (LLNL 1-D model).
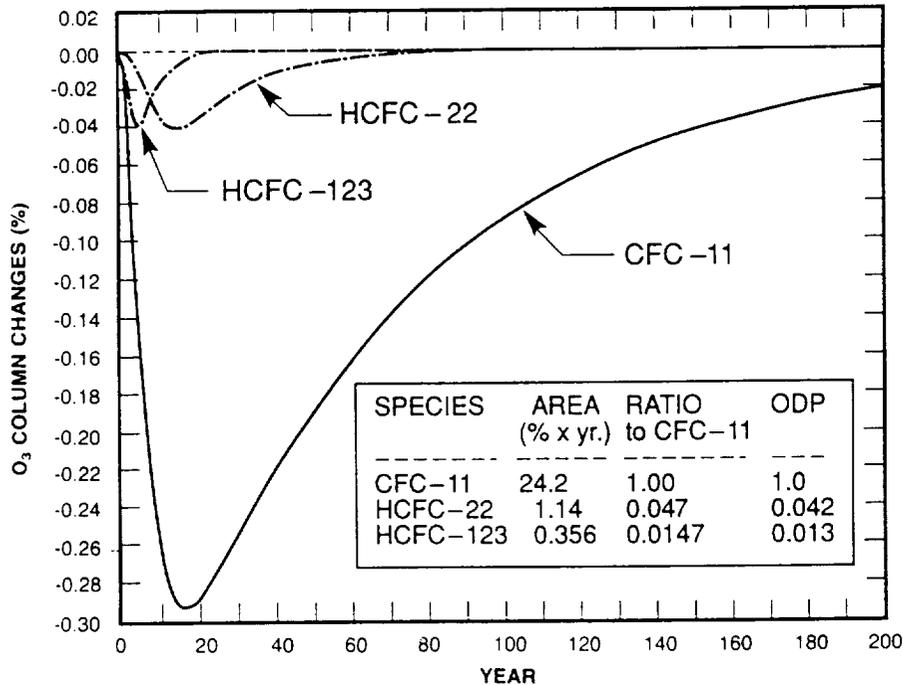
Figure 4.2. Calculated column ozone change following a pulsed input of 5 x 10^9 kg (for one year) of specified gas (DuPont 1-D model).

Sensitivity analyses indicate that ODPs are affected to only a minor degree (≤ 20%) by assumed variations in background levels of N_2O, CH_4, CO_2, CO, total stratospheric chlorine, and total stratospheric bromine.

4.3 Halocarbon Global Warming Potentials

Halocarbon Global Warming Potential is defined as the ratio of the calculated steady-state net infrared flux change forcing at the tropopause for any halocarbon for each unit mass emitted relative to the same for CFC-11. This definition quantifies the relative cumulative greenhouse warming per unit mass emitted.

Changes in the infrared fluxes in the surface troposphere system have been calculated for a number of halocarbons of these gases using a line-by-line radiative transfer model (GFDL). In addition, radiative forcing and surface temperature changes for these gases have been calculated using two one-dimensional radiative-convective models (AER and DuPont).

Halocarbon Global Warming Potentials (halocarbon GWPs) have been calculated from these results and scaled to a reference set of lifetimes (see Table 4.4). Agreement of ratio values is good, although direct radiative forcing values for individual gases differ systematically among models (between line-by-line and band models).

Halocarbon GWPs for fully halogenated compounds are larger than those for the hydrogenated halocarbons. Fully halogenated CFCs have halocarbon GWP values ranging from 1.0 to 7.5, whereas HCFCs and HFCs range from 0.02 to 0.7.

Halocarbon GWP values differ between species because of differences in infrared absorbances and differences in lifetimes. The range on absorbances is approximately a factor of 4, while the lifetimes vary by a factor of 250. Thus, the range of 600 among the halocarbon GWP values is primarily a result of differences in lifetimes.

Halocarbon GWP values are nearly insensitive to changes in background concentrations of CO_2, CH_4 and N_2O. Minor effects ($\leq 20\%$) do result from influences on chemical lifetimes, but these do not affect the relative radiative forcing.

Calculated time-dependent relative global warmings for halocarbons are initially on order unity, but decrease or increase depending on whether their lifetimes are shorter or longer than that of the reference gas. At long lifetimes the relative global warmings asymptotically approach halocarbon GWP values.

Table 4.4. Halocarbon Global Warming Potentials (Halocarbon GWPs) scaled relative to reference set of halocarbon lifetimes.

Species	Reference* Lifetime(Yrs)	AER**	DuPont**	GFDL**
CFC-11	60.0	1.0	1.0	1.0
CFC-12	120.0	3.4	2.8	3.0
CFC-113	90.0	1.4	1.4	1.3
CFC-114	200.0	4.1	3.7	
CFC-115	400.0	7.5	7.6	7.4
HCFC-22	15.3	0.37	0.34	0.32
HCFC-123	1.6	0.020	0.017	0.017
HCFC-124	6.6	0.10	0.092	
HFC-125	28.1	0.65	0.51	
HFC-134a	15.5	0.29	0.25	0.24
HCFC-141b	7.8	0.097	0.087	0.084
HCFC-142b	19.1	0.39	0.34	0.35
HFC-143a	41.0	0.76	0.72	
HFC-152a	1.7	0.033	0.026	0.028
CCl$_4$	50.0	0.34	0.35	
CH$_3$CCl$_3$	6.3	0.022	0.026	

* Lifetimes are based on estimates used in scenarios development (Section 3.3.1) for CFCs and from the analysis in Section 4.2 for HCFCs and HFCs.

** AER and DuPont results are based on surface temperatures perturbations calculated using radiative-convective models. The GFDL results are based on line-by-line determined radiative forcing.

Volume II

THE AFEAS REPORT

I. SUMMARY

The AFEAS report is the outcome of the Alternative Fluorocarbon Environmental Acceptability Study (AFEAS). AFEAS was organized to evaluate the potential effects on the environment of alternative compounds targeted to replace fully halogenated chlorofluorocarbons (CFCs). The objective was to:

Evaluate all relevant current scientific information to determine the environmental acceptability of the alternative fluorocarbons with special emphasis on:

- The potential of the compounds to affect stratospheric ozone,
- Their potential to affect tropospheric ozone,
- Their potential to contribute to model calculated global warming,
- the atmospheric degradation mechanisms of the compounds, in order to identify their products and hence,
- The potential environmental effects of the decomposition products.

The alternative compounds to be studied were hydrofluorocarborns (HFCs) with one or two carbon atoms and one or more each of fluorine and hydrogen and hydrochlorofluorocarbons (HCFCs) with one or two carbon atoms and one or more each of fluorine, chlorine and hydrogen. Because they contain hydrogen atoms, HFCs, and HCFCs are less stable in the atmosphere than CFCs and thus have greatly reduced ozone depletion potentials. Additionally, HFCs do not contain chlorine atoms which are the key factor in ozone depletion. All compounds meeting the above criteria were evaluated where data exists but emphasis was placed on evaluating the following.

HCFC 123	CCl_2HCF_3
HCFC 141b	CCl_2FCH_3
HCFC 142b	$CClF_2CH_3$
HCFC 22	$CClF_2H$
HCFC 124	$CClFHCF_3$
HFC 134a	CF_3CFH_2
HFC 152a	CF_2HCH_3
HFC 125	CF_3CF_2H

There were 52 scientists worldwide involved in AFEAS. Experts prepared review papers on all aspects of the topic and each paper was reviewed by one or more scientists. In addition, model calculations were carried out on ozone depletion and halocarbon global warming potentials. A meeting was held in Boulder, Colorado in May 1989 under the chairmanship of Dr. R. T. Watson of the National Aeronautics and Space Administration (NASA) for experts and reviewers to discuss and reach a consensus. The papers in this report are the outcome of that meeting. Summaries of these papers formed part of the 1989 UNEP Science Assessment.

AFEAS was conducted by independent scientists but was organized and sponsored by fifteen CFC producers from around the world as part of cooperative industry efforts to study the safety and environmental acceptability of CFC alternatives.

This report consists of the individual papers prepared for the Boulder meeting, revised to take account of reviewers' opinions and discussion. They are arranged in sections according to subject matter. Where there is more than one paper on a topic, a combined summary and conclusions was prepared to introduce the papers in that section.

II. PHYSICAL PROPERTIES

Physical Properties of Alternatives to the Fully Halogenated Chlorofluorocarbons
by M. O. McLinden

This section is concerned with physical properties of possible alternatives to the fully halogenated Chlorofluorocarbons (CFCs) used as refrigerants, solvents, and foam blowing agents. Specifically considered are the fixed points of the fluids (triple point and boiling point temperatures, and critical temperature, pressure, and density), vapor pressure, saturated liquid density, solubility in water, and hydrolysis rates. These properties directly or indirectly influence the fate of a chemical in the environment and also include the key thermophysical data necessary to estimate other properties. The fluids considered are hydrogen-containing halogenated methanes and ethanes. Included are R125, R22, R134a, R152a, R124, R142b, R123, R141b, and methyl chloroform.

A wide variety of data sources have been considered including published data, surveys and compilations of properties, and unpublished data provided by several of the companies which are members of the Alternative Fluorocarbon Environmental Acceptability Study (AFEAS) consortium. These data have been compiled and evaluated. Recommended values are tabulated for the fluid fixed points. The temperature dependencies of vapor pressure, saturated liquid density and solubility in pure water are presented in terms of correlations and as a tabulation of values calculated from these correlations.

The data vary greatly in quality and reliability, and are sometimes conflicting. At least limited data were available for the fixed points, vapor pressure and liquid density of all of the compounds. The values presented here are felt to be reasonable, although the lack of documentation in many cases makes an objective assessment of accuracy impossible, and revisions will certainly be necessary as additional data become available. Identified as high priority needs are improved vapor pressure data for R124, R142b, and, especially R141b, and improved liquid density data for R142b.

For solubility in water, the data were much more limited. Published, fully documented data were available only for R22. For the other fluids, unpublished data provided by the chemical manufacturers were used; again, while these data may be reliable, an assessment of their accuracy was not possible. The solubility information was correlated in terms of the Henry's law constant. The use of Henry's law in extrapolating from the saturation vapor pressure condition's employed in most of the measurements to the extremely low partial pressures that can be expected in the atmosphere is a source of uncertainty. For solubility in salt water, only data for R22 and methyl chloroform were found; an empirical 'salting parameter' evaluated from data for these two fluids can be applied to the other fluids in the absence of data.

Finally, hydrolysis is considered. Hydrolysis represents one possible mechanism for the environmental decomposition of a compound dissolved in the oceans or in cloud water. The data for hydrolysis rates were quite sparse; except for R22 and methyl chloroform, recommended values could not be developed. In view of the very limited solubilities of these compounds, even the order of magnitude-type information that can be estimated or extrapolated from the available

36

data may be sufficient to determine whether dissolution in water and subsequent hydrolysis is a significant destruction mechanism for these compounds. Thus, complete data on solubility and hydrolysis may be needed only for methyl chloroform. This point is considered in detail in a study by Wine and Chameides presented in Section VII, Liquid Phase Processes.

III. REACTION RATE CONSTANTS

Evaluated Rate Constants for Selected HCFCs and HFCs with OH and $O(^1D)$
by R. F. Hampson, M. J. Kurylo and S. P. Sander

The chemistry of HCFCs and HFCs in the troposphere is controlled by reactions with OH in which a hydrogen atom is abstracted from the halocarbon to form water and an halo-alkyl radical. The halo-alkyl radical subsequently reacts with molecular oxygen to form a peroxy radical. The reactions of HCFCs and HFCs with $O(^1D)$ atoms are unimportant in the troposphere but may be important in producing active chlorine or OH in the stratosphere.

In this chapter, the rate constants for the reactions of OH and $O(^1D)$ with many HFCs and HCFCs have been evaluated. Recommendations are given for the five HCFCs and three HFCs specified by AFEAS as primary alternatives as well as for all other isomers of C_1 and C_2 HCFCs and HFCs where rate data exist. In addition, recommendations are included for CH_3CCl_3, CH_2Cl_2, and CH_4.

The format used for the presentation of the recommended rate constant data is the same as that used by the NASA Panel for Data Evaluation (see DeMore et al., JPL Publication 87-41, September 15, 1987). The rate constant tabulation is given in Arrhenius form, $k(T) = A \exp(-E/RT)$, and contains the following information:

1. Reaction stoichiometry and products (if known).
2. Arrhenius A factor (in units of cm^3 molecule^{-1} s^{-1}.
3. Temperature dependence ("activation temperature," E/R) and associated uncertainty (Δ E/R).
4. Rate constant at 298 K (in units of cm^3 molecule^{-1} s^{-1}.
5. Uncertainty factor at 298 K.

All of the uncertainties are one standard deviation, 1σ. Hence, 95% confidence limits are given by 2σ. The uncertainty (1σ) at any temperature can be calculated from the expression:

$$f(T) = f(298)\exp\{\Delta E/R(1/T - 1/298)\}$$

For all of the OH reactions, the recommendations were derived from linear least squares Arrhenius fits of the selected data bases for temperatures below 400 K. This temperature restriction was made due to the observed Arrhenius curvature for several of the reactions over more extended temperature ranges. For some reactants, the necessary temperature dependent data do not exist, and the E/R values were estimated by comparison with other similar reactants and the A factor back-calculated using k_{298}. Reasonable values of E/R can be estimated from compounds appearing in a homologous series and by noting that most values of E/R for reactions of OH with halocarbons lie between 1000 and 2000 K. An alternative approach would have involved estimating, or calculating from transition state theory, the A factor and using k_{298} to obtain E/R. These two approaches yield similar results if the data are not extrapolated very far from room

37

temperature and, thus, are nearly equivalent for the calculation of ozone depletion or greenhouse warming potentials. These two estimation procedures can result in significant differences when used for extrapolations over a wide temperature range. In addition, they can yield disparate predictions when there are no direct kinetic data for either the species of interest or for one of similar structure.

Recommended rate constants and uncertainties for reactions of OH with selected HFCs and HCFCs.

Reaction	Fluorocarbon Number	A[1]	E/R ± ΔE/R[2]	k_{298}[1]	f(298)
OH + $CHFCl_2$	HCFC-21	1.2(-12)	1100 ± 150	3.0(-14)	1.1
OH + CHF_2Cl	HCFC-22	1.2(-12)	1650 ± 150	4.7(-15)	1.1
OH + CHF_3	HFC-23	1.5(-12)	2650 ± 500	2.1(-16)	1.5
OH + CH_2Cl_2	30	5.8(-12)	1100 ± 250	1.4(-13)	1.2
OH + CH_2FCl	HCFC-31	3.0(-12)	1250 ± 200	4.5(-14)	1.15
OH + CH_2F_2	HFC-32	2.5(-12)	1650 ± 200	1.0(-14)	1.2
OH + CH_3F	HFC-41	5.4(-12)	1700 ± 300	1.8(-14)	1.2
OH + CH_4	50	2.3(-12)	1700 ± 200	7.7(-15)	1.2
OH + $CHCl_2CF_3$	HCFC-123	6.4(-13)	850 ± 250	3.7(-14)	1.2
OH + $CHFClCF_3$	HCFC-124	6.6(-13)	1250 ± 300	1.0(-14)	1.2
OH + CHF_2CF_3	HFC-125	8.9(-13)	1750 ± 500	2.5(-15)	2.0
OH + CH_2ClCF_2Cl	HCFC-132b	3.6(-12)	1600 ± 400	1.7(-14)	2.0
OH + CH_2ClCF_3	HCFC-133a	5.2(-13)	1100 ± 300	1.3(-14)	1.3
OH + CHF_2CHF_2	HFC-134	8.7(-13)	1500 ± 500	5.7(-15)	2.0
OH + CH_2FCF_3	HFC-134a	1.7(-12)	1750 ± 300	4.8(-15)	1.2
OH + CH_3CCl_3	140	5.0(-12)	1800 ± 300	1.2(-14)	1.3
OH + CH_3CFCl_2	HCFC-141b	4.2(-13)	1200 ± 300	7.5(-15)	1.3
OH + CH_3CF_2Cl	HCFC-142b	9.6(-13)	1650 ± 250	3.8(-15)	1.2
OH + CH_2FCHF_2	HFC-143	2.8(-12)	1500 ± 500	1.8(-14)	2.0
OH + CH_3CF_3	HFC-143a	6.0(-13)	1750 ± 500	1.7(-15)	2.0
OH + CH_2FCH_2F	HFC-152	1.7(-11)	1500 ± 500	1.1(-13)	2.0
OH + CH_3CHF_2	HFC-152a	1.5(-12)	1100 ± 200	3.7(-14)	1.1
OH + CH_3CH_2F	HFC-161	1.3(-11)	1200 ± 300	2.3(-13)	2.0

1 units are cm^3 molecule^{-1} s^{-1}
2 units are K

Rate constants for the $O(^1D)$ reactions are associated with actual chemical reaction (leading to chemical breakdown of the HCFC or HFC) and do not include contributions due to simple physical deactivation (quenching) of the excited oxygen atom. Temperature data do not exist for most of the $O(^1D)$ reactions and the estimated temperature independencies are taken from comparisons with the few HCFCs and CFCs for which such data do exist. The following two tables summarize the results of this evaluation.

Recommended rate constants and uncertainties for reactions of $O(^1D)$ with selected HFCs and HCFCs.

Reaction	Fluorocarbon Number	A^1	$E/R \pm \Delta E/R^2$	$k_{298}{}^1$	$f(298)$
$O(^1D) + CHFCl_2$	HCFC-21	1.9(-10)	0 ± 100	1.9(-10)	1.3
$O(^1D) + CHF_2Cl$	HCFC-22	1.0(-10)	0 ± 100	1.0(-10)	1.3
$O(^1D) + CHF_3$	HFC-23	1.9(-12)	0 ± 500	1.9(-12)	3.0
$O(^1D) + CH_2F_2$	HFC-32	5.0(-11)	0 ± 100	5.0(-11)	2.0
$O(^1D) + CH_3F$	HFC-41	1.0(-10)	0 ± 100	1.0(-10)	2.0
$O(^1D) + CHCl_2CF_3$	HCFC-123	2.3(-10)	0 ± 100	2.3(-10)	2.0
$O(^1D) + CHFClCF_3$	HCFC-124	1.0(-10)	0 ± 100	1.0(-10)	3.0
$O(^1D) + CHF_2CF_3$	HFC-125	5.0(-11)	0 ± 100	5.0(-11)	2.0
$O(^1D) + CH_2ClCF_2Cl$	HCFC-132b	1.7(-10)	0 ± 100	1.7(-10)	2.0
$O(^1D) + CH_2ClCF_3$	HCFC-133a	1.6(-10)	0 ± 100	1.6(-10)	2.0
$O(^1D) + CH_2FCF_3$	HFC-134a	5.0(-11)	0 ± 100	5.0(-11)	3.0
$O(^1D) + CH_3CFCl_2$	HCFC-141b	1.5(-10)	0 ± 100	1.5(-10)	3.0
$O(^1D) + CH_3CF_2Cl$	HCFC-142b	1.4(-10)	0 ± 100	1.4(-10)	2.0
$O(^1D) + CH_3CF_3$	HFC-143a	6.0(-11)	0 ± 100	6.0(-11)	2.0
$O(^1D) + CH_3CHF_2$	HFC-152a	1.0(-10)	0 ± 100	1.0(-10)	3.0

1 units are cm^3 molecule^{-1} s^{-1}
2 units are K

IV. ABSORPTION CROSS SECTIONS

Review of Ultraviolet Absorption Cross Sections of a Series of Alternative Fluorocarbons
by M. J. Molina

Solar photolysis is likely to contribute significantly to the stratospheric destruction of those alternative fluorocarbons (HFCs) which have two or more chlorine atoms bonded to the same carbon atom. Two of the eight HFCs considered in this review fall into this category, namely HFC-123 and HFC-141b. For these two species there is good agreement among the various measurements of the ultraviolet cross sections in the wavelength region which is important for atmospheric photodissociation, that is, around 200 nm. There is also good agreement for HFC-124, HFC-22 and HFC 142b; these are the three species which contain one chlorine atom per molecule. The agreement in the measurements is poor for the other species, i.e. those that do not contain chlorine, except in so far as to corroborate that solar photolysis should be negligible relative to destruction by hydroxyl radicals.

V. TROPOSPHERIC OH AND HCFC/HFC LIFETIMES

The Tropospheric Lifetimes of Halocarbons and their Reactions with OH Radicals: An Assessment Based on the Concentration of ^{14}CO
by R.G. Derwent and A. Volz-Thomas

Tropospheric Hydroxyl Concentrations and the Lifetimes of Hydrochlorofluorocarbons (HCFCs)
by M.J. Prather

The atmospheric lifetime of HCFCs is determined predominantly by reaction with tropospheric OH. Stratospheric loss is secondary and may contribute at most 10% of the total budget.

The lifetimes of HCFCs are determined here by three separate approaches:

(1)   2-D chemical transport model with semi-empirical fit to ^{14}CO;
(2)   photochemical calculation of 3-D OH fields and integrated loss;
(3)   scaling of the inferred $CH_3 CCl_3$ lifetime by rate coefficients.

Resulting lifetimes from all three independent approaches generally agree within 15%, as shown in the table below. The integrated losses calculated from the global OH fields in the models (1 & 2) are constrained by modelling of the observations and budgets for ^{14}CO and CH_3CCl_3 (respectively). Method (3) may be expressed simply as

lifetime (HCFC) = 6.3 yr x k($CH_3 CCl_3$ at 277 K) / k(HCFC at 277 K),

where the current estimate of the lifetime for methyl chloroform (6.3 yr) is based on the ALE/GAGE analysis (Prinn et al., 1987). Some of the errors associated with this scaling have been tested with the 3-D OH fields from method (2); method (3) should be reliable for calculating HCFC lifetimes in the range 1 to 30 years.

The calculated local concentrations of OH in these models (1 & 2) are not well tested since there are few observations of OH with which to compare. Based on method (2), the middle tropical troposphere (2-6 km) dominates the atmospheric loss and would be an important region in which to make observations of OH.

Estimated uncertainties in the HCFC lifetimes between 1 and 30 years are ± 50% for (1) and ± 40% for (2) & (3). Global OH values that give lifetimes outside of these ranges of uncertainty are inconsistent with detailed analyses of the observed distributions for ^{14}CO and CH_3CCl_3. The expected spatial and seasonal variations in the global distribution of HCFCs with lifetimes of 1 to 30 yr have been examined with methods (1) & (2) and found to have insignificant effect on the calculated lifetimes. Larger uncertainties apply to gases with lifetimes shorter than one year; however, for these species our concern is for destruction on a regional scale rather than global accumulation.

Future changes in the oxidative capacity of the troposphere, due to changing atmospheric composition, will affect HCFC lifetimes and introduce additional uncertainties of order ± 20%.

Atmospheric Lifetimes for HCFCs

HCFC	k (cm^3 molec^{-1} s^{-1})		lifetime (yr) for method*		
			(1)	(2)	(3)
CH_3CCl_3	5.0×10^{-13}	exp(-1800/T)	5	5.4	6.3
(range)			(3-7)	(4-7)	(5.4-7.5)
CH_3F	5.4×10^{-12}	exp(-1700/T)	3.3	3.8	4.1
CH_2F_2	2.5×10^{-12}	exp(-1650/T)	6.0	6.8	7.3
CHF_3	7.4×10^{-13}	exp(-2350/T)	635.	289.	310.
CH_2FCl	3.0×10^{-12}	exp(-1250/T)	1.26	1.33	1.44
$CHFCl_2$	1.2×10^{-12}	exp(-1100/T)	1.80	1.89	2.10
CHF_2Cl (22)	1.2×10^{-12}	exp(-1650/T)	13.0	14.2	15.3
CH_3CH_2F	1.3×10^{-11}	exp(-1200/T)	0.31	0.25	0.28
CH_2FCH_2F (152a)	1.7×10^{-11}	exp(-1500/T)	0.60	0.58	0.63
CH_3CHF_2	1.5×10^{-12}	exp(-1100/T)	1.46	1.53	1.68
CH_2FCHF_2	2.8×10^{-12}	exp(-1500/T)	3.2	3.5	3.8
CH_3CF_3	2.6×10^{-13}	exp(-1500/T)	40.	38.	41.
CHF_2CHF_2	8.7×10^{-13}	exp(-1500/T)	10.4	11.4	12.3
CH_2FCF_3 (134a)	1.7×10^{-12}	exp(-1750/T)	13.1	14.4	15.5
CHF_2CF_3 (125)	3.8×10^{-13}	exp(-1500/T)	24.9	26.1	28.1
CH_3CFCl_2 (141b)	2.7×10^{-13}	exp(-1050/T)	6.7	6.7	7.8
CH_3CF_2Cl (142b)	9.6×10^{-13}	exp(-1650/T)	16.6	17.8	19.1
CH_2ClCF_2Cl	3.6×10^{-12}	exp(-1600/T)	3.5	4.0	4.2
CH_2ClCF_3	5.2×10^{-13}	exp(-1100/T)	4.1	4.4	4.8
$CHCl_2CF_3$ (123)	6.4×10^{-13}	exp(-850/T)	1.40	1.42	1.59
$CHFClCF_3$ (124)	6.6×10^{-13}	exp(-1250/T)	5.5	6.0	6.6

*Lifetimes from method (1) do not include stratospheric loss; those from method (2) include small additional stratospheric loss. Method (3) is based on scaling the methylchloroform lifetime of 6.3 yrs from Prinn et al. (Science, 238, 945-950, 1988) by the ratio of the rate coefficients at 277 K.

VI. DEGRADATION MECHANISMS

Tropospheric Reactions of the Haloalkyl Radicals Formed from Hydroxyl
Radical Reaction with a Series of Alternative Fluorocarbons
by R. Atkinson

Degradation Mechanisms of Selected Hydrochlorofluorocarbons in the
Atmosphere: An Assessment of Current Knowledge
by R. A.Cox and R. Lesclaux

An Assessment of Potential Degradation Products in the Gas-Phase
Reactions of Alternative Fluorocarbons in the Troposphere
by H. Niki

Atmospheric Degradation Mechanisms of Hydrogen Containing
Chlorofluorocarbons (HCFCs) and Fluorocarbons (HFCs)
by R. Zellner

Tropospheric reaction with the OH radical is the major and rate determining loss process for the HFCs and HCFCs in the atmosphere.

There are virtually no experimental data available concerning the subsequent reactions occurring in the atmospheric degradation of these molecules. By consideration of data for degradation of alkanes and chloroalkanes it is possible to postulate the reaction mechanisms and products formed in the troposphere from HCFCs and HFCs. However, the results are subject to large qualitative and quantitative uncertainty, and may even be incorrect.

The current level of support for laboratory work is inadequate to enable significant improvement in the state of knowledge in this area in the near future.

Using the above mentioned analysis, a large variety of chlorine and fluorine containing intermediate products such as hydroperoxides, peroxynitrates, carbonyl halides, aldehydes and acids can be expected from the degradation of the 8 proposed CFC substitutes. These are listed in the accompanying table.

Based on the available knowledge of gas phase chemistry only four of these products appear to be potentially significant carriers of chlorine to the stratosphere. These are $CClFO$, CF_3CClO, $CClF_2CO_3NO_2$ and $CCl_2FCO_3NO_2$. However physical renewal processes may reduce this potential. In addition, the possibility of pathways and products not predicted by the arguments-by-analogy are a cause for concern.

A large part of the uncertainty of the mechanistic details of the HCFC oxidation arises from all insufficient knowledge of the thermal stability and reactivity of halogenated alkoxyradicals. In particular, the mechanism of oxidation of the CF_3O radical, which is assumed to produce CF_2O, is not known for atmospheric conditions and needs further study.

Particular attention should be paid to obtaining data on the photochemistry, gas phase reactivity and solubility of the carbonyl, acetyl and formyl halides, in order to assess their removal rates and mechanisms.

42

Based on current knowledge, the products identified are unlikely to cause significant changes to the effective greenhouse warming potential of the 8 proposed CFC substitutes. This conclusion would be modified if long-lived products such as CF_3H were formed by unidentified pathways.

Laboratory tests and atmospheric measurements are urgently needed to test the validity of the proposed degradation mechanisms for HCFCs and HCFs.

Fluorine-containing products in the atmospheric degradation of selected fluorocarbons.

Compound	Formula	Atom & Radical	Carbonyl	Acid	Hydroxide	Nitrate
HCFC 123	$HCCl_2CF_3$	CF_3CCl_2OO CF_3CCl_2O CF_3OO CF_3O	CF_3CClO		CF_3CCl_2OOH CF_3OOH CF_3OH	$CF_3CCl_2OONO_2$ CF_3OONO_2 CF_3ONO_2
HCFC 141B	CCl_2FCH_3	CCl_2FCH_2OO CCl_2FCH_2O CCl_2FOO CCl_2FO $CCl_2FC(O)OO$	CCl_2FCHO $CClFO$	 $CCl_2FC(O)OOH$ $CCl_2FC(O)OH$	CCl_2FCH_2OOH CCl_2FOOH	$CCl_2FCH_2OONO_2$ CCl_2FOONO_2 $CCl_2FC(O)OONO_2$
HCFC 142b	$CClF_2CH_3$	$CClF_2CH_2OO$ $CClF_2CH_2O$ $CClF_2OO$ $CClF_2O$ $CClF_2C(O)OO$	$CClF_2CHO$ CF_2O	 $CClF_2(O)OOH$ $CClF_2C(O)OH$	$CClF_2CH_2OOH$ $CClF_2OOH$	$CClF_2CH_2OONO_2$ $CClF_2OONO_2$ $CClF_2C(O)OONO_2$
HCFC 22	$CHClF_2$	$CClF_2OO$ $CClF_2O$	CF_2O		$CClF_2OOH$	$CClF_2OONO_2$
HCFC 124	$CHClFCF_3$	$CF_3CClFOO$ CF_3CClFO CF_3OO CF_3O	CF_3CFO		$CF_3CClFOOH$ CF_3OOH CF_3OH	$CF_3CClFOONO_2$ CF_3OONO_2 CF_3ONO_2
HCF 134a	CH_2FCF_3	CF_3CHFOO CF_3CHFO CF_3OO CF_3O CFO	$CHFO$ CF_3CHFO		$CF_3CHFOOH$ CF_3OOH CF_3OH $CF(O)OOH$	$CF_3CHFOONO_2$ CF_3OONO_2 CF_3ONO_2 $CF(O)OONO_2$
HFC 52a	CHF_2CH_3	CH_3CF_2Oo CH_3CF_2O CHF_2CH_2OO CHF_2CH_2O CHF_2OO CHF_2O $CHF_2C(O)OO$ CFO	CF_2O CHF_2CHO $CHFO$	 $CHF_2C(O)OOH$ $CHF_2C(O)OH$ $CF(O)OOH$	CH_3CF_2OOH CHF_2CH_2OOH CHF_2OOH	$CH_3CF_2OONO_2$ $CHF_2CH_2OONO_2$ CHF_2OONO_2 $CHF_2C(O)OONO_2$ $CF(O)OONO_2$
HCF 125	CHF_2CF_3	CF_3CF_2OO CF_3CF_2O CF_3OO CF_3O	CF_2O CF_3CFO		CF_3CF_2OOH CF_3OOH CF_3OH	$CF_3CF_2OONO_2$ CF_3OONO_2 CF_3ONO_2

VII. LIQUID PHASE PROCESSES

Possible Atmospheric Lifetimes and Chemical Reaction Mechanisms for
Selected HCFCs, HFCs, CH$_3$CCl$_3$, and their Degradation Products
Against Dissolution and/or Degradation in Seawater and Cloudwater
by P.H. Wine and W.L. Chameides

The rates at which eight potential alternative HCFCs and HFCs and methyl chloroform (CH$_3$CCl$_3$) can be removed from the atmosphere by dissolution and reaction in the oceans and in cloudwater have been estimated from the species' thermodynamic and chemical properties using simple mathematical formulations to simulate the transfer of gases from the atmosphere to the aqueous phase. The HCFCs and HFCs considered are CHCl$_2$CF$_3$ (HCFC-123), CFCl$_2$CH$_3$, (HCFC-141b), CF$_2$ClCH3 (HCFC-142b), CHF$_2$Cl (HCFC-22), CHFClCF$_3$, (HCFC-124), CH$_2$FCF$_3$ (HFC-134a), CHF$_2$CH$_3$ (HFC-152a), and CHF$_2$CF$_3$ (HFC-125).

Cloudwater is found to be of no importance as an atmospheric sink for any of the above compounds. Best-estimate lifetimes for all eight HCFCs and HFCs toward removal in the oceans are greater than 77 years, with only HCFC-22, HCFC-123, and HCFC-141b having lifetimes shorter than 200 years. The most reactive of the nine species considered toward removal in the oceans is methyl chloroform with a best-estimated lifetime of 42 years and a minimum reasonable lifetime of 22 years. Important removal mechanisms for methyl chloroform, HCFC-22, HCFC-123, and HCFC-141b in seawater are hydrolysis and reaction with hydrated electrons. Improved hydrolysis kinetics data and Henry's law solubility data for methyl chloroform HCFC-22, HCFC-123, and HCFC-141b in seawater are hydrolysis and reaction with hydrated electrons. Improved hydrolysis kinetics data and Henry's law solubility data for methyl chloroform, HCFC-22, HCFC-123, and HCFC-141b would help to reduce the uncertainties in the aqueous phase removal rates of these species, as would improved estimates of the hydrated electron concentration in water.

Gas phase degradation products of the eight HCFCs and HFCs include a large variety of halo-substituted carbonyls, acids, peroxyacids, hydroperoxides, alcohols, nitrates, peroxynitrates, and peroxyacetylnitrates. Although handicapped by the total absence of Henry's law solubility data for any of the compounds of interest and the limited availability of relevant kinetic data, an assessment of the rates and mechanisms of aqueous phase removal of the gas phase degradation products has been carried out.

The species X$_2$CO, HXCO, CH$_3$CXO, CF$_3$OH, CX$_3$OONO$_2$ and ROOH (X = F or Cl, R = halosubstituted methyl or acetyl) are all expected to be removed from the atmosphere on time scales limited by transport to cloudy regions or the marine boundary layer (i.e. about 1 month); aqueous phase reactions of these species result in the formation of chloride, fluoride, and carbon dioxide, as well as formic, acetic, and oxalic acids. The species CX$_3$CXO, CX$_3$CX$_2$OOH, CX$_3$CX$_2$OONO$_2$, CX$_3$C(O)OONO$_2$, and CX$_3$C(O)OOH are also expected to be removed from the atmosphere rapidly, and their aqueous phase reactions result in the formation of halo-substituted acetates, CX$_3$C(O)O$^-$.

The species CX$_3$C(O)OH are very acidic and, as a result, are highly soluble in cloudwater. These acids are expected to be rapidly removed from the atmosphere by rainout. However, the aqueous phase species CX$_3$C(O)O$^-$ are expected to be resistant to chemical degradation. Trichloroacetate can thermally decompose on a time scale of 2-10 years to yield carbon dioxide and chloroform. In fresh water, the reaction of CCl$_3$C(O)O$^-$, with the hydrated electron is also expected to occur on a time scale of a few years. The species CFCl$_2$C(O)O$^-$, CF$_2$ClC(O)O$^-$ and

$CF_3C(O)O^-$ may have very long aqueous phase lifetimes. The longest lived species, $CF_3C(O)O^-$, could have a lifetime in natural waters as long as several hundred years. Processes which could possibly degrade $CF_nCl_{3-n}C(O)O^-$ on shorter times scales than suggested above, but whose rates cannot be estimated with any degree of confidence at this time, include oxidation by photochemically generated valence band holes in semiconductor particles and hydrolysis catalyzed by enzymes in microorganisms and plants; further research aimed at characterizing these processes is needed.

One possible gas phase degradation product about very little is known is CF_3ONO_2. This compound has never been observed, and may be thermally unstable. If CF_3ONO_2 is thermally stable, then it may have a long lifetime toward aqueous phase removal. Henry's law solubility data and hydrolysis kinetics data for CF_3ONO_2 are needed before its aqueous phase removal rate can be assessed with any degree of confidence

VIII. OZONE DEPLETION POTENTIALS

Relative Effects on Stratospheric Ozone of Halogenated Methanes and
Ethanes of Social and Industrial Interest
by D.A. Fisher, C.H.Hales, D.L. Filkin, M.K.W. Ko, N.D. Sze, P.S. Connell,
D.J. Wuebbles, I. S. A. Isaksen, and F. Stordal

Ozone Depletion Potentials (ODPs) have been defined and calculated in order to allow estimates of the relative effects of halocarbons on stratospheric ozone. Models using representations of homogeneous atmospheric chemical processes have estimated relative effects on global ozone. These estimates indicate that the ODPs of the hydrohalocarbons are generally one-tenth or less those of the CFC-11 and -12. The reduction in ODP that might be expected due to replacement of uses of a CFC by a hydrohalocarbon can be estimated by taking the ratio of the ODP of the hydrohalocarbon to the ODP of the CFC it might replace. For example, the reduction in ODP in replacing uses of CFC-12 by HCFC-22 is $(0.049 \pm .015)/(.93) = .053 \pm .015$. Of course, the relative quantities of the compound required in the use application must also be taken into account.

Although the values of ODPs reported here agree reasonably well among models, uncertainties in the values still exist due to the uncertainties in modeled chemistry and dynamics. Since reaction with OH dominates the chemistry of the HCFCs, uncertainties in the model calculated OH values remain a major source of uncertainty for both lifetimes and ODPs of these compounds. Uncertainties for some compounds may be reduced with new laboratory data on the ultraviolet absorption properties and the rate constants with hydroxyl for the HCFCs and HFCs.

Sensitivity analyses reveal that the global ODP values are affected to only a minor degree by the levels of N_2O, CH_4, CO_2, CO, and Brx used in model calculations. Latitudinal relative effects on ozone depletion depend on the species — species with high altitude sinks show more latitudinal dependency than CFC-11. Those species destroyed in the lower stratosphere have latitudinal effects equivalent to CFC-11. Seasonal variation of relative ozone depletions are second order.

Another major uncertainty centers on the potential effects of heterogeneous chemistry in the lower stratosphere, particularly near the poles in winter-time. While these effects are believed to cause the Antarctic springtime ozone decreases, they are not included in any of the model

45

calculations of ODPs. Due to the cold stratospheric temperatures, polar stratospheric clouds become activation sites for chlorine compounds (by-products from the decomposition of the chlorocarbons) resulting in increased chlorine catalytic loss for ozone. Since ODP is defined relative to CFC-11, the effect of including heterogeneous chemistry will have little effect on the local ODP value compared to values determined assuming only homogeneous chemistry. However, polar contribution to global ozone loss would be greater such that global ODP values would be more heavily weighted by the polar values. Thus, species with large, positive latitudinal gradients in ODP would have global ODPs that are fractionally increased. On the other hand, inclusion of stronger polar dynamics would affect both the transport and the distribution of chlorine species and would directly impact both the local and global ODP values.

Upper bounds are placed on the local effects by a chlorine loading potential, i.e., the relative amount of chlorine added to the stratosphere by a given gas. A less conservative estimate derived from the relative values of Cly in the lower polar stratosphere in spring indicates that the potential effect can be substantially less than the Chlorine Loading Potential but would be above the homogeneous chemistry ODP value. The geographic extent of the heterogeneous effect on global ODP outside of the polar vortex is impossible to estimate at the present time.

Time-dependent Relative Ozone Depletions and Relative Chlorine Loading for HCFCs have values above the ODP and CLP values derived from steady-state calculations. For longer lived CFCs, the time-dependent values are always less than the ODP and CLP values.

Range of Ozone Depletion Potentials (ODP) determined by 1-D and 2-D models, assuming scaling for HCFC ODPs by CH_3CCl_3 observed lifetime (6.3 years).

Species	1-D Models*	2-D Models**
CFC-11	1.0	1.0
CFC-12	0.9-1.0	0.9
CFC-113	0.8-0.9	0.8-0.9
CFC-114	0.6-0.8	0.6-0.8
CFC-115	0.4-0.5	0.3-0.4
HCFC-22	0.4-0.05	0.04-0.06
HCFC-123	0.013-0.016	0.013-0.022
HCFC-124	0.016-0.018	0.017-0.024
HFC-125	0	0
HFC-134a	0	0
HCFC-141b	0.07-0.08	0.09-0.11
HCFC-142b	0.05-0.06	0.05-0.06
HFC-134a	0	0
HFC-152a	0	0
CCl_4	1.0-1.2	1.0-1.2
CH_3CCl_3	0.10-0.12	0.13-0.16

*   1-D models from AER, LLNL and DuPont.
** 2-D models from AER, LLNL, University of Oslo, and DuPont.

IX. HALOCARBON GLOBAL WARMING POTENTIALS

Relative Effects on Global Warming of Halogenated Methanes and Ethanes
of Social and Industrial Interest
by D.A. Fisher, C. H. Hales,
Wei-Chyung Wang, M.K.W. Ko and N.D. Sze

Halocarbon Global Warming Potentials have been defined and calculated in order to allow estimates of the relative environmental effects of halocarbons to be made. The results presented here indicate that the HGWPs of the hydrohalocarbons depend primarily on the atmospheric lifetime of the compounds and to a lesser degree on the molecular IR absorption characteristics.

The reduction in HGWP that might be expected due to use replacement of a CFC by a hydrohalocarbon can be estimated by taking the ratio of the HGWP of the hydrohalocarbon to the HGWP of the CFC it would replace. For example, the reduction in HGWP in replacing uses of CFC-12 by HCFC-134a is $(0.26 \pm .010)/(3.05) = 0.085 \pm 0.003$. Of course, the relative quantities of the compound required in the use application must also be taken into account.

Although the HGWP values reported here agree between models reasonably well once accounting is made for the differences in lifetimes, uncertainties in the values still exist due to the uncertainties in modeled chemistry and dynamics and their direct effect on the chemical lifetimes of these compounds. We expect that these values will be updated once better data is available for the ultraviolet reactions and the hydroxyl radical reactions with the respective compounds.

The HGWP values appear to be reasonably robust parameters since their calculated values are nearly insensitive to assumed values of other radiative gases. The minor shifting of the HGWP values in primarily influenced by the changes in calculated lifetimes and therefore the abundance in the atmosphere.

Calculated time-dependent relative global warmings for halocarbons are initially on order unity but decrease or increase depending on whether their lifetimes are shorter than that of the reference gas. At longer times, the Relative Global Warmings asymptotically approach the HGWP values.

X. IMPACT ON PHOTOCHEMICAL OXIDANTS INCLUDING TROPOSPHERIC OZONE

An Assessment of Potential Impact of Alternative Fluorocarbons on
Tropospheric Ozone
by H. Niki

One type of tropospheric impact of the alternative halocarbons may arise from their possible contribution as precursors to the formation of O_3 and other oxidants on urban and global scales. In the present assessment the following specific issues related to tropospheric oxidants are addressed:

1.	Is it likely that the HFCs and HCFCs would contribute to production of photochemical oxidants in the vicinity of release?

2. On a global basis, how would emissions of HCFCs and HCFs compare to natural sources of O_3 precursors?

Since almost all CFCs are emitted in urban environments, the first question deals primarily with urban "smog" formation. Salient features of chemical relationships between oxidants and their precursors as well as the relevant terminologies are described briefly in order to provide a framework for the discussion of these two issues.

Based on an analysis of the atmospheric concentrations of various O_3 precursors, and their atmospheric reactivity and O_3 forming potential, the maximum projected contributions of the alternative fluorocarbons to O_3 production in both urban and global atmospheres have been derived as follows:

1: Urban Atmosphere (values in parenthesis in units of $10^{-3}\%$ of the total contribution of all O_3 precursors):

HFCs: CH_3CHF_2-152a (59), CH_2FCF_3-134a (8), CHF_2CF_3-125 (4)

HCFCs: $CHClF_2$-22 (8), CH_3CClF_2-142b (6), CH_3CHClF-124 (16),

CH_3CCl_2F-141b (13), $CHClCF_3$-123 (59)

2: Global Atmosphere (values in parenthesis in units of $10^{-3}\%$ of the total contribution of all O_3 precursors):

HFCs: CH_3CHF_2-152a (92), CH_2FCF_3-134a (11), CHF_2CF_3-125 (7)

HCFCs: $CHClF_2$-22 (11), CH_3CClF_2-142b (10), CH_3CHClF-124 (25),

CH_3CCl_2F-141b (20), $CHClCF_3$-123 (92)

XI. NATURAL SOURCES

Natural Chlorine and Fluorine in the Atmosphere, Water and Precipitation
by J.P. Friend

The geochemical cycles of chlorine and fluorine are surveyed and summarized as framework for the understanding of the global natural abundances of these species in the atmosphere, water and precipitation. In the cycles the fluxes into and out of the atmosphere can be balanced within the limits of our knowledge of the natural sources and sinks. Sea salt from the ocean surfaces represent the predominant portion of the source of chlorine. It is also an important source of atmospheric fluorine, but volcanos are likely to be more important fluorine sources. Dry deposition or sea salt returns about 85% of the salt released there. Precipitation removes the remainder. Most of the sea salt material is considered to be cyclic, moving through sea spray over the oceans and either directly back to the oceans (about 90%) or deposited dry and in precipitation on land (about 10%), whence it runs off into rivers and streams and returns to the oceans. Most of the natural chlorine in the atmosphere is in the form of particulate chloride ion with lesser amounts as gaseous inorganic chloride (most likely HlC) and methyl chloride vapor. Fluorine is emitted

48

from volcanos primarily as HF. It is possible that HF may be released directly from the ocean surface but this has not been confirmed by observation. HCl and most likely HF gases are released into the atmosphere by sea salt aerosols. The mechanism for the release is likely to be the provision of protons from the so-called excess sulfate (that which results from the oxidation of SO_2) and HNO_3. Sea salt aerosol contains fluorine as F^-, MgF^+ and CaF^+ and NaF. The concentrations of the various species of chlorine and fluorine that characterize primarily natural, unpolluted atmospheres are summarized in tables and are discussed in relation to their fluxes through the geochemical cycle.

XII. BIOLOGICAL AND HEALTH EFFECTS

Toxicology of Atmosphere of Atmospheric Degradation Products of Selected
Hydrochlorofluorocarbons
by L.S. Kaminsky

Assessment of Effects on Vegetation of Degradation Products from
Alternative Fluorocarbons
by D.C. McCune and L.H. Weinstein

There is a need for more information on exposure, especially to organic breakdown products. This should include estimates of ground level concentrations, modes of deposition (wet and dry) and should extend to identification of half-lives in soil and water, and the products of microbial transformation.

Nothing is known of the toxicology to humans, animals or plants of any of the organic breakdown products other than trifluoroacetic acid. It was considered dubious to extrapolate from analogous compounds (e.g. trichloroacetic acid). The limited work on toxicology of TFA was with very high concentrations compared with those potentially arising from HCFCs and CFCs. Studies should aim to determine the long-term threshold level for toxicological effects.

One of the major uncertainties is the fate of $-CF_3$ as there is conflict of opinion about the stability of the C-F bond. The biological evidence (from toxicology and pesticide biochemistry) indicates that $-CF_3$, is recalcitrant and may persist in the environment but an opinion was expressed that there may be significant chemical defluorination at room temperature. Because of the mammalian toxicity of monofluoroacetate, the possibility of defluorination of trifluoro- to monofluoro- needs to be firmly clarified.

In contrast with position regards organic products, and notwithstanding uncertainties about rates of deposition, it can be stated with a high degree of confidence that inorganic fluoride (HF) does not present a significant risk to human, animals, plants, or soil.

Likewise HCl is of no direct risk to humans, animals or plants. Acidity from inorganic acids or as a result of mineralization of organic products does not add any significant burden to the environment in the form of acid deposition.

SECTION C

Transient Scenarios for Atmospheric Chlorine and Bromine

Michael J. Prather and Robert T. Watson
NASA Headquarters, Code SEU, Washington, DC 20546

1.0 INTRODUCTION

The rise in atmospheric chlorine levels due to the industrial production and emission of chlorofluorocarbons (CFCs) and other halocarbons is now believed to be the cause of the dramatic appearance of the Antarctic ozone hole in the late 1970s. Further increases in the chlorine and bromine content of the stratosphere are inevitable over the next decade, and the consequences for ozone abundances over the Antarctic, Arctic and the globe are uncertain. Only stringent controls over the production of chlorine-containing hydrocarbons will enable our atmosphere to return to chlorine abundances prevalent prior to the occurrence of the ozone hole, about 2 ppb (parts per billion = molecules per 10^9 molecules of air).

Bromine in the stratosphere, present at concentrations of about 0.02 ppb, also contributes globally to ozone loss. The role of bromine, as BrO, in formation of the Antarctic ozone hole has been demonstrated but not yet been fully quantified. Catalytic cycles involving BrO and ClO are greatly enhanced in the Antarctic ozone hole relative to the rest of the stratosphere. During the austral spring of 1987, bromine is estimated to be responsible for 10 to 30% of the ozone depletion with chlorine alone responsible for the majority.

A sensitivity study of chlorine-loading scenarios is presented for a range of global emissions for compounds currently regulated under the Montreal Protocol (CFC-11 = $CFCl_3$, CFC-12 = CF_2Cl_2, CFC-113 = $CF_2ClCFCl_2$, CFC-114 = CF_2ClCF_2Cl, CFC-115 = CF_3CF_2Cl), for other gases not specified in the Montreal Protocol (carbon tetrachloride = CCl_4, methyl chloroform = CH_3CCl_3, HCFC-22 = CHF_2Cl), and for possible new hydro-halocarbon substitutes (HCFCs). A subset of these scenarios is also shown for atmospheric bromine loading, being driven by the increases in the halons listed under the Montreal Protocol (CF_3Br, CF_2ClBr, $C_2F_4Br_2$) with fixed levels of CH_3Br.

After complete cessation of all halocarbon emissions, the decline in atmospheric chlorine levels below 2 ppb is determined by the decay of the long-lived CFCs produced prior to the phaseout and would not occur until the latter half of the 21st century. We show here that the use of short-lived HCFC substitutes would not significantly affect this time scale if the substitutes were eliminated sometime between 2030 and 2050, depending on the lifetime of the substitute. The elimination of the Antarctic ozone hole sometime in the future relies predominantly on reducing chlorine levels to 2 ppb or less, but will also depend in part on the local meteorology and changes in other trace gases such as methane.

The maximum concentration of atmospheric chlorine that will be reached in the next several decades is controlled by the amount of chlorine-containing halocarbons (CFCs, CCl_4, CH_3CCl_3, and HCFC-22) added to the atmosphere thus far, and by the amount that will be produced and eventually released to the atmosphere prior to a complete phaseout. The scenarios shown here demonstrate the obvious result that the key factor in reducing the peak chlorine loading is the rapid cutback in CFC emissions. They also show the less evident result that substitution of modest amounts of short-lived HCFCs for the CFCs will not increase the maximum chlorine levels.

Largest ozone depletions in the future are expected to coincide with the peak chlorine loading of the atmosphere. Global-scale losses, largest in the upper stratosphere, are predicted from the gas-phase chemical reactions of chlorine monoxide with atomic oxygen. Ozone depletion throughout the stratosphere in the southern mid-latitudes may become more extensive if the Antarctic ozone hole enlarges. Over Antarctica, and possibly in the Arctic, losses are driven by chlorine-catalyzed destruction of ozone following heterogeneous reactions on polar stratospheric clouds in winter. The rapid appearance of the ozone hole over the last decade demonstrates the extremely non-linear response of polar ozone to increasing chlorine levels. We must be prepared for new thresholds of accelerated ozone loss in the Arctic as chlorine concentrations continue to rise above the current (record) levels of about 3 ppb.

2.0 CHLORINE LOADING AND ODPs

The atmospheric chlorine loading is calculated here as the instantaneous, bulk tropospheric mixing ratio (ppb) of chlorine atoms in the form of all the halocarbons noted above, plus the natural source CH_3Cl (0.6 ppb). This definition of chlorine loading of the atmosphere is a conservative (maximum) measure of the amount of stratospheric chlorine that may be active in catalytic ozone destruction because not all of the chlorine will be available (i.e., photochemically released from the halocarbon source gas). For the year 1985, the table below gives the relative contribution of the individual gases to the total chlorine loading (3.0 ppb). The projected chlorine loading can be used to demonstrate the contribution of individual halocarbons to overall chlorine levels as a function of time.

Atmospheric Chlorine Loading in the Year 1985

industrial sources	
CFC-11	22 %
CFC-12	25 %
CFC-113	3 %
CFC-114	<1 %
CFC-115	<1 %
HCFC-22	3 %
carbon tetrachloride	13 %
methyl chloroform	13 %
natural sources	
methyl chloride	20 %

The Ozone Depletion Potential (ODP) of a halocarbon is calculated with a chemical model for stratospheric ozone, assuming that the gas is in steady state between emissions and atmospheric loss. For most CFCs the time to approach within 10% of steady-state conditions is more than a century. The ODP of a halocarbon is defined relative to CFC-11 (dimensionless) rather than in absolute units (e.g., % ozone loss per kg of gas emitted). Greenhouse Warming Potentials (GWP) are calculated similarly with a model for steady-state climate change. ODPs (or GWPs) therefore reflect the relative chronic ozone destruction (or warming potential) of CFCs after nearly constant emissions for a century. Transient ozone depletion potentials have also been used, but they do not clearly reflect the contribution of different halocarbons to the amount of chlorine in the atmosphere over the next century.

Even in the limit of steady state, the relative chlorine loading of a halocarbon can differ from its ODP because the calculation of an ODP includes the effectiveness of the gas in releasing its chlorine within the stratosphere. Most of the chlorine atoms in CFC-11 are released by photolysis in the lower stratosphere and thus are available to participate in the catalytic destruction

of ozone at all altitudes in the stratosphere. Other CFCs, such as CFC-12 and HCFC-22, are more slowly photolyzed; in the lower stratosphere much of their chlorine is retained in the halocarbon; and most of their chlorine atoms are available only in the upper stratosphere or in the winter polar stratosphere. (Air in the winter polar stratosphere appears to be photochemically aged, having descended from the upper stratosphere.) For such compounds, the model derived ODPs (relative to CFC-11) will be less than the relative chlorine loading in these scenarios. A warning about the accuracy of ODP calculations must be made: the current assessment models are limited to gas-phase chemistry and predict future ozone depletion predominantly in the middle stratosphere; they do not predict the Antarctic ozone hole or the possibility of similar heterogeneously driven ozone loss in the Arctic lower stratosphere.

The following scenarios were constructed as a sensitivity study to examine several possible approaches to limiting atmospheric chlorine content. The scenarios for the halocarbon source gases are similar, but not identical, to those used to calculate ozone depletion by the UNEP/WMO assessment. Two particular differences are that the lifetime of HCFC-22 is assumed here to be 15 years (rather than 20 years) based on more recent analyses of HCFC lifetimes, and that the assumed CFC cutback in emissions occurs entirely at the end of a given year rather than being phased in over 5 years from 1996 to 2000.

3.0 THE MODEL FOR CHLORINE/BROMINE LOADING

The data for halocarbons used in the model for chlorine and bromine loading are based on compilations from the recent ozone assessment (UNEP/WMO, 1990) and the workshop on alternative fluorocarbons (AFEAS, 1990). The data and method of calculating the mean abundance of the halocarbons are given in Table 1. The atmospheric lifetimes in Table 1 are taken from these recent reports and have an estimated uncertainty of 25 %. Lifetimes for those species destroyed predominantly in the troposphere (CH_3CCl_3 and HCFC-22) are based on the AFEAS review. The fluxes in Table 1 (1 kt/yr = 1,000 metric tons per yr) are based on estimates of production in the year 1985 and total 1,000,000 metric tons for CFCs alone. Growth in production from 1985 through 1990 (kt/yr per yr) is assumed to be 4 %/yr for all industrial halocarbons; such increases are consistent with growth in the production of CFC-11 and CFC-12, compounds for which we have reliable estimates. The initial concentrations in 1985 (parts per trillion $=1/10^{12}$) represent a tropospheric average based on available observations (IOTP, 1990). The factor (kt/ppt) used to convert mixing ratio (ppt) to total abundance (kt) assumes the compound is well mixed throughout 95 % of the atmosphere.

A simple numerical model is used: for example, the concentration in 1986 is calculated by reducing the 1985 value by a factor equal to exp[-1/lifetime(yr)] and then by adding the total emissions in 1986 which have also been reduced by a factor depending on the lifetime (see notes in Table 1). Thus, concentrations refer to the end of the specified year. Fluxes of CFCs and all other chlorine- and bromine-containing species, except CH_3Cl and CH_3Br, are defined according to the scenario, and cuts are assumed to take place instantly at the end of the specified year. More accurate numerical models for the calculation of halocarbon concentrations are available. For example, such models might include the effects of the delay between production and emission of CFCs according to use, of shifts in atmospheric circulation due to climate change, or of changes in tropospheric chemistry (e.g., HCFC and CH_3CCl_3 losses) due to increasing concentrations of other gases such as methane. However, increasing the complexity of the model is not justified for this work because uncertainties (e.g., lifetimes, see Objective 7; release of chlorine in the stratosphere, see ODP discussion) overwhelm the differences between such models.

The reference scenario assumes control over atmospheric emissions of all industrial halocarbons as a group (CFCs, CCl_4, HCFC-22, CH_3CCl_3 and the halons). It begins in 1985,

53

Table 1. Halocarbon Data for Model

Halocarbon		Lifetime (yr)	Flux (kt yr^{-1})	Growth (kt yr^{-1}yr^{-1})	Concen-tration (ppt)	Factor (kt ppt^{-1})
CFC-11	CFCl$_3$	60	360	14.4	220	23.2
CFC-12	CF$_2$Cl$_2$	120	450	18.0	375	20.4
CFC-113	C$_2$F$_3$Cl$_3$	90	165	6.6	30	31.6
CFC-114	C$_2$F$_4$Cl$_2$	200	15	0.6	5	28.9
CFC-115	C$_2$F$_5$Cl	400	10	0.4	4	26.1
Carbon tetrachloride	CCl$_4$	50	80	3.2	100	25.9
HCFC-22	CHF$_2$Cl	15	140	5.6	80	14.6
methylchloroform	CH$_3$CCl$_3$	6	600	24.0	130	22.4
methylchloride	CH$_3$Cl	1.5			600	
(sub. X)	C$_x$Cl	15			0	19.3
(sub. Y)	C$_x$Cl	6			0	19.3
halon-1211	CF$_2$BrCl	15	10	0.40	1.5	27.9
halon-1301	CF$_3$Br	110	9	0.36	1.7	25.1
methylbromide	CH$_3$Br	1.5			15	

Lifetime (yr) is the global abundance divided by the annual average loss rate.
Flux (kt/yr = 1,000 tons per year) equals the atmospheric emissions during 1985.
Growth (kt/yr/yr) equals the increment to the flux each year from 1986 through 1990.
Concentration (ppt = parts per trillion = 1/10^{12}) is the average (well mixed) tropospheric abundance in 1985.
Factor (kt/ppt) relates concentration (ppt) to global content (kt).
Methyl chloride and methyl bromide concentrations are fixed.
The concentration (conc) in year+1 is calculated from the equation:
    conc[year+1] = conc[year] x decay + flux[year+1] x (1-decay) x lifetime / factor
    where decay = exp(-1 / lifetime).

assumes growth for the years 1986 through 1990, freezes emissions into the atmosphere at the 1990-rate, and cuts all emissions to zero at the end of the year 2000. From then on the atmospheric abundance of chlorine or bromine is determined solely by the slow decay of gases already in the atmosphere in this reference scenario. Under the current Montreal Protocol the cutback to 50% of CFC emissions refers to 1986 production levels. Also, the earlier implementation of these reductions may result in smaller emissions during the period 1990-2000 than in this scenario.

4.0 TIME DELAYS AND BANKING OF CFCs

The absolute timing of the atmospheric response in these calculations may be imprecise not only due to the basic uncertainties in modeling atmospheric composition, but also because certain simplifying assumptions have been made. For example, stratospheric destruction of halocarbons (predominant loss for the long-lived CFCs) will lag emissions by about 2 years, the time it takes for air to travel from the upper troposphere to the middle stratosphere. This effect will be important only when tropospheric concentrations are changing rapidly and is not included here. Furthermore, the ozone depletion in response to halocarbons will also be delayed by the time for tropospheric air to circulate through the stratosphere. Air over the winter pole may represent a mix of tropospheric halocarbons from as long ago as 5 years previous.

A more important and obviously systematic omission in these calculations is the failure to simulate the delay between halocarbon production and emissions (see CMA, 1988). Depending on

use, the halocarbons produced in a given year may not be emitted into the atmosphere until several years later. For examples, CFC-11 used in blowing closed-cell insulating foams may take more than 10 years to escape into the atmosphere, and CFC-12 used in hermetically sealed refrigeration systems will not be released until the refrigerant coils break, on average 20 years later. The accumulation, or banking, of the CFCs makes it difficult to stop emissions (as in the reference scenario) immediately upon cessation of production. On the other hand, CFC-113 and CH_3CCl_3 are used primarily as cleaning agents, and their production reflects the amount lost during the cleaning process, presumably to the atmosphere. Most of the CFCs are used in products that release the gases to the atmosphere within 3 years of production. The total bank of CFCs as of 1987 in products with average retention times greater than 2 years is estimated to be less than 2 years of the annual production of all CFCs (CMA, 1988). The net effect of CFC banking may look similar to the scenario in which there is a 15-year delay in compliance with CFC cuts (Objective 4 below); however, the banking may be offset by partial cuts in CFCs before the year 2000 as already agreed upon in the current Montreal Protocol.

In spite of these uncertainties in the timing of atmospheric effects, we expect that the comparison between scenarios, such as the difference in peak chlorine loading or the variance in times to reach 2 ppb chlorine, will be accurate. These scenarios describe controls over emissions rather than production and, with this caveat, the calculations provide a useful relative measure of the potential damage to stratospheric ozone associated with each option.

5.0   SUBSTITUTION

Substitution for the phased-out halocarbons is considered in many scenarios. In such cases we assume a kg-per-kg replacement (in %) of the sum of halocarbon cuts referenced to their 1985 emission levels (1,000 kt/yr of CFCs, 80 kt/yr of CCl_4, 140 kt/yr of HCFC-22, 600 kt/yr of CH_3CCl_3). We are interested here only in substitutes containing chlorine or bromine. The chemical industry has estimated that replacement with chlorinated compounds would capture about 30% of the CFC market (350 kt/yr in 1985). Substitution for CCl_4, HCFC-22 and CH_3CCl_3--if these compounds were phased out--are likely not to involve chlorinated replacements. Hence, in the reference scenario with a complete cut in all halocarbons (1,820 kt/yr in 1985), the industry estimates would correspond to a substitution rate of about 20% in these scenarios. We have not considered the possibility of bromine-containing compounds as substitutes for the halons.

Two substitute chemicals are considered as replacements for the reductions in the industrial halocarbons (CFCs, CCl_4, HCFC-22, and CH_3CCl_3):

- compound X has a 15 year lifetime (like HCFC-22) with a single chlorine atom and a mean molecular weight of 115, corresponding to a steady-state chlorine loading factor of 0.10 relative to CFC-11;

- compound Y has a 6 year lifetime (like CH_3CCl_3) with a single chlorine atom and a mean molecular weight of 115, corresponding to a steady-state chlorine loading factor of 0.04 relative to CFC-11.

These substitutes are examples of the types of alternative halocarbons included by AFEAS (1990) in its review of alternative fluorocarbons, but do not correspond to any specific compound. Choosing substitute X to replace some of the cutbacks in CFCs, CCl_4, CH_3CCl_3, and HCFC-22, is almost equivalent to continuing, and possibly expanding, the use of HCFC-22. The chlorine loading of HCFC-22 is slightly larger, 0.13, but its ODP is currently modelled to be smaller, 0.05, as discussed above. Thus substitute X would mimic the temporal behavior of HCFC-22 with a slightly different scale factor for its emissions (in kg). Similarly, substitute Y would mimic CH_3CCl_3 but has only one chlorine.

55

6.0 OBJECTIVES

Possible environmental goals might be based on the levels of atmospheric chlorine in the past. Some key chlorine abundances to remember are: (1) the natural abundance of chlorine is 0.6 ppb; (2) chlorine levels in the Antarctic stratosphere before the ozone hole were 1.5 to 2.0 ppb; and (3) today's abundance of chlorine is about 3.0 ppb.

One could not expect the depletion of Antarctic ozone to cease much before the middle of the next century when atmospheric chlorine concentrations would reach 2 ppb or less under the most stringent controls over halocarbon emissions. In order to return to near pristine conditions below 1 ppb chlorine, however, we must wait for the longest-lived CFCs to be almost completely destroyed in the atmosphere. Even without further emissions, this condition would not be met until well into the 22nd century. Without the ozone hole, the difference between 1 and 2 ppb of chlorine is predicted to lead to small, less than 2%, changes in global column ozone (IOTP, 1990).

A number of scenarios were performed to understand what possible actions control the peak chlorine loading, the rate at which the atmospheric abundance of chlorine decreases, and the date at which the atmospheric abundance of chlorine drops below 2 ppb. Specific objectives involve the testing of the impact of:

1. the timing of a phaseout (100% cut) in CFCs, CCl_4, CH_3CCl_3, and HCFC-22 (complete phaseout without substitution in 1995, 2000 [reference case] and 2005);

2. incomplete phaseout (cut in 2000 to 10%, 20%, 50% of 1985 emissions, or freeze the 1990 emissions);

3. different substitution scenarios for compound X and compound Y (phaseout of all halocarbons in 2000 with varying % substitution of X and Y by weight continued until 2015, 2030, 2045 and even 2100);

4. delayed compliance of phaseout by some countries (cut back to 10% or 20% of 1985 emissions in 2000, complete phaseout in 2015, any substitution is similarly lagged by 15 years);

5. graduated phase-in of halocarbon cuts (cut halocarbon emission to 50% of 1985 emissions in 1995 and completely phaseout in 2000; substitutes have similar 5 yr phase lag);

6. continued use of CH_3CCl_3 (freeze emissions of CH_3CCl_3 at 1990 levels, phaseout in 2030);

7. current uncertainties in the atmospheric lifetimes of halocarbons;

8. halon emissions on bromine loading (cut emissions of CF_3Br and CF_2ClBr in 2000 to 0%, 10%, 20%, 50% of 1985 emissions, or freeze at 1990 levels).

The chlorine loading from these scenarios is summarized in Tables 2a-h and the bromine loading in Table 3. Figures 1-12 display the evolution of chlorine from 1985 to 2100 for a selection of these cases and always compare with the reference calculation (complete phaseout of CFCs, CCl_4, CH_3CCl_3, and HCFC-22 emissions in the year 2000 with no substitutions).

6.1   OBJECTIVE 1.   Test the impact of the timing of a phaseout (100% cut) in CFCs, CCl4, CH3CCl3, and HCFC-22

This objective was examined by eliminating the emissions of all halocarbons as a group (CFCs, CCl4, CH3CCl3 and HCFC-22) at the end of years 1995, 2000 (reference case), and 2005, all without substitution of any new chlorine containing compound.

Table 2a and Figure 1 show the results of these scenarios. (Tables 2a-2-h and Table 3 follow at the end in order to provide easy reference.) It is evident that each 5 year delay in the total phaseout of these chemicals results in the peak chlorine loading increasing by about 0.5 ppb (87% of it due to the CFCs) and in the date taken for the atmospheric abundance of chlorine to drop below 2 ppb increasing by about 18 years. The delay in reaching an atmospheric loading of 2 ppb is due to the timing of the phaseout of the long-lived halocarbons (CFCs and CCl4) and is not influenced by the timing of the phaseout of short-lived halocarbons (CH3CCl3 and HCFC-22). Banking of these gases, especially the long-lived CFCs, and possible non-compliance (see Objectives 2 and 4), make the effective dates for cessation of CFC emissions slip further into the future.

The key information from these scenarios is that an early phaseout of these substances results in a lower peak chlorine loading (0.1 ppb per year earlier phaseout) and in an earlier date for the atmospheric chlorine loading to drop below 2 ppb (3.6 years per year earlier phaseout), corresponding to the most optimistic time for elimination of the Antarctic ozone hole. The table below summarizes the peak chlorine loading and the date of 2 ppb chlorine for these scenarios.

Peak Chlorine Loading and Time to Reach 2 ppb

scenario (phaseout=100% cut)	peak chlorine (ppb)	year when chlorine falls below 2 ppb
1995 phaseout	4.24	2055
2000 phaseout (ref#)	4.78	2073
2005 phaseout	5.28	2091
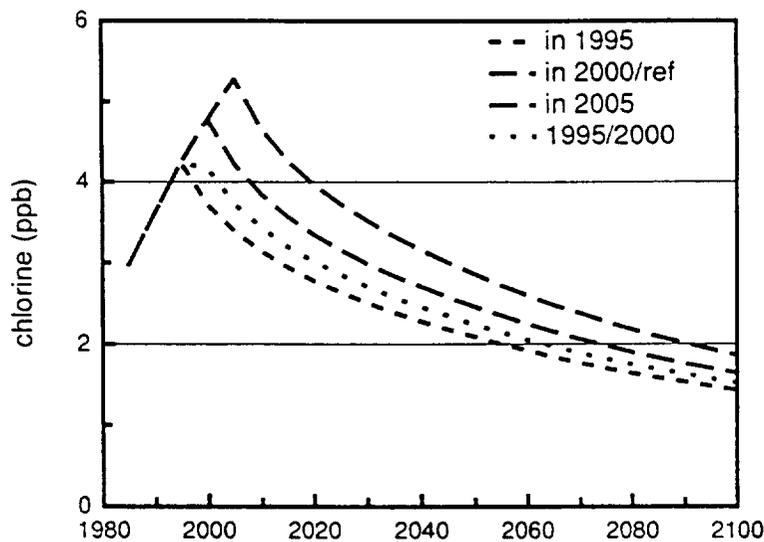
Figure 1.   100% cut of all halocarbons.

6.2 OBJECTIVE 2. Test the impact of incomplete phaseout.

This objective examined the impact of a partial phaseout (90%, 80%, 50%, 0%) in the emissions of all halocarbons as a group (CFCs, CCl_4, CH_3CCl_3 and HCFC-22) without substitution of any new chlorine containing compound. All reductions (90%, 80% and 50%) were made to reach a fraction of the year 1985 emissions (10%, 20% and 50% respectively), and all occurred at the end of year 2000. The calculation with no reductions continued the year 1990 emission levels of all halocarbons until the year 2100.

Table 2a and Figure 2 show the results of these scenarios. For partial phaseouts of 90% and 80% the peak chlorine loading is not affected, but the rate of decrease in the atmospheric chlorine and its long-term steady state value are significantly impacted. In the reference case (100% reduction) the atmospheric abundance of chlorine has decreased to 2 ppb by the year 2073. With a 90% reduction the chlorine abundance reaches 2.4 ppb in the year 2100 and is not expected to decrease to 2 ppb until after the year 2175. With an 80% reduction the chlorine abundance is 3.1 ppb in the year 2100 and will eventually approach its steady-state limit of about 2.8 ppb. With 50% reductions the peak chlorine loading drops briefly after the year 2000 and then continues to rise above 5.3 ppb by the year 2100. Without a cutback in the 1990 emissions the chlorine abundance in the atmosphere is expected to rise rapidly, exceeding 8.5 ppb by the year 2050 and 10.5 ppb by the end of the 21st century.
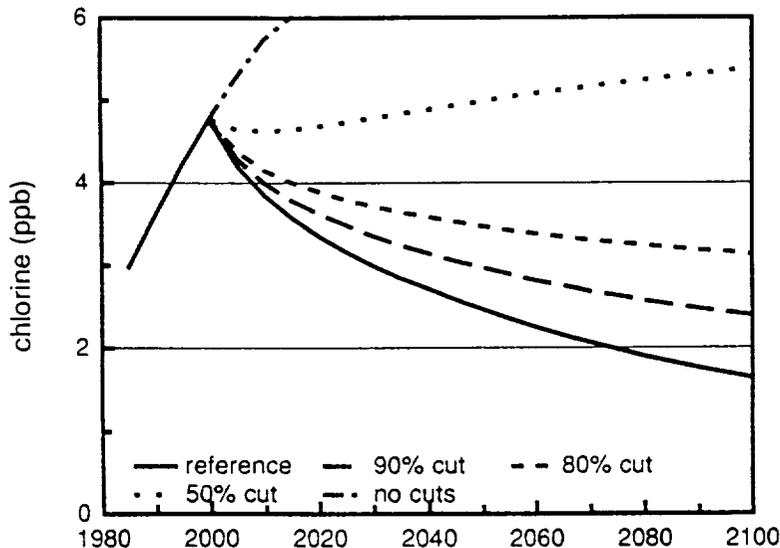
Figure 2. Cut all halocarbons in 2000.

The key conclusion to be drawn from these scenarios is that a complete phaseout of almost all emission of halocarbons (CFCs, CCl_4, CH_3CCl_3, and HCFC-22) as a group is needed in order to decrease the atmospheric abundance of chlorine below 2 ppb before the year 2100. The required timing of these phaseouts will depend on the lifetime of the specific halocarbon. The long-term decline in chlorine abundances is controlled by the long-lived CFCs and CCl_4. Therefore, a long-term non-compliance with the 100% reduction, by even as little as 5 to 10%, limits our chance of eliminating the Antarctic ozone hole before the year 2100. The table below summarizes the peak chlorine loading and the date of 2 ppb chlorine for these scenarios.

Peak Chlorine Loading and Time to Reach 2 ppb

scenario (phaseout=100% cut)	peak chlorine (ppb)	year when chlorine falls below 2 ppb
2000 phaseout (ref#)	4.78	2073
2000 (90% cut)	4.78	2175
2000 (80% cut)	4.78	never

6.3 OBJECTIVE 3. Test the impact of different substitution scenarios for compound X and compound Y

This objective was examined by eliminating the emissions of the halocarbons (CFCs, CCl_4, CH_3CCl_3 and HCFC-22) as a group in the year 2000 (reference case) and then by substituting for a fraction of these emissions (1,820 kt/yr) with either compound X (15 year lifetime, ODP = 0.1) or compound Y (6 year lifetime, ODP = 0.04). Substitution of either X or Y begins in the year 2001 at a level of 25%, 50% or 100%, corresponding to annual fluxes of 455, 910 and 1,820 kt, respectively. In addition, a scenario with 50% substitution is considered in which use of the substitute (X or Y) is allowed to grow annually at a compounded rate of 3 %/yr (denoted by *50%). In general, the time period of substitution is assumed to be 30 years, from year 2001 through year 2030. In some cases the period of substitution is shortened to 15 years or extended to 45 or even 100 years.

Tables 2b-d and Figures 3-6 show the results of these many scenarios. We discuss only a few of them below.

For the levels of substitution and the limits on their growth considered in these scenarios, the peak chlorine loading occurs at the phaseout of CFCs and is not affected by the substitution. In the case of 100% substitution of compound X, however, the chlorine loading remains high, above 4 ppb, out to the year 2032 (Figure 3). Equivalent substitution of compound Y has a much smaller impact on atmospheric chlorine because of the shorter lifetime (Figure 4). Substitution by either compound X or Y at 50% of the halocarbon emissions followed by 3 %/yr compounded growth becomes equivalent to 100% substitution by the year 2030 and would greatly exceed that level if continued for another 15 years (Figures 3 and 4).

Substitution between the years 2000 and 2030 with compound X at less than 25%, or compound Y at less than 50% of all halocarbon emissions, results in a rapid decrease in peak chlorine loading. The increase in atmospheric chlorine abundance above the base case (no substitution) is
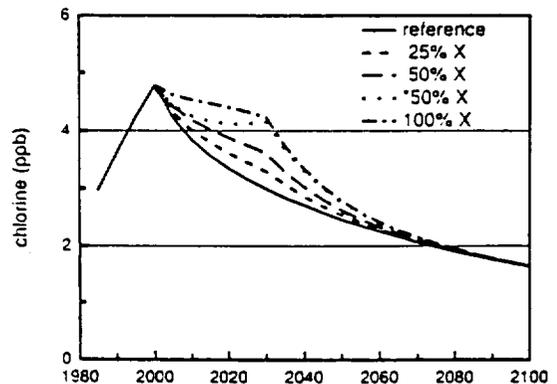
Figure 3. Substitution for 30 yrs (*=growth).
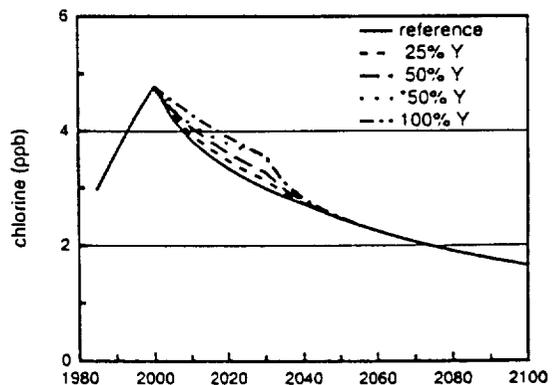
Figure 4. Substitution for 30 yrs (*=growth)..

59

greatest in the year 2030 and never exceeds 0.3 ppb under these conditions. The assessment of the International Technical Panel (part of the UNEP assessment) is that about 30% of the current CFC market will be replaced by short-lived substitutes containing chlorine, and that this market will grow at 3 %/yr until terminated. Such a scenario is about equivalent to following the 25% substitution-curve in the early years (2000-2010) and increasing to chlorine levels slightly above the 50% substitution-curve by the year 2030.

Figure 5. Substitution for different periods.

When compound X is phased out before the year 2030 or compound Y before the year 2045, the earliest date when the atmospheric abundance of chlorine falls to 2 ppb is delayed by at most 4 years relative to the reference case with no substitutions (Figure 5). With indefinite substitution of compound X or Y, even at 50% of the halocarbon emissions, it is difficult or impossible to achieve chlorine concentrations below 2 ppb by the end of the 21st century (Figure 6).

Figure 6. Substitution until 2100.

The key conclusions to be drawn from these scenarios are that substitution of all halocarbons (CFCs, CCl$_4$, CH$_3$CCl$_3$ and HCFC-22) as a group, between the years 2000 and 2030 by compound X, and between the years 2000 and 2045 by compound Y, would have little influence on the date when the atmospheric abundance of chlorine can be expected to fall below 2 ppb, approximately the year 2073. With a limited period of substitution of the short-lived substitutes, the chlorine loading of the atmosphere beyond the year 2075 is governed by the CFCs and CCl$_4$ emitted prior to their phaseout. Furthermore, such substitutions can still result in a rapid decrease in the peak chlorine abundance if substitution rates close to 25% for X or 50% for Y are used. Substitution by compound Y is preferable to substitution by compound X because of its shorter lifetime: compound Y makes a smaller contribution to the chlorine loading and in addition allows for more rapid recovery of atmospheric chlorine following cessation of emissions.

6.4 OBJECTIVE 4. Test the impact of delayed compliance of phaseout by some countries.

This objective was examined by reducing emissions of all halocarbons (CFCs, CCl$_4$, CH$_3$CCl$_3$ and HCFC-22) to a fraction (10% or 20%) of their 1985 levels in the year 2000 and allowing this fraction of emissions to continue for 15 years until the end of year 2015. Substitution of compounds X and Y was also considered as above for a 30-year time period. The final phaseout of CFCs in the year 2015 was followed by a similar period of fractional substitution until the year 2045. This form of delayed compliance would allow a fraction of the world community further time to implement a complete halocarbon phaseout.

Table 2e and Figures 7-8 show the results of these scenarios. There is no additional penalty in the peak chlorine loading for a 15-year lag in the final 10% or 20% of the halocarbon cuts. However, the 15-year lag in 10% of the phaseout results in a 6-year delay in the time to reach 2 ppb chlorine, and the lag in 20% adds 11 years to this time. The effects of substitution of
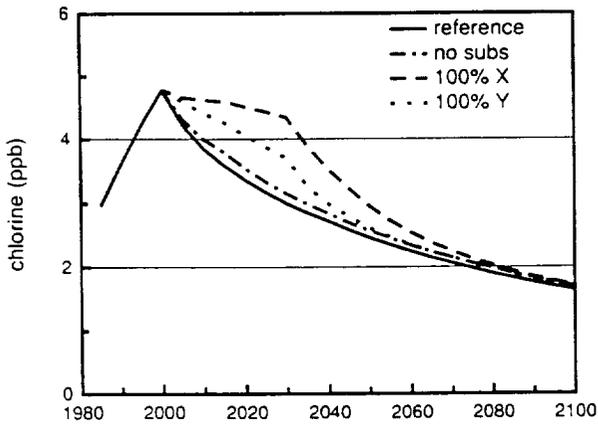
Figure 7. 10% of CFC cuts/subs lag 15 yr.
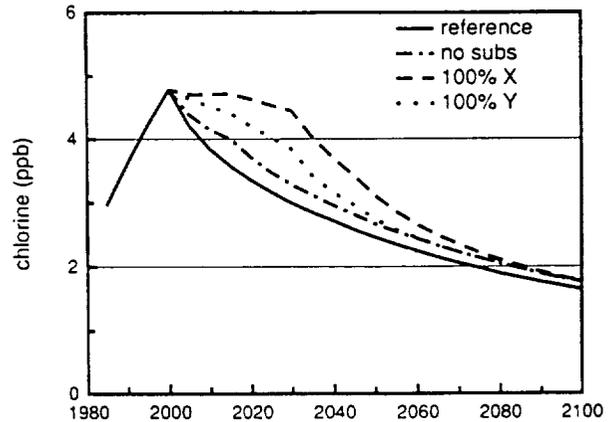
Figure 8. 20% of CFC cuts/subs lag 15 yr.

compounds X or Y are similar to the reference case (complete phaseout) except that the baseline of total chlorine is higher during the substitution period, by a maximum in the year 2015 of about 0.2 ppb (10%) and 0.4 ppb (20%). The 15-year delay in the phaseout does extend the duration of higher chlorine levels. In the case where only 80% of the CFCs are cut and replaced 100% by compound X, the peak chlorine loading in the year 2000 (4.78 ppb) is maintained out to the year 2015 (4.72 ppb).

The key point here is that a 15-year lag in compliance of the phaseout of CFCs by a *small fraction*, 10-20%, of the community should have no effect on peak chlorine levels and have only a small delay in the time to reach 2 ppb total chlorine. The average chlorine levels in the first half of the next century would be higher in this scenario, but may be compensated for by reducing use of the longer-lived of the two substitutes, compounds X. The table below summarizes the peak chlorine loading and the date of 2 ppb chlorine for these scenarios.

Peak Chlorine Loading and Time to Reach 2 ppb

scenario (phaseout=100% cut)	peak chlorine (ppb)	year when chlorine falls below 2 ppb
2000 phaseout (ref#)	4.78	2073
2000/2015 (90/10%)	4.78	2079
2000/2015 (80/20%)	4.78	2084

6.5 OBJECTIVE 5. Test the impact of a graduated phase-in of halocarbon cuts.

This objective was examined by reducing the emissions of all halocarbons (CFCs, CCl_4, CH_3CCl_3 and HCFC-22) to 50% of their 1985 levels at the end of year 1995 and completely to zero at the end of year 2000. Substitution of compound X or Y for a period of 30 years (staggered 5 years as for halocarbon cuts) at 50% of the 1985 halocarbon emissions is also considered. This complex scenario for phaseout of CFCs may be a more realistic approach to elimination of halocarbon emissions, recognizing the ability of some parts of the CFC market to phaseout earlier than others and also the net impact of banking in delaying release of CFCs to the atmosphere.

61

Table 2f and Figure 9 show the results of these scenarios. As expected, the history of chlorine abundance from the 50%/50% scenario lies between that of the year-1995 phaseout and that of the year-2000 phaseout. Peak chlorine loading occurs in 1995, and the year when chlorine levels fall below 2 ppb is 2063, about 10 years earlier than in the reference case. Moderate substitution (50% of cuts) with compounds X or Y until the year 2030 give chlorine histories that resemble the reference case without substitution for the first half of the 21st century.

The key result from this scenario is that an earlier partial phaseout of CFCs has distinct advantages: reducing the peak chlorine loading, approaching more rapidly the 2 ppb level (probably eliminating the Antarctic ozone hole), and allowing for substitution without significant increase in the average chlorine levels over the next 50 years. The table below summarizes the peak chlorine loading and the date of 2 ppb chlorine for these scenarios.
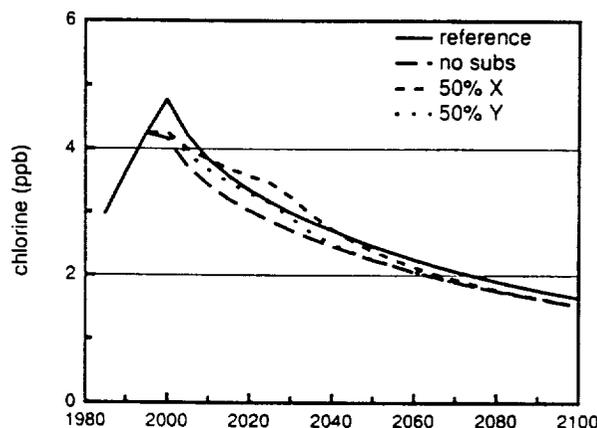
Figure 9. 50/50% cuts in 1995/2000 with subs.

Peak Chlorine Loading and Time to Reach 2 ppb

scenario (phaseout=100% cut)	peak chlorine (ppb)	year when chlorine falls below 2 ppb
2000 phaseout (ref#)	4.78	2073
1995/2000 (50/50%)	4.24	2063

6.6 OBJECTIVE 6. Test the impact of continued use of CH_3CCl_3

This objective was examined by eliminating the emissions of CFCs, CCl_4, and HCFC-22 at the end of year 2000, but continuing CH_3CCl_3 emissions (1990 levels) until the year 2030. Substitution of compound X or Y for a period of 30 years is considered as above, but substitution percentages now refer to a lesser halocarbon budget of 1,220 kt/yr. This scenario recognizes that methyl chloroform is a short-lived halocarbon (about 6 yr) and has properties similar to those of possible CFC substitutes (i.e., compound Y).
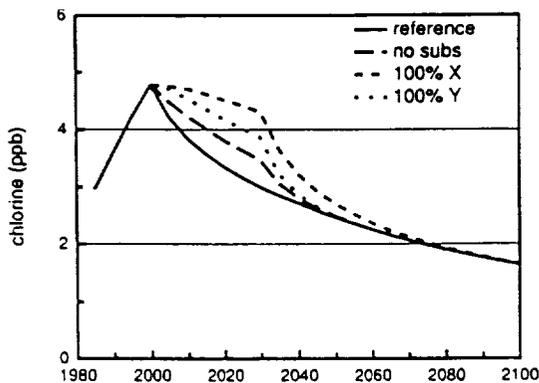
Figure 10. CH_3CCl_3 to 2030, cut/sub for others.

Table 2g and Figure 10 show the results of these scenarios. Compared with the reference scenario, there is no increase in peak chlorine loading and little change in the date at which the atmospheric abundance of chlorine drops below 2 ppb. Substitutions for the phased-out compounds (CFCs, CCl_4 and HCFC-22) show similar properties as in Objective 3, although 100% replacement with compound X maintains near-peak chlorine levels above 4.5 ppb out to the year 2020. Continued use of methyl chloroform is equivalent to substitution with 1,800 kt/yr of compound Y.

62

When the cuts in CH3CCl3 and CFC *production* are simultaneous the *emissions* of CH3CCl3 are expected to drop rapidly but those of CFCs will continue at some reduced level as the bank of CFCs is released (see previous discussion). The bank of CFCs as of 1987 (CMA, 1988) would produce only a modest extension of CFC release following a cut in production: emissions would drop to about 30% of production levels in 3 years and continue at an average level of less than 10% out to 20 years. Details of the CFC banking in relation to the timing of the cut in CH3CCl3 may slightly affect the peak chlorine loading.

The key point from this scenario is that the phaseout of CH3CCl3 production is expected to lead to a rapid cessation of emissions and would result in a relatively rapid decrease of as much as 0.5 ppb in atmospheric chlorine.

6.7   OBJECTIVE 7.   Test the impact of current uncertainties in the atmospheric lifetimes of halocarbons;

This objective was examined by increasing or decreasing the recommended atmospheric lifetimes of the halocarbons by 25% for the reference scenario (phaseout of all halocarbons in the year 2000). These limits are extreme (e.g., CFC-11 lifetimes from 45 yr to 75 yr) and cover the most probable range in CFC lifetimes from the best current atmospheric models and from the budget analyses using observations and historical emissions. Assuming that future halocarbon emissions are known, this scenario represents the largest uncertainty in the absolute abundance of atmospheric chlorine from these calculations.

Table 2h and Figure 11 show the results of these scenarios. When halocarbon lifetimes are reduced by 25%, the more rapid destruction of these compounds lowers the peak chlorine concentration by about 0.3 ppb (to 4.5 ppb) and reduces the time to reach 2 ppb chlorine by 20 years (to the year 2053). When halocarbon lifetimes are increased by 25%, the slower destruction of these compounds raises the peak chlorine concentration by about 0.2 ppb (to 5.0 ppb) and increases the time to reach 2 ppb chlorine by 22 years (to the year 2095).
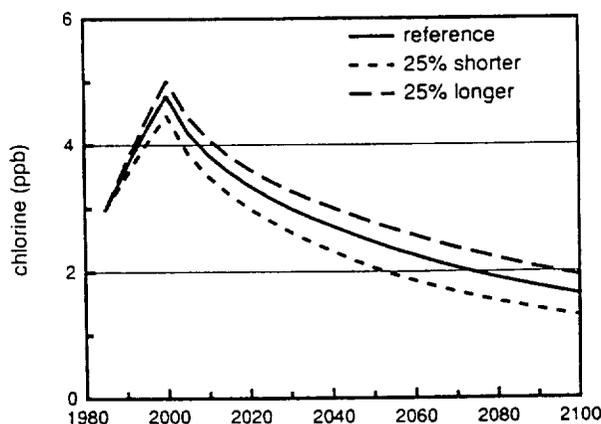
Figure 11. Uncertainty in lifetimes

The key point from these calculations is that the uncertainty in predicting atmospheric chlorine levels in the future, given the history of atmospheric emissions, is not large. More specifically, all of the options to the reference scenario considered above (Objectives 1-6) may need to be shifted up or down, by less than 0.3 ppb, as our understanding and modeling of the atmospheric chemical losses of these compounds improves.

6.8 OBJECTIVE 8. Evaluate the impact of halon emissions on bromine loading.

The atmospheric abundance of bromine in these scenarios is predicted to result from emissions of methyl bromide (CH_3Br) and the halons 1301 (CF_3Br) and 1211 (CF_2ClBr). The other halon specified in the current Montreal Protocol, halon-2402 or $C_2F_4Br_2$, is assumed to be negligible at present and in the future. (The short-lived compound bromoform, $CHBr_3$, is observed occasionally at high concentrations near the ocean surface, but is expected to contribute little to stratospheric bromine.) This scenario is similar to that for chlorine loading and examines the effects of cutting halon emissions to 0%, 20% and 50% of 1985 levels, as well as freezing emissions at their 1990 levels (see Table 3). The assumption here that production and release of halons occurs simultaneously is also incorrect as discussed for CFCs above.

Results are shown in Table 3 and Figure 12. In 1985 the halons 1301 and 1211 together contributed about 3 ppt to the atmospheric abundance of bromine (18 ppt). If their emissions continued at the estimated 1990 production levels then the atmospheric abundance of bromine in the future would approximately triple from about 18 ppt (3 ppt halons) in the year 1985 to 53 ppt (38 ppt halons) by the year 2100.
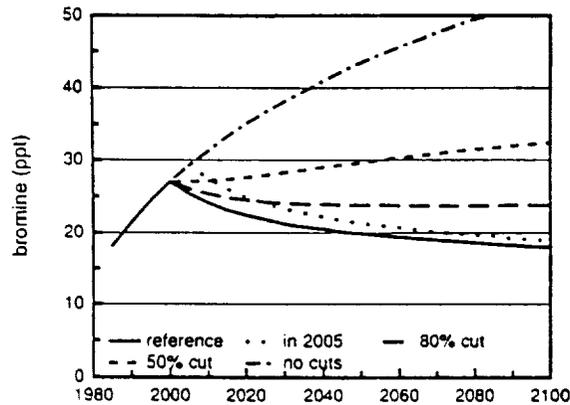
Figure 12. Cut all halocarbons in 2000.

To relate the impact of increases in atmospheric bromine to that of chlorine increases, it would be useful to define a factor relating bromine to chlorine. Such a simple factor is difficult to derive because bromine-catalyzed destruction of ozone is important both globally and in the special environment of the Antarctic ozone hole. Furthermore, much of the loss is coupled to the chlorine abundance as noted above. Currently, one estimate of this factor is about 30 (with a large uncertainty ranging from 10 to 50), and thus the rise in bromine with a freeze on 1990 emissions (increase of 33 ppt) would be about the equivalent of adding 1 ppb of chlorine to the atmosphere.

These calculations, however, assumed that CH_3Br remains constant. There is clear evidence that a substantial fraction of atmospheric CH_3Br is associated with northern continental sources and human activity (e.g., grain fumigation), and thus its concentration may increase in the future.

The key result of these bromine scenarios is that a phaseout or 80% reduction of halon emissions in the near future would stabilize the atmospheric abundance of bromine at about 24 ppt (9 ppt of halons).

7.0 CONCLUSIONS

In order to minimize future ozone depletion, or the potential of damage to the protective stratospheric ozone layer, and to facilitate the elimination of the Antarctic ozone hole it is desirable to:

• phase out production/emission of long-lived halocarbons (CFCs and CCl_4) as soon as possible,

• achieve as great as possible compliance with such a phaseout of CFCs and CCl_4 at the expense of substituting short-lived HCFCs,

• if it becomes necessary to rapidly reduce the peak chlorine loading, make significant cutbacks in the emissions of abundant, short-lived, non-banked halocarbons, particularly CH_3CCl_3,

• phase out in addition the halocarbon substitutes sometime in the middle of the next century if the Antarctic ozone hole is expected to disappear before the end of the next century,

• stabilize the atmospheric bromine concentration at today's level or below.

REFERENCES

UNEP/WMO, Scientific Assessment of Stratospheric Ozone: 1989, Vol. I, World Meteorological Organization Global Ozone Research and Monitoring Project, Report No. 20, 1990.

AFEAS, Alternative Fluorocarbon Environmental Acceptability Study; Scientific Assessment of Stratospheric Ozone: 1989, Vol. II, The AFEAS Report, World Meteorological Organization Global Ozone Research and Monitoring Project, Report No. 20, 1990.

1987 Production and Sales of Chlorofluorocarbons CFC-11 and CFC-12 (Chemical Manufacturers Association, Fluorocarbon Program Panel, Washington, DC 1988).

IOTP, Report of the International Ozone Trends Panel: 1988, World Meteorological Organization Global Ozone Research and Monitoring Project, Report No. 18, 1990.

UNEP/Technical Panel Report, 1989.

Table 2a. Atmospheric Chlorine (ppb = $1/10^9$) following Cut in all Halocarbon Emissions without Substitutes

year cut	1995 100%	2000 100%#	2005 100%	2000 90%	2000 80%	2000 50%	2000 0%
1985	2.98	2.98	2.98	2.98	2.98	2.98	2.98
1990	3.62	3.62	3.62	3.62	3.62	3.62	3.62
1995	4.24	4.24	4.24	4.24	4.24	4.24	4.24
2000	3.71	4.78	4.78	4.78	4.78	4.78	4.78
2005	3.38	4.21	5.28	4.30	4.39	4.65	5.28
2010	3.14	3.84	4.67	3.99	4.15	4.63	5.74
2015	2.95	3.57	4.27	3.78	4.00	4.65	6.17
2020	2.78	3.35	3.97	3.62	3.89	4.69	6.57
2025	2.64	3.16	3.73	3.48	3.79	4.74	6.95
2030	2.51	2.99	3.52	3.35	3.71	4.79	7.30
2035	2.39	2.84	3.33	3.24	3.64	4.84	7.64
2040	2.28	2.71	3.16	3.14	3.58	4.89	7.95
2045	2.18	2.58	3.00	3.05	3.52	4.94	8.25
2050	2.09	2.46	2.86	2.97	3.47	4.99	8.53
2055	2.00	2.35	2.72	2.89	3.42	5.04	8.80
2060	1.92	2.25	2.60	2.81	3.38	5.08	9.05
2065	1.84	2.15	2.48	2.75	3.34	5.12	9.28
2070	1.77	2.06	2.38	2.68	3.30	5.16	9.51
2075	1.70	1.98	2.27	2.63	3.27	5.20	9.72
2080	1.64	1.90	2.18	2.57	3.24	5.24	9.92
2085	1.58	1.83	2.09	2.52	3.21	5.28	10.11
2090	1.53	1.76	2.01	2.47	3.18	5.31	10.28
2095	1.48	1.70	1.93	2.43	3.16	5.35	10.45
2100	1.43	1.64	1.86	2.39	3.13	5.38	10.61

reference case in all following tables = ref#

Table 2b. Halocarbon Cuts (ref = 100% in 2000) with Substitutes to 2030
(* = +3%/yr growth in substitute)

Atmospheric Chlorine (ppb = $1/10^9$)

subs %	none ref#	X 25%	X 50%	X 100%	X *50%	Y 25%	Y 50%	Y 100%	Y *50%
1985	2.98	2.98	2.98	2.98	2.98	2.98	2.98	2.98	2.98
1990	3.62	3.62	3.62	3.62	3.62	3.62	3.62	3.62	3.62
1995	4.24	4.24	4.24	4.24	4.24	4.24	4.24	4.24	4.24
2000	4.78	4.78	4.78	4.78	4.78	4.78	4.78	4.78	4.78
2005	4.21	4.31	4.41	4.61	4.43	4.29	4.37	4.53	4.38
2010	3.84	4.01	4.18	4.53	4.25	3.95	4.07	4.30	4.12
2015	3.57	3.79	4.02	4.47	4.16	3.70	3.83	4.09	3.93
2020	3.35	3.61	3.87	4.40	4.12	3.49	3.62	3.90	3.78
2025	3.16	3.45	3.74	4.32	4.12	3.30	3.44	3.72	3.67
2030	2.99	3.30	3.61	4.23	4.15	3.14	3.28	3.56	3.59
2035	2.84	3.07	3.29	3.73	3.67	2.91	2.97	3.09	3.10
2040	2.71	2.86	3.02	3.34	3.30	2.73	2.76	2.81	2.82
2045	2.58	2.69	2.81	3.03	3.00	2.59	2.60	2.63	2.63
2050	2.46	2.54	2.62	2.79	2.76	2.47	2.47	2.48	2.48
2055	2.35	2.41	2.47	2.58	2.57	2.35	2.35	2.36	2.36
2060	2.25	2.29	2.33	2.42	2.40	2.25	2.25	2.25	2.25
2065	2.15	2.18	2.21	2.27	2.26	2.15	2.15	2.15	2.15
2070	2.06	2.09	2.11	2.15	2.14	2.06	2.06	2.06	2.06
2075	1.98	2.00	2.01	2.04	2.04	1.98	1.98	1.98	1.98
2080	1.90	1.91	1.93	1.95	1.94	1.90	1.90	1.90	1.90
2085	1.83	1.84	1.85	1.86	1.86	1.83	1.83	1.83	1.83
2090	1.76	1.77	1.77	1.78	1.78	1.76	1.76	1.76	1.76
2095	1.70	1.70	1.71	1.71	1.71	1.70	1.70	1.70	1.70
2100	1.64	1.64	1.64	1.65	1.65	1.64	1.64	1.64	1.64

Table 2c.   Halocarbon Cuts (ref = 100% in 2000) and 100% Substitution
for different periods: until 2015, 2030 & 2045

Atmospheric Chlorine (ppb = $1/10^9$)

subs until	none ref#	X 2015	X 2030	X 2045	Y 2030	Y 2045
1985	2.98	2.98	2.98	2.98	2.98	2.98
1990	3.62	3.62	3.62	3.62	3.62	3.62
1995	4.24	4.24	4.24	4.24	4.24	4.24
2000	4.78	4.78	4.78	4.78	4.78	4.78
2005	4.21	4.61	4.61	4.61	4.53	4.53
2010	3.84	4.53	4.53	4.53	4.30	4.30
2015	3.57	4.47	4.47	4.47	4.09	4.09
2020	3.35	3.99	4.40	4.40	3.90	3.90
2025	3.16	3.62	4.32	4.32	3.72	3.72
2030	2.99	3.33	4.23	4.23	3.56	3.56
2035	2.84	3.08	3.73	4.14	3.09	3.41
2040	2.71	2.88	3.34	4.04	2.81	3.28
2045	2.58	2.70	3.03	3.94	2.63	3.15
2050	2.46	2.55	2.79	3.43	2.48	2.71
2055	2.35	2.41	2.58	3.05	2.36	2.46
2060	2.25	2.29	2.42	2.75	2.25	2.30
2065	2.15	2.19	2.27	2.51	2.15	2.17
2070	2.06	2.09	2.15	2.32	2.06	2.07
2075	1.98	2.00	2.04	2.16	1.98	1.98
2080	1.90	1.91	1.95	2.03	1.90	1.90
2085	1.83	1.84	1.86	1.92	1.83	1.83
2090	1.76	1.77	1.78	1.83	1.76	1.76
2095	1.70	1.70	1.71	1.75	1.70	1.70
2100	1.64	1.64	1.65	1.67	1.64	1.64

68

Table 2d. Halocarbon Cuts (ref = 100% in 2000) and Substitution to 2100

Atmospheric Chlorine (ppb = $1/10^9$)

subs %	none ref#	X 25%	X 50%	Y 25%	Y 50%	X&Y 50%
1985	2.98	2.98	2.98	2.98	2.98	2.98
1990	3.62	3.62	3.62	3.62	3.62	3.62
1995	4.24	4.24	4.24	4.24	4.24	4.24
2000	4.78	4.78	4.78	4.78	4.78	4.78
2005	4.21	4.31	4.41	4.29	4.37	4.57
2010	3.84	4.01	4.18	3.95	4.07	4.41
2015	3.57	3.79	4.02	3.70	3.83	4.28
2020	3.35	3.61	3.87	3.49	3.62	4.14
2025	3.16	3.45	3.74	3.30	3.44	4.02
2030	2.99	3.30	3.61	3.14	3.28	3.90
2035	2.84	3.17	3.49	2.99	3.13	3.78
2040	2.71	3.04	3.37	2.85	2.99	3.65
2045	2.58	2.92	3.26	2.72	2.86	3.54
2050	2.46	2.80	3.15	2.60	2.75	3.44
2055	2.35	2.70	3.05	2.49	2.64	3.34
2060	2.25	2.60	2.95	2.39	2.53	3.23
2065	2.15	2.51	2.86	2.30	2.44	3.15
2070	2.06	2.42	2.77	2.21	2.35	3.06
2075	1.98	2.34	2.69	2.12	2.27	2.98
2080	1.90	2.26	2.61	2.05	2.19	2.90
2085	1.83	2.19	2.54	1.97	2.12	2.83
2090	1.76	2.12	2.48	1.91	2.05	2.77
2095	1.70	2.06	2.41	1.84	1.98	2.69
2100	1.64	2.00	2.35	1.78	1.92	2.63

Table 2e. Developed/Undeveloped Scenarios:

100% cut & substitution of all halocarbons, but delay
10% to 20% of cuts (& substitution) by 15 yr.

Atmospheric Chlorine (ppb = $1/10^9$)

cut 2000 cut 2015 subs	100% ref# none	90% 10% none	90% 10% 100%X	90% 10% 100%Y	80% 20% none	80% 20% 100%X	80% 20% 100%Y
1985	2.98	2.98	2.98	2.98	2.98	2.98	2.98
1990	3.62	3.62	3.62	3.62	3.62	3.62	3.62
1995	4.24	4.24	4.24	4.24	4.24	4.24	4.24
2000	4.78	4.78	4.78	4.78	4.78	4.78	4.78
2005	4.21	4.30	4.66	4.59	4.39	4.71	4.64
2010	3.84	3.99	4.62	4.41	4.15	4.71	4.52
2015	3.57	3.78	4.60	4.25	4.00	4.72	4.42
2020	3.35	3.53	4.51	4.06	3.71	4.63	4.21
2025	3.16	3.32	4.43	3.87	3.47	4.54	4.02
2030	2.99	3.14	4.34	3.70	3.28	4.45	3.84
2035	2.84	2.98	3.88	3.25	3.11	4.02	3.41
2040	2.71	2.83	3.51	2.98	2.95	3.69	3.15
2045	2.58	2.69	3.22	2.79	2.81	3.42	2.96
2050	2.46	2.57	2.95	2.61	2.67	3.11	2.74
2055	2.35	2.45	2.72	2.47	2.55	2.86	2.58
2060	2.25	2.34	2.54	2.35	2.44	2.66	2.45
2065	2.15	2.24	2.38	2.24	2.33	2.49	2.33
2070	2.06	2.15	2.25	2.15	2.23	2.35	2.23
2075	1.98	2.06	2.13	2.06	2.14	2.22	2.14
2080	1.90	1.98	2.03	1.98	2.05	2.11	2.05
2085	1.83	1.90	1.94	1.90	1.97	2.01	1.97
2090	1.76	1.83	1.85	1.83	1.89	1.92	1.89
2095	1.70	1.76	1.78	1.76	1.82	1.84	1.82
2100	1.64	1.70	1.71	1.70	1.76	1.77	1.76

Table 2f. Phased Halocarbon Cuts spread over 5 years:
50% cut back in 1995 and remaining 50% in 2000
Substitutes similarly cut back in 2025 and 2030

Atmospheric Chlorine (ppb = $1/10^9$)

subs	ref#	none	50%X	50%Y
1985	2.98	2.98	2.98	2.98
1990	3.62	3.62	3.62	3.62
1995	4.24	4.24	4.24	4.24
2000	4.78	4.16	4.26	4.24
2005	4.21	3.72	4.00	3.92
2010	3.84	3.43	3.83	3.67
2015	3.57	3.20	3.69	3.47
2020	3.35	3.02	3.57	3.30
2025	3.16	2.86	3.46	3.14
2030	2.99	2.71	3.24	2.92
2035	2.84	2.58	2.96	2.67
2040	2.71	2.46	2.73	2.50
2045	2.58	2.35	2.54	2.36
2050	2.46	2.24	2.38	2.25
2055	2.35	2.15	2.25	2.15
2060	2.25	2.05	2.13	2.06
2065	2.15	1.97	2.02	1.97
2070	2.06	1.89	1.93	1.89
2075	1.98	1.82	1.85	1.82
2080	1.90	1.75	1.77	1.75
2085	1.83	1.69	1.70	1.69
2090	1.76	1.63	1.64	1.63
2095	1.70	1.57	1.58	1.57
2100	1.64	1.52	1.52	1.52

Table 2g. CH₃CCl₃ continued until 2030:

All other halocarbons cut 100% in 2000 with subs until 2030
(* = +3%/yr growth, compounded)

Atmospheric Chlorine (ppb = $1/10^9$)

subs %	none ref#	none 0%	X 25%	X 100%	X *50%	Y 25%	Y 100%	Y *50%
1985	2.98	2.98	2.98	2.98	2.98	2.98	2.98	2.98
1990	3.62	3.62	3.62	3.62	3.62	3.62	3.62	3.62
1995	4.24	4.24	4.24	4.24	4.24	4.24	4.24	4.24
2000	4.78	4.78	4.78	4.78	4.78	4.78	4.78	4.78
2005	4.21	4.48	4.55	4.75	4.63	4.53	4.70	4.60
2010	3.84	4.23	4.34	4.70	4.51	4.30	4.54	4.42
2015	3.57	4.01	4.16	4.62	4.41	4.10	4.36	4.25
2020	3.35	3.81	3.99	4.52	4.33	3.91	4.18	4.11
2025	3.16	3.64	3.83	4.42	4.28	3.73	4.01	3.98
2030	2.99	3.47	3.68	4.31	4.25	3.57	3.86	3.88
2035	2.84	3.05	3.20	3.65	3.61	3.09	3.22	3.23
2040	2.71	2.80	2.90	3.22	3.19	2.81	2.87	2.87
2045	2.58	2.62	2.69	2.92	2.90	2.63	2.65	2.65
2050	2.46	2.48	2.53	2.70	2.68	2.48	2.49	2.49
2055	2.35	2.36	2.40	2.52	2.50	2.36	2.36	2.36
2060	2.25	2.25	2.28	2.36	2.36	2.25	2.25	2.25
2065	2.15	2.15	2.17	2.23	2.23	2.15	2.16	2.16
2070	2.06	2.06	2.08	2.12	2.12	2.06	2.06	2.06
2075	1.98	1.98	1.99	2.02	2.02	1.98	1.98	1.98
2080	1.90	1.90	1.91	1.93	1.93	1.90	1.90	1.90
2085	1.83	1.83	1.84	1.85	1.85	1.83	1.83	1.83
2090	1.76	1.76	1.77	1.78	1.78	1.76	1.76	1.76
2095	1.70	1.70	1.70	1.71	1.71	1.70	1.70	1.70
2100	1.64	1.64	1.64	1.65	1.65	1.64	1.64	1.64

Table 2h.   Uncertainty in Halocarbon Lifetimes

Atmospheric Chlorine (ppb = $1/10^9$)

	ref#	25% shorter	25% longer
1985	2.98	2.98	2.98
1990	3.62	3.49	3.71
1995	4.24	4.01	4.40
2000	4.78	4.47	5.01
2005	4.21	3.87	4.46
2010	3.84	3.50	4.10
2015	3.57	3.22	3.82
2020	3.35	2.99	3.61
2025	3.16	2.80	3.43
2030	2.99	2.62	3.27
2035	2.84	2.46	3.13
2040	2.71	2.32	3.00
2045	2.58	2.18	2.88
2050	2.46	2.06	2.76
2055	2.35	1.95	2.66
2060	2.25	1.85	2.56
2065	2.15	1.76	2.46
2070	2.06	1.68	2.37
2075	1.98	1.60	2.29
2080	1.90	1.53	2.21
2085	1.83	1.47	2.13
2090	1.76	1.41	2.06
2095	1.70	1.35	2.00
2100	1.64	1.30	1.93

Table 3. Atmospheric Bromine (ppt = $1/10^{12}$)
Following Cut in all Halocarbon Emissions without Substitutes

year %cut	1995 100%	2000 100%	2005 100%	2000 90%	2000 80%	2000 50%	2000 0%
1985	18.2	18.2	18.2	18.2	18.2	18.2	18.2
1990	21.4	21.4	21.4	21.4	21.4	21.4	21.4
1995	24.4	24.4	24.4	24.4	24.4	24.4	24.4
2000	23.0	27.0	27.0	27.0	27.0	27.0	27.0
2005	22.0	25.3	29.3	25.7	26.0	27.0	29.3
2010	21.2	24.1	27.4	24.7	25.3	27.1	31.3
2015	20.6	23.1	26.0	24.0	24.8	27.3	33.2
2020	20.1	22.4	24.9	23.4	24.5	27.6	35.0
2025	19.7	21.8	24.0	23.0	24.2	27.9	36.6
2030	19.4	21.2	23.3	22.7	24.1	28.3	38.1
2035	19.1	20.8	22.7	22.4	23.9	28.6	39.5
2040	18.9	20.5	22.2	22.2	23.9	29.0	40.9
2045	18.6	20.1	21.7	22.0	23.8	29.3	42.2
2050	18.5	19.9	21.3	21.8	23.8	29.6	43.4
2055	18.3	19.6	21.0	21.7	23.8	30.0	44.5
2060	18.1	19.4	20.7	21.6	23.7	30.3	45.6
2065	18.0	19.2	20.4	21.4	23.7	30.6	46.6
2070	17.8	19.0	20.1	21.3	23.7	30.9	47.6
2075	17.7	18.8	19.9	21.3	23.7	31.2	48.6
2080	17.6	18.6	19.7	21.2	23.7	31.5	49.5
2085	17.5	18.4	19.5	21.1	23.7	31.7	50.3
2090	17.3	18.3	19.2	21.0	23.8	32.0	51.2
2095	17.2	18.1	19.1	20.9	23.8	32.2	51.9
2100	17.1	18.0	18.9	20.9	23.8	32.4	52.7

SECTION D

CHEMICAL KINETICS AND PHOTOCHEMICAL DATA FOR USE IN STRATOSPHERIC MODELING

1.0 Introduction

This compilation (JPL Publication 90-1) is the ninth evaluation of rate constants and photochemical cross sections prepared by the NASA Panel for Data Evaluation. The Panel was established in 1977 for the purpose of providing a critical tabulation of the latest kinetic and photochemical data for use in the modeling of stratospheric processes with particular emphasis on the ozone layer and its possible perturbation by anthropogenic and natural phenomena. Copies of the complete evaluation are available from the Jet Propulsion Laboratory, Documentation Section, 111-116B, California Institute of Technology, Pasadena, California, 91109.

2.0 Basis of the Recommendations

The recommended rate constants and cross sections are based on laboratory measurements. In order to provide recommendations that are as up to date as possible, preprints and written private communications are accepted, but only when it is expected that they will appear as published journal articles. In no cases are rate constants adjusted to fit observations of stratospheric concentrations. The Panel considers the question of consistency of data with expectations based on chemical kinetic theory, and when a discrepancy appears to exist, this fact is pointed out in the accompanying note. The major use of theoretical extrapolation of data is in connection with three-body reactions, in which the required pressure or temperature dependence is sometimes unavailable from laboratory measurements, and can be estimated by use of appropriate theoretical treatment. In the case of important rate constants for which no experimental data are available, the Panel may provide estimates of rate constant parameters based on analogy to similar reactions for which data are available.

3.0 Recent Changes and Current Needs of Laboratory Kinetics

There are approximately forty changes in the rate constant recommendations in the present evaluation, but these are, for the most part, minor. However, some notable improvements have been made in the photochemistry related to Antarctic ozone depletion, as discussed in more detail in later sections. Seventy-two new reactions have been added, many of which are related to the chemistry of hydrochlorofluorocarbons (HCFCs). These latter compounds are being considered as possible industrial alternatives to the fully halogenated chlorofluorocarbons, and the new reactions deal with the chemical fate of the HCFCs in the atmosphere. As in previous evaluations, some reactions thought to be unimportant in the atmosphere are, nevertheless, included for completeness and for possible applications to laboratory studies. A section dealing with laboratory data on heterogeneous chemistry has been added, although this field is not yet fully amenable to evaluation. The table of enthalpy data which, since the last evaluation (JPL Publication 87-41) has been included as an appendix, has been updated and extended.

At the time of publication of the previous evaluation, the phenomenon of Antarctic ozone depletion had focussed intense interest on three areas particularly relevant to polar chemistry: (1)

certain second-order reactions of halogen radicals, such as ClO + ClO and ClO + BrO; (2) heterogeneous chemistry, especially on polar stratospheric clouds; and (3) photochemical kinetics below about 220 K.

In the intervening two years, considerable progress has been made in establishing a database for gas phase (i.e., non-heterogeneous) polar photochemistry. The rates and product distributions of the bimolecular ClO and BrO reactions have been measured more accurately, and there has been further elucidation of the chemistry and photochemistry on the ClO dimer, which is now believed to exist in the atmosphere only in the symmetric form, ClOOCl. Some important gaps remain, however, such as the identity of the photolysis products of ClOOCl.

It is now well-recognized that heterogeneous processes are crucial to stratospheric chemistry in the polar regions, and may play roles in mid-latitudinal regions as well. The heterogeneous chemistry enhances the efficiency of the chlorine catalyzed destruction of stratospheric ozone by converting inactive "reservoir" species such as HCl and $ClONO_2$ to Cl_2 and HOCl. These compounds are photolyzed upon return of sunlight to the polar region, thereby enhancing the levels of active forms of chlorine such as atomic chlorine and the ClO radical. The particles also sequester nitrogen oxides from the stratosphere, in the form of absorbed HNO_3. Thus, the reformation of $ClONO_2$ is suppressed and accelerated ozone destruction occurs during the early Antarctic spring.

Laboratory experiments on heterogeneous chemistry are very complex compared to those for homogeneous chemistry, and experimental techniques are not as well developed. As a consequence, we are not able to make recommendations with the confidence, reliability, and well-defined uncertainty limits that have been characteristic of the homogeneous chemistry. Nonetheless, experiments by several groups have demonstrated a high surface efficiency for key reactions which shift the equilibrium between the chlorine reservoirs and the chemically active forms of chlorine. Quantitative application of the laboratory results to the stratospheric situation is difficult, however, because of uncertainties associated with the nature of the surfaces in question and problems relating to particle microphysics and thermochemistry. These issues are discussed in somewhat more detail in the section on heterogeneous processes.

As mentioned in the previous evaluation, relatively few kinetics measurements have been made below about 220 K, and rate constants for this temperature regime are obtained by extrapolation of data from higher temperatures, using a simple Arrhenius temperature coefficient. The accuracy of such extrapolations is somewhat questionable, however, because several key reactions seem to show non-Arrhenius temperature dependence in this regime. Additional experiments are needed in the 200 K region to verify the accuracy of rate data being used in the models.

3.1 O_x Reactions

The kinetics of the O, O_2, and O_3 system are relatively well-established. The ozone forming reaction, O + O_2 + M, is of fundamental importance in atmospheric chemistry because the extent of ozone destruction is determined by the relative rates of it and competing reactions such as O + O_3, O + NO_2, O + OH, and O + ClO. Thus, additional studies of the O + O_2 + M reaction, or of its relative rate compared to the competing reactions, would be useful at very low temperatures.

3.2 $O(^1D)$ Reactions

The recommended rate coefficients for the $O(^1D)$ reactions correspond to the rate of removal of $O(^1D)$, which includes both chemical reactions and physical quenching of the excited O atoms. Details on the branching ratios are given in the notes in JPL Publication 90-1.

The $O(^1D)$ reactions of 17 fluorine-containing compounds have been added to this review. Most of the compounds are hydrogen-containing fluorocarbons and chlorofluorocarbons that are under consideration as replacements for CFMs. These compounds are reactive toward OH radicals or are photolyzed, so the $O(^1D)$ reactions will generally be minor atmospheric loss processes. On the other hand, SF_6, CF_4, and C_2F_6 do not react with OH and are not readily photolyzed, so the $O(^1D)$ reactions could play an important role in their atmospheric degradation. The small amount of data available on these compounds indicates that the rate coefficients are relatively small, and there is no evidence of significant chemical reaction. The database for most of the new reactions is sparse, and additional measurements of the rate coefficients and branching ratios would be useful.

The kinetic energy or hot atom effects of photolytically generated $O(^1D)$ are probably not important in the atmosphere, although the literature is rich with studies of these processes and with studies of the dynamics of many $O(^1D)$ reactions. The important atmospheric reactions of $O(^1D)$ include: (1) deactivation by major gases, N_2 and O_2, which limit the $O(^1D)$ steady state concentrations; (2) reaction with trace gases, e.g., H_2O, CH_4, and N_2O, which generate radicals; and (3) reaction with long lived trace gases, e.g., HCN, which have relatively slow atmospheric degradation rates. Studies of the $O(^1D)$ reactions with HCN, CF_4, C_2F_6, and SF_6 would contribute to defining the atmospheric lifetimes of these minor species.

3.3 HO$_x$ Reactions

There has been little change in the database for HO_x chemistry since the last evaluation. The OH + HO_2 rate coefficient has been changed slightly to reflect the latest published data. The rate coefficient for the OH + H_2O_2 reaction at 298 K has not been changed, although the Arrhenius parameters have been revised slightly and the data set has been reevaluated to account for revisions in the H_2O_2 UV absorption cross section recommendations. The HO_2 + O_3 reaction rate coefficient remains one of the most significant uncertainties in the HO_x system. High quality data at low temperatures are needed for this key reaction.

3.4 NO$_x$ Reactions

The changes to the database for NO_x reactions are relatively minor. There are new entries for the reactions of OH and HO_2 with NO_3, and for the bimolecular channel of the NO_2 + NO_3 reaction, for which the first direct evidence for the channel giving NO + NO_2 + O_2 is presented. Whether or not this channel actually occurs is still a matter of some controversy, however. There have been some minor updates and revisions to the reactions N + O_2, N + O_3, and NO_2 + O_3.

As noted in the previous evaluation, a few of the important reactions in the NO_x family require additional work. These include the reactions which produce and remove peroxynitric acid, HO_2NO_2. Additional studies of the HO_2 + NO_2 + M recombination are needed, focusing on the temperature dependence of the low pressure limit. In addition, the temperature dependence of the important OH + HO_2NO_2 reaction is still poorly characterized. Additional work on the reactions of NH_2 radicals and subsequent oxidation steps are necessary, particularly under atmospheric conditions.

3.5 Hydrocarbon Oxidation

Our understanding of hydrocarbon oxidation in the atmosphere has improved considerably in the past few years. All hydrocarbons are released at the surface of the earth, and their degradation in the troposphere is initiated by reaction with OH (and with ozone in the case of olefins). Depending on their reactivity with OH, only a fraction of the surface flux of

hydrocarbons is transported to the stratosphere, where their oxidation serves as a source of water vapor. In addition, the reaction of atomic chlorine with these hydrocarbons (mainly CH_4) constitutes one of the major sink mechanisms for active chlorine. Even though CH_4 is the predominant hydrocarbon in the stratosphere, we have included in this evaluation certain reactions of a few heavier hydrocarbon species.

In the stratosphere, CH_4 oxidation leads initially to formation of CH_3, which immediately is converted to CH_3O_2. Some of the subsequent chemistry is not clear, primarily because the key reaction of CH_3O_2 with HO_2 is not well-characterized, even though there have been three new studies of this reaction. Not all the products of the reaction have been identified. Some of the recent work suggests that, in addition to CH_3OOH, CH_2O is also formed. Our understanding of the reaction between OH and CH_3OOH has improved significantly since the last evaluation. Even though the rate constants for some of the reactions mentioned above are not well-defined, the effects of these uncertainties on stratospheric ozone perturbation are negligible.

One area of hydrocarbon oxidation which has seen a great deal of improvement is that of product analysis. However, some additional work may be required to measure branching ratios for reactions such as $CH_3O_2 + CH_3O_2$ and $CH_3O_2 + HO_2$.

The rates of the reactions of higher hydrocarbons with OH are sufficiently well-measured to permit their rate of transport to the stratosphere to be calculated. However, the oxidation scheme for these hydrocarbons has not been fully elucidated. In most cases, it is expected that the radicals formed from the initial OH or Cl attack will follow courses analogous to that of CH_3, and ultimately lead to CO. In this evaluation, we have included some, but not all, of the reactions in the oxidation of ethane to CO. We have also added the reactions of OH with CH_3OH and C_2H_5OH, the most abundant alcohols in the stratosphere.

3.6 Halogen Chemistry

The kinetics database for halogen reactions has shown significant expansion and improvement since the previous evaluation. It now contains rate coefficients for the reaction of OH with a large number of potential alternatives to the fully halogenated CFCs, [nine hydrochlorofluorocarbons (HCFCs) and eleven hydrofluorocarbons (HFCs)]. The chemistry of these species in the troposphere is controlled by their reactions with OH whereby a hydrogen atom is abstracted and a hydrocarbon radical produced. There are now also upper limits for the rate constants for the reactions of OH with four brominated fully halogenated halocarbons (Halons). Other new entries include several reactions of Cl_2O_2, the dimer formed by recombination of two ClO radicals, several reactions of OClO, and reactions of NO_3 with several bromine species. The important recombination of ClO radicals to produce Cl_2O_2 has now been directly studied under polar stratospheric conditions and found to be significantly slower than had been believed on the basis of earlier studies. The bimolecular channels for the ClO + ClO reaction have been shown to be unimportant under the same conditions. The important BrO + ClO reaction has now been directly studied under polar stratospheric conditions, and has been found to proceed through three reaction channels for which reliable temperature dependent rate expressions have been derived. With these expansions and improvements, the kinetics database for homogeneous reactions of halogen species appears to be relatively well established.

3.7 SO$_x$ Reactions

The database on homogeneous sulfur chemistry has seen only minor changes in the recommendations for the reactions that were included in the previous evaluation. However, this section has been expanded significantly to include many reactions that are important in the atmospheric oxidation of reduced compounds of natural and anthropogenic origin. These new entries include the reactions of OH and NO_3 radicals with simple organic sulfides, as well as

several reactions representing the oxidation of the radical products CH_3S and CH_3SO. There have not been significant improvements in our understanding of the oxidation of SO_2 into sulfuric acid, although there have been several direct measurements of the $HOSO_2$ intermediate. There is still a need for further information on the atmospheric reactivity of this species and, perhaps, even on reactions involving its possible complexes with O_2 or H_2O. Along these same lines, further information on the reactions of SO_3 with other atmospheric species is needed to assess the competition of these reactions with SO_3 hydrolysis. Finally, further details have been provided on the mechanism for CS_2 atmospheric oxidation. The database has also been expanded to include the reactions of NO_3 with both OCS and CS_2.

3.8 Metal Chemistry

Sodium is deposited in the upper atmosphere by meteors along with larger amounts of silicon, magnesium, and iron; comparable amounts of aluminum, nickel, and calcium; and smaller amounts of potassium, chromium, manganese, and other elements. The interest is greatest in the alkali metals because they form the least stable oxides and thus free atoms can be regenerated through photolysis and reactions with O and O_3. The other meteoric elements are expected to form more stable oxides.

The total flux of alkali metals through the atmosphere is relatively small, e.g., one or two orders of magnitude less than CFCs. Therefore extremely efficient catalytic cycles are required in order for Na to have a significant effect on stratospheric chemistry. There are no measurements of metals or metal compounds in the stratosphere which indicate a significant role.

It has been proposed that the highly polar metal compounds may polymerize to form clusters and that the stratospheric concentrations of free metal compounds are too small to play a significant role in the chemistry.

Some studies have shown that the polar species NaO and NaOH associate with abundant gases such as O_2 and CO_2 with very fast rates in the atmosphere. It has been proposed that reactions of this type will lead to the production of clusters with many molecules attached to the sodium compounds. Photolysis is expected to compete with the association reactions and to limit the cluster concentrations in daylight. If atmospheric sodium does form large clusters, it is unlikely that Na species can have a significant role in stratospheric ozone chemistry. In order to assess the importance of these processes, data are needed on the association rates and the photolysis rates involving the cluster species.

3.9 Photochemical Cross Sections

Absorption spectra of a few species which have highly structured spectra have now been included in graphical, as well as tabular, form (JPL Publication 90-1). These figures are only a guide to the spectra, and should not be used for quantitative purposes, because the measured cross sections may be resolution dependent. Spectra of the haloethanes have been included to show the shape of the spectra.

The absorption cross sections of the Cl_2O_2 molecule formed by the association of two ClO radicals have also been included. The quantum yield for the photo-dissociation of the dimer is believed to be unity. The products have not been established, although it is probable that Cl + ClOO are produced with unit efficiency.

The cross sections for many halocarbons which are expected to be replacements for the chlorofluoromethanes have been included and the cross sections for bromocarbons updated.

79

The temperature dependence of the absorption cross sections of species such as HO_2NO_2 and H_2O_2 in the 300 nm region may be important. We have thus included the measured temperature dependence for H_2O_2 in this latest evaluation. Data on HO_2NO_2 are not available. In the case of haloethanes, there are large discrepancies between the available sets of data and, therefore, we have not included these results. Additional laser experiments are needed.

The recommendation for the wavelength dependence of the $O(^1D)$ quantum yield in ozone photolysis has been modified to represent more closely the results obtained from laser photolysis experiments. The latter have better resolution than the earlier monochromator measurements, and thus are believed to reproduce the fall-off behavior more accurately. However, the laser results are not in complete agreement, particularly at the longest wavelengths. Furthermore, the temperature dependence of the $O(^1D)$ quantum yield has not been measured using laser sources, and it was necessary in this evaluation to use monochromator results for the temperature dependence. The laser experiments should be performed.

4.0 Atmospheric Chemistry

4.1 Overview

The ozone content of earth's atmosphere can be considered to exist in three distinct regions; the troposphere, stratosphere, and mesosphere. The unpolluted troposphere contains small amounts of ozone, which come from both downward transport from the stratosphere and from in situ photochemical production. The chemistry of the global troposphere is complex, with both homogeneous and heterogeneous (e.g., rain-out) processes playing important roles. The homogeneous chemistry is governed by coupling between the carbon, nitrogen, hydrogen, and oxygen systems and can be considered to be more complex than the chemistry of the stratosphere, due to the presence of higher hydrocarbons, long photochemical relaxation times, higher total pressures, and the high relative humidity which may affect the reactivity of certain key species such as HO_2. Significant progress is being made in understanding the coupling among the different chemical systems, especially the mechanism of methane oxidation which partially controls the odd hydrogen budget. This is an important development, as reactions of the hydroxyl radical are the primary loss mechanism for compounds containing C-H (CH_4, CH_3Cl, CHF_2Cl, etc.) or C=C (C_2Cl_4, C_2HCl_3, C_2H_4, etc.), thus limiting the fraction transported into the stratosphere.

The stratosphere is the region of the atmosphere where the bulk of the ozone resides, with the concentration reaching a maximum value of about 5×10^{12} molecule cm^{-3} at an altitude of ~25 km. Ozone in the stratosphere is removed predominantly by catalytic processes, but assignment of the relative importance of different catalytic cycles and the prediction of their future impact are dependent on a detailed understanding of chemical reactions which form, remove and interconvert the catalytic species. A model calculation of stratospheric composition may include some 150 chemical reactions and photochemical processes, which vary greatly in their importance in controlling the density of ozone. Laboratory measurements of the rates of these reactions have progressed rapidly in recent years, and have given us a basic understanding of the processes involved, particularly in the upper stratosphere. Despite the basically sound understanding of overall stratospheric chemistry which presently exists, much remains to be done to quantify errors, to identify reaction channels positively, and to measure reaction rates both under conditions corresponding to the lower stratosphere (~210 K, ~75 torr), as well as the top of the stratosphere (~270 K, ~1 torr). As previously mentioned, Antarctic conditions require the consideration of even lower temperatures.

The chemistry of the upper stratosphere, i.e. 30-50 km, is thought to be reasonably well defined, although there appear to be some significant differences between the predicted and observed chemical composition of this region of the atmosphere, which may be due to inaccurate

rate data or missing chemistry. In this region, the composition of the atmosphere is predominantly photochemically controlled, and the photolytic lifetimes of temporary reservoir species such as $HOCl$, HO_2NO_2, $ClONO_2$, N_2O_5 and H_2O_2 are short; and, hence, they play a minor role. Thus, the important processes above 30 km all involve atoms and small molecules. The majority of laboratory studies of these reactions have been carried out under the conditions of pressure and temperature which are encountered in the upper stratosphere, and their overall status appears to be good. No significant changes in rate coefficients for the key reactions, such as $Cl + O_3$, $NO + ClO$, $NO + O_3$, etc., have occurred in the last few years. Historically, a major area of concern in the chemistry of the upper stratosphere has involved the reaction between HO and HO_2 radicals, which has had considerable uncertainty in the rate constant. This HO_x termination reaction plays an important role in determining the absolute concentrations of HO and HO_2, and since HO plays a central role in controlling the catalytic efficiencies of both NO_x and ClO_x, it is a reaction of considerable importance. The uncertainty in the rate coefficient for the reaction is thought to be about a factor of 1.3 to 1.8 over the range of atmospheric conditions. It should be noted that the $HO + H_2O_2$, $HO + HNO_3$ and $HO + HO_2NO_2$ reactions have little effect on controlling the HO_x concentrations above 30 km. For reactions such as $O + HO$ and $O + HO_2$, which control the HO_x radical partitioning above 40 km, the database can be considered to be quite good.

One area in which additional studies may be needed is that of excited state chemistry, i.e., studies to determine whether electronic or vibrational states of certain atmospheric constituents may be more important than hitherto recognized. Possible examples are O_2^*, O_3^*, HO^*, or N_2^*.

The chemistry of the lower stratosphere is quite complex, with significant coupling between the HO_x, NO_x and ClO_x families. In this region of the atmosphere (15-30 km), both dynamics and photochemistry play key roles in controlling the trace gas distributions. It is also within this region that the question of the pressure and temperature dependences of the rate coefficients is most critical, due to the low temperatures (210 K and lower) and the high total pressures (30-200 torr).

4.2   Heterogeneous Effects

A continuing question in stratospheric modeling is whether or not aerosols perturb the homogeneous chemistry to a significant degree. As mentioned earlier, this question has assumed much greater importance in connection with the role of polar stratospheric clouds in Antarctic chemistry. On a global scale, effects have been suggested through the following processes:

(1) Surface catalysis of chemical reactions.

(2) Production or removal of active species.

(3) Effects of aerosol precursors such as SO_2.

In NASA Reference Publications 1010 and 1049, processes 1 and 2 above were discussed in general terms. It was shown that, with a few possibly significant exceptions, surface catalysis of chemical reactions is not expected to compete with the rates of homogeneous gas phase reactions. The essential reason is that the frequency of collision of a gas phase molecule with the aerosol surface is typically of the order of 10^{-5} sec^{-1}, whereas most of the key gas phase reactions occur with much greater frequency, for example, conversion of atomic chlorine to HCl by the $Cl + CH_4$ reaction (10^{-2} sec^{-1}). Thus, even in the unlikely case of unit reaction efficiency on the aerosol surface the heterogeneous process cannot be significant. Possible exceptions occur for reactions which are extremely slow in the gas phase, such as hydrolysis of an anhydride, as in the reaction $N_2O_5 + H_2O \rightarrow 2HNO_3$. There remains some uncertainty with regard to the role of these latter processes.

It was also shown in NASA Publications 1010 and 1049 that there is no evidence that aerosols serve as significant sources or sinks of the major active species such as chlorine compounds. However, it has been suggested that dust particles of meteoritic origin may scavenge metallic atoms and ions and, in particular, may remove Na diffusing from the mesosphere in the form of absorbed NaOH or Na_2SO_4.

Although it appears that aerosols do not greatly perturb the ambient concentrations of active species through direct interaction with the surfaces, the aerosol precursors may significantly perturb the stratospheric cycles through removal of species such as OH radicals. For example, a large injection of SO_2, such as that which occurred in the El Chichon eruption, has the potential of significantly depleting HO_x radical concentrations. It must be reiterated, however, that recent studies of the mechanism of SO_2 oxidation have shown that OH plays a catalytic role, and, therefore, the process does not result in a net loss of OH from the system.

The effects of aerosols on the radiation field and on the temperature may also need to be considered. These effects are probably small, however.

There are two problems with regard to detecting the effects of aerosol injections such as that following the El Chichon eruption. One is that no adequate baseline exists for the unperturbed atmosphere, and therefore a given observation cannot unambiguously be assigned to the enhanced presence of the aerosol loading. A second problem is that, as already discussed, the effects are expected to be subtle and probably of small magnitude. Thus, in spite of large changes that may occur in the aerosol content of the lower stratosphere, effects on the chemical balance will be difficult to detect.

5.0   Rate Constant Data

In Table 1 (Rate Constants for Second Order Reactions) the reactions are grouped into the classes O_x, $O(^1D)$, HO_x, NO_x, Hydrocarbon Reactions, ClO_x, BrO_x, FO_x, and SO_x. The data in Table 2 (Rate Constants for Three-Body Reactions), while not grouped by class, are presented in the same order as the bimolecular reactions. Further, the presentation of photochemical cross section data follows the same sequence.

5.1   Bimolecular Reactions

Some of the reactions in Table 1 are actually more complex than simple two-body reactions. To explain the anomalous pressure and temperature dependences occasionally seen in reactions of this type, it is necessary to consider the bimolecular class of reactions in terms of two subcategories, direct (concerted) and indirect (non-concerted) reactions.

A direct or concerted bimolecular reaction is one in which the reactants A and B proceed to products C and D without the intermediate formation of an AB adduct which has appreciable bonding, i.e., no stable A-B molecule exists, and there is no reaction intermediate other than the transition state of the reaction, $(AB)^{\#}$.

$$A + B \rightarrow (AB)^{\#} \rightarrow C + D$$

The reaction of OH with CH_4 forming $H_2O + CH_3$ is an example of a reaction of this class.

Very useful correlations between the expected structure of the transition state $(AB)^{\#}$ and the A-factor of the reaction rate constant can be made, especially in reactions which are constrained

to follow a well-defined approach of the two reactants in order to minimize energy requirements in the making and breaking of bonds. The rate constants for these reactions are well represented by the Arrhenius expression $k = A \exp(-E/RT)$ in the 200-300 K temperature range. These rate constants are not pressure dependent.

The indirect or non-concerted class of bimolecular reactions is characterized by a more complex reaction path involving a potential well between reactants and products, leading to a bound adduct (or reaction complex) formed between the reactants A and B:

$$A + B \rightarrow (AB)^* \rightarrow C + D$$

The intermediate $(AB)^*$ is different from the transition state $(AB)^\#$, in that it is a bound molecule which can, in principle, be isolated. (Of course, transition states are involved in all of the above reactions, both forward and backward, but are not explicitly shown.) An example of this reaction type is ClO + NO, which normally produces $Cl + NO_2$ as a bimolecular product, but which undoubtedly involves ClONO (chlorine nitrite) as an intermediate. This can be viewed as a chemical activation process forming $(ClONO)^*$ which decomposes to the ultimate products, $Cl + NO_2$. Reactions of the non-concerted type can have a more complex temperature dependence, can exhibit a pressure dependence if the lifetime of $(AB)^*$ is comparable to the rate of collisional deactivation of $(AB)^*$. This arises because the relative rate at which $(AB)^*$ goes to products $C + D$ vs. reactants $A + B$ is a sensitive function of its excitation energy. Thus, in reactions of this type, the distinction between the bimolecular and termolecular classification becomes less meaningful, and it is especially necessary to study such reactions under the temperature and pressure conditions in which they are to be used in model calculations.

The rate constant tabulation for second-order reactions (Table 1) is given in Arrhenius form: $k(T) = A \exp((-E/R)(1/T))$ and contains the following information:

(1) Reaction stoichiometry and products (if known). The pressure dependences are included, where appropriate.

(2) Arrhenius A-factor.

(3) Temperature dependence and associated uncertainty ("activation temperature" $E/R +/- \Delta E/R$).

(4) Rate constant at 298 K.

(5) Uncertainty factor at 298 K.

5.2 Termolecular Reactions

Rate constants for 3rd order reactions (Table 2) of the type $A + B \leftrightarrow (AB)^* \rightarrow AB$ are given in the form

$$k_0(T) = k_0^{300}(T/300)^{-n} \text{ cm}^6 \text{ molecule}^{-2} \text{ s}^{-1}$$

(where the value is suitable for air as the third body), together with the recommended value of n. Where pressure fall-off corrections are necessary, an additional entry gives the limiting high pressure rate constant in a similar form:

$$k_\infty(T) = k_\infty^{300}(T/300)^{-m} \text{ cm}^3 \text{ molecule}^{-1} \text{ s}^{-1}$$

To obtain the effective second-order rate constant for a given condition of temperature and pressure (altitude), the following formula is used:

$$k(Z) = k(M,T) = (\{k_0(T)[M]\}/\{1+k_0(T)[M]/k_\infty(T)\})0.6^{\frac{1}{\alpha}}$$

where

$$\alpha = 1 + \{\log_{10}(k_0(T)[M]/k_\infty(T))\}^2$$

The fixed value 0.6 which appears in this formula fits the data for all listed reactions adequately, although in principle this quantity may be different for each reaction.

Thus, a compilation of rate constants of this type requires the stipulation of the four parameters, $k_0(300)$, n, $k_\infty(300)$, and m. These can be found in Table 2. The discussion that follows outlines the general methods we have used in establishing this table.

5.2.1 Low-Pressure Limiting Rate Constant [$k^x_0(T)$]

Troe (J. Chem. Phys. 66, 4745 (1977)) has described a simple method for obtaining low-pressure limiting rate constants. In essence this method depends on the definition:

$$k^x_0(T) = \beta_x k^x_{0,sc}(T)$$

Here sc signifies "strong" collisions, x denotes the bath gas, and β_x is an efficiency parameter $(0 < \beta_x < 1)$, which provides a measure of energy transfer.

The coefficient β_x is related to the average energy transferred in a collision with gas x, $<\Delta E>_x$, via:

$$\beta_x/(1-\beta_x^{0.5}) = <\Delta E>_x/F_E kT$$

Notice that $<\Delta E>_x$ is quite sensitive to β. F_E is the correction factor of the energy dependence of the density of states (a quantity of the order of 1.1 for most species of stratospheric interest).

For many of the reactions of possible stratospheric interest reviewed here, there exist data in the low-pressure limit (or very close thereto), and we have chosen to evaluate and unify this data by calculating $k^x_{0,sc}(T)$ for the appropriate bath gas x and computing the value of β_x corresponding to the experimental value. A recent compilation (Patrick and Golden, Int. J. Chem. Kinet. 15, 1189 (1983)) gives details for many of the reactions considered here.

From the β_x values (most of which are for N_2, i.e., β_{N2}), we compute $<\Delta E>_x$ according to the above equation. Values of $<\Delta E>_{N2}$ of approximately 0.3 - 1.0 kcal mole[-1] are generally expected. If multiple data exist, we average the values of $<\Delta E>_{N2}$ and recommend a rate constant corresponding to the β_{N2} computed in the equation above.

Where no data exist we have estimated the low-pressure rate constant by taking $\beta_{N2} = 0.3$ at T = 300 K, a value based on those cases where data exist.

5.2.2 Temperature Dependence of Low-Pressure Limiting Rate Constants: n

The value of n recommended here comes from a calculation of $<\Delta E>_{N2}$ from the data at 300 K, and a computation of $\beta_{N2}(200\ K)$ assuming that $<\Delta E>_{N2}$ is independent of temperature in this range. This $\beta_{N2}(200\ K)$ value is combined with the computed value of $k_{0,sc}(200\ K)$ to give

the expected value of the actual rate constant at 200 K. This latter in combination with the value at 300 K yields the value of n.

This procedure can be directly compared with measured values of $k_0(200$ K) when those exist. Unfortunately, very few values at 200 K are available. There are often temperature-dependent studies, but some ambiguity exists when one attempts to extrapolate these down to 200 K. If data are to be extrapolated beyond the measured temperature range, a choice must be made as to the functional form of the temperature dependence. There are two general ways of expressing the temperature dependence of rate constants. Either the Arrhenius expression $k_0(T) = A\exp(-E/RT)$ or the form $k_0(T) = A'T^{-n}$ is employed. Since neither of these extrapolation techniques is soundly based, and since they often yield values that differ substantially, we have used the method explained earlier as the basis of our recommendations.

5.2.3 High-Pressure Limit Rate Constants, $k_\infty(T)$

High-pressure rate constants can often be obtained experimentally, but those for the relatively small species of atmospheric importance usually reach the high-pressure limit at inaccessibly high pressures. This leaves two sources of these numbers, the first being guesses based upon some model, and the second being extrapolation of fall-off data up to higher pressures. Stratospheric conditions generally render reactions of interest much closer to the low-pressure limit, and thus are fairly insensitive to the high-pressure value. This means that while the extrapolation is long, and the value of $k_\infty(T)$ not very accurate, a "reasonable guess" of $k_\infty(T)$ will then suffice. In some cases we have declined to guess since the low-pressure limit is effective over the entire range of stratospheric conditions.

5.2.4 Temperature Dependence of High-Pressure Limit Rate Constants: m

There are very little data upon which to base a recommendation for values of m. Values in Table 2 are estimated, based on models for the transition state of bond association reactions and whatever data are available.

5.2.5 Isomer Formation

A particular problem with association reactions arises when there are easily accessible isomeric forms of the molecule AB. In this situation, if the laboratory measurement of the rate constant is accomplished by following the disappearance of reactants, the value ascertained may be the sum of two or more processes that should be measured and tabulated independently. A specific example of such a case is found in Table 2 for the reactions of Cl-atoms with NO_2. These reactants may come together to form either $ClNO_2$ or $ClONO$. Whether or not isomer formation, such as discussed above, is important depends on the relative stability of the possible products. At the moment the only case that we are sure about is the above example. In the past however, there was some thought that data on the reaction between ClO radicals and NO_2 could be understood only in terms of the formation of both chlorine nitrate ($ClONO_2$) and other isomers ($ClOONO$, $OClONO$). Experiments have shown that this is not the case and that chlorine nitrate is the sole product.

There are many other possibilities for isomer formation in the reactions listed in Table 2. Even for reactions where no mention is made of isomers, because we felt that they could not contribute under atmospheric conditions, extrapolation to higher pressures and lower temperatures should be done with the possibilities kept in mind.

5.3 Uncertainty Estimates

For second-order rate constants in Table 1, an estimate of the uncertainty at any given temperature may be obtained from the following expression:

$$f(T) = f(298)\exp((\Delta E/R)(1/T - 1/298))$$

An upper or lower bound (corresponding approximately to one standard deviation) of the rate constant at any temperature T can be obtained by multiplying or dividing the value of the rate constant at that temperature by the factor f(T). The quantities f(298) and $\Delta E/R$ are, respectively, the uncertainty in the rate constant at 298 K and in the Arrhenius temperature coefficient, as listed in Table 1. This approach is based on the fact that rate constants are almost always known with minimum uncertainty at room temperature. The overall uncertainty normally increases at other temperatures, because there are usually fewer data and it is almost always more difficult to make measurements at other temperatures. It is important to note that the uncertainty at a temperature T cannot be calculated from the expression $\exp(\Delta E/RT)$. The above expression for f(T) must be used to obtain the correct result.

The uncertainty represented by f(298) is normally symmetric; i.e., the rate constant may be greater than or less than the central value, k(298), by the factor f(298). In a few cases in Table 1 asymmetric uncertainties are given in the temperature coefficient.

For these cases, the factors by which a rate constant are to be multiplied or divided to obtain, respectively, the upper and lower limits are not equal, except at 298 K where the factor is simply f(298K). Explicit equations are given below for the case where the temperature dependence is (E/R +a, -b):

For T > 298K, multiply by the factor

$$f(298K) \times e^{[a \times (1/298-1/T)]}$$

and divide by the factor

$$f(298K) \times e^{[b \times (1/298-1/T)]}.$$

For T < 298K, multiply by the factor

$$f(298K) \times e^{[b \times (1/T-1/298)]}$$

and divide by the factor
$$f(298K) \times e^{[a \times (1/T-1/298)]}.$$

For three-body reactions (Table 2) a somewhat analogous procedure is used. Uncertainties expressed as increments to k_0 and k_∞ are given for these rate constants at room temperature. The additional uncertainty arising from the temperature extrapolation is expressed as an uncertainty in the temperature coefficients n and m.

The assigned uncertainties represent the subjective judgment of the Panel. They are not determined by a rigorous, statistical analysis of the database, which generally is too limited to permit such an analysis. Rather, the uncertainties are based on a knowledge of the techniques, the difficulties of the experiments, and the potential for systematic errors. There is obviously no way to quantify these "unknown" errors. The spread in results among different techniques for a given reaction may provide some basis for an uncertainty, but the possibility of the same, or

86

compensating, systematic errors in all the studies must be recognized. Furthermore, the probability distribution may not follow the normal, Gaussian form. For measurements subject to large systematic errors, the true rate constant may be much further from the recommended value than would be expected based on a Gaussian distribution with the stated uncertainty. As an example, the recommended rate constants for the reactions $HO_2 + NO$ and $Cl + ClONO_2$ have changed by factors of 30-50, occurrences which could not have been allowed for with any reasonable values of σ in a Gaussian distribution.

5.4 Units

The rate constants are given in units of concentration expressed as molecules per cubic centimeter and time in seconds. Thus, for first-, second-, and third-order reactions the units of k are s^{-1}, cm^3 molecule^{-1} s^{-1}, and cm^6 molecule^{-2} s^{-1}, respectively. Cross sections are expressed as cm^2 molecule^{-1}, base e.

Table 1. Rate Constants for Second Order Reactions[a]

Reaction	A-Factor[a]	E/R±(ΔE/R)	k(298 K)	f(298)[b]
O_x Reactions				
$O + O_2 \xrightarrow{M} O_3$	(See Table 2)			
$O + O_3 \rightarrow O_2 + O_2$	8.0×10^{-12}	2060 ± 250	8.0×10^{-15}	1.15
$O(^1D)$ Reactions				
$O(^1D) + N_2O \rightarrow N_2 + O_2$	4.9×10^{-11}	0 ± 100	4.9×10^{-11}	1.3
$\rightarrow NO + NO$	6.7×10^{-11}	0 ± 100	6.7×10^{-11}	1.3
$O(^1D) + H_2O \rightarrow OH + OH$	2.2×10^{-10}	0 ± 100	2.2×10^{-10}	1.2
$O(^1D) + CH_4 \rightarrow OH + CH_3$	1.4×10^{-10}	0 ± 100	1.4×10^{-10}	1.2
$\rightarrow H_2 + CH_2O$	1.4×10^{-11}	0 ± 100	1.4×10^{-11}	1.2
$O(^1D) + H_2 \rightarrow OH + H$	1.0×10^{-10}	0 ± 100	1.0×10^{-10}	1.2
$O(^1D) + N_2 \rightarrow O + N_2$	1.8×10^{-11}	$-(110 \pm 100)$	2.6×10^{-11}	1.2
$O(^1D) + N_2 \xrightarrow{M} N_2O$	(See Table 2)			
$O(^1D) + O_2 \rightarrow O + O_2$	3.2×10^{-11}	$-(70 \pm 100)$	4.0×10^{-11}	1.2
$O(^1D) + CO_2 \rightarrow O + CO_2$	7.4×10^{-11}	$-(120 \pm 100)$	1.1×10^{-10}	1.2
$O(^1D) + O_3 \rightarrow O_2 + O_2$	1.2×10^{-10}	0 ± 100	1.2×10^{-10}	1.3
$\rightarrow O_2 + O + O$	1.2×10^{-10}	0 ± 100	1.2×10^{-10}	1.3
$O(^1D) + HCl \rightarrow products$	1.5×10^{-10}	0 ± 100	1.5×10^{-10}	1.2
$O(^1D) + HF \rightarrow OH + F$	1.4×10^{-10}	0 ± 100	1.4×10^{-10}	2.0
$O(^1D) + HBr \rightarrow products$	1.5×10^{-10}	0 ± 100	1.5×10^{-10}	2.0
$O(^1D) + Cl_2 \rightarrow products$	2.8×10^{-10}	0 ± 100	2.8×10^{-10}	2.0
$O(^1D) + CCl_4 \rightarrow products$	3.3×10^{-10}	0 ± 100	3.3×10^{-10}	1.2
$O(^1D) + CFCl_3 \rightarrow products$	2.3×10^{-10}	0 ± 100	2.3×10^{-10}	1.2
$O(^1D) + CF_2Cl_2 \rightarrow products$	1.4×10^{-10}	0 ± 100	1.4×10^{-10}	1.3
$O(^1D) + CF_4 \rightarrow CF_4 + O$	-	-	$< 1.8 \times 10^{-13}$	-
$O(^1D) + CCl_2O \rightarrow products$	3.6×10^{-10}	0 ± 100	3.6×10^{-10}	2.0

Table 1. (Continued)

Reaction	A-Factor[a]	E/R±(ΔE/R)	k(298 K)	f(298)[b]
$O(^1D)$ + CFClO → products	1.9×10^{-10}	0±100	1.9×10^{-10}	2.0
$O(^1D)$ + CF_2O → products	7.4×10^{-11}	0±100	7.4×10^{-11}	2.0
$O(^1D)$ + NH_3 → OH + NH_2	2.5×10^{-10}	0±100	2.5×10^{-10}	1.3
$O(^1D)$ + $CHFCl_2$ → products	1.9×10^{-10}	0±100	1.9×10^{-10}	1.3
$O(^1D)$ + CHF_2Cl → products	9.5×10^{-11}	0±100	9.5×10^{-11}	1.3
$O(^1D)$ + CHF_3 → products	8.4×10^{-12}	0±100	8.4×10^{-12}	5.0
$O(^1D)$ + CH_2F_2 → products	9×10^{-11}	0±100	9×10^{-11}	3.0
$O(^1D)$ + CH_3F → products	1.4×10^{-10}	0±100	1.4×10^{-10}	2.0
$O(^1D)$ + $CHCl_2CF_3$ → products	2.2×10^{-10}	0±100	2.2×10^{-10}	2.0
$O(^1D)$ + $CHFClCF_3$ → products	1×10^{-10}	0±100	1×10^{-10}	3.0
$O(^1D)$ + CHF_2CF_3 → products	5×10^{-11}	0±100	5×10^{-11}	3.0
$O(^1D)$ + CH_2ClCF_2Cl → products	1.6×10^{-10}	0±100	1.6×10^{-10}	2.0
$O(^1D)$ + CH_2ClCF_3 → products	1.5×10^{-10}	0±100	1.5×10^{-10}	2.0
$O(^1D)$ + CH_2FCF_3 → products	1×10^{-10}	0±100	1×10^{-10}	3.0
$O(^1D)$ + CH_3CFCl_2 → products	1.5×10^{-10}	0±100	1.5×10^{-10}	3.0
$O(^1D)$ + CH_3CF_2Cl → products	1.4×10^{-10}	0±100	1.4×10^{-10}	2.0
$O(^1D)$ + CH_3CF_3 → products	1.0×10^{-10}	0±100	1.0×10^{-10}	3.0
$O(^1D)$ + CH_3CHF_2 → products	1×10^{-10}	0±100	1×10^{-10}	3.0
$O(^1D)$ + C_2F_6 → O + C_2F_6	-	-	$<2 \times 10^{-13}$	-
$O(^1D)$ + SF_6 → products	-	-	$<4.5 \times 10^{-14}$	-

HO_x Reactions

H + O_2 $\xrightarrow{M}$ HO_2	(See Table 2)			
H + O_3 → OH + O_2	1.4×10^{-10}	470±200	2.9×10^{-11}	1.25
H + HO_2 → products	8.1×10^{-11}	0±200	8.1×10^{-11}	1.3

Table 1. (Continued)

Reaction	A-Factor[a]	E/R±(ΔE/R)	k(298 K)	f(298)[b]
O + OH → O$_2$ + H	2.2×10^{-11}	-(120±100)	3.3×10^{-11}	1.2
O + HO$_2$ → OH + O$_2$	3.0×10^{-11}	-(200±100)	5.9×10^{-11}	1.2
O + H$_2$O$_2$ → OH + HO$_2$	1.4×10^{-12}	2000±1000	1.7×10^{-15}	2.0
OH + HO$_2$ → H$_2$O + O$_2$	4.8×10^{-11}	-(250±200)	1.1×10^{-10}	1.3
OH + O$_3$ → HO$_2$ + O$_2$	1.6×10^{-12}	940±300	6.8×10^{-14}	1.3
OH + OH → H$_2$O + O	4.2×10^{-12}	240±240	1.9×10^{-12}	1.4
$\xrightarrow{M}$ H$_2$O$_2$	(See Table 2)			
OH + H$_2$O$_2$ → H$_2$O + HO$_2$	2.9×10^{-12}	160±100	1.7×10^{-12}	1.2
OH + H$_2$ → H$_2$O + H	5.5×10^{-12}	2000±400	6.7×10^{-15}	1.2
HO$_2$ + HO$_2$ → H$_2$O$_2$ + O$_2$	2.3×10^{-13}	-(600±200)	1.7×10^{-12}	1.3
$\xrightarrow{M}$ H$_2$O$_2$ + O$_2$	1.7×10^{-33}[M]	-(1000±400)	4.9×10^{-32}[M]	1.3
HO$_2$ + O$_3$ → OH + 2O$_2$	1.1×10^{-14}	500^{+500}_{-100}	2.0×10^{-15}	1.3

NO$_x$ Reactions

Reaction	A-Factor[a]	E/R±(ΔE/R)	k(298 K)	f(298)[b]
N + O$_2$ → NO + O	1.5×10^{-11}	3600±400	8.5×10^{-17}	1.25
N + O$_3$ → NO + O$_2$	-	-	$<2.0 \times 10^{-16}$	-
N + NO → N$_2$ + O	3.4×10^{-11}	0±100	3.4×10^{-11}	1.3
N + NO$_2$ → N$_2$O + O	-	-	3.0×10^{-12}	3.0
O + NO $\xrightarrow{M}$ NO$_2$	(See Table 2)			
O + NO$_2$ → NO + O$_2$	6.5×10^{-12}	-(120±120)	9.7×10^{-12}	1.1
O + NO$_2$ $\xrightarrow{M}$ NO$_3$	(See Table 2)			
O + NO$_3$ → O$_2$ + NO$_2$	1.0×10^{-11}	0±150	1.0×10^{-11}	1.5
O + N$_2$O$_5$ → products	-	-	$<3.0 \times 10^{-16}$	-
O + HNO$_3$ → OH + NO$_3$	-	-	$<3.0 \times 10^{-17}$	-
O + HO$_2$NO$_2$ → products	7.8×10^{-11}	3400±750	8.6×10^{-16}	3.0

Table 1. (Continued)

Reaction	A-Factor[a]	E/R±(ΔE/R)	k(298 K)	f(298)[b]
$O_3 + NO \rightarrow NO_2 + O_2$	2.0×10^{-12}	1400 ± 200	1.8×10^{-14}	1.2
$NO + HO_2 \rightarrow NO_2 + OH$	3.7×10^{-12}	$-(240 \pm 80)$	8.3×10^{-12}	1.2
$NO + NO_3 \rightarrow 2NO_2$	1.7×10^{-11}	$-(150 \pm 100)$	2.9×10^{-11}	1.3
$OH + NO \xrightarrow{M} HONO$	(See Table 2)			
$OH + NO_2 \xrightarrow{M} HNO_3$	(See Table 2)			
$OH + NO_3 \rightarrow products$	-	-	2.3×10^{-11}	2.0
$OH + HNO_3 \rightarrow H_2O + NO_3$	(See ≠ below)		1.3	
$OH + HO_2NO_2 \rightarrow products$	1.3×10^{-12}	$-(380 \pm ^{270}_{500})$	4.6×10^{-12}	1.5
$HO_2 + NO_2 \xrightarrow{M} HO_2NO_2$	(See Table 2)			
$HO_2 + NO_3 \rightarrow products$	-	-	4.1×10^{-12}	2.0
$O_3 + NO_2 \rightarrow NO_3 + O_2$	1.2×10^{-13}	2450 ± 150	3.2×10^{-17}	1.15
$O_3 + HNO_2 \rightarrow O_2 + HNO_3$	-	-	$< 5.0 \times 10^{-19}$	-
$NO_2 + NO_3 \xrightarrow{M} N_2O_5$	(See Table 2)			
$NO_2 + NO_3 \rightarrow NO + NO_2 + O_2$				
$N_2O_5 + H_2O \rightarrow 2HNO_3$	-	-	$< 2.0 \times 10^{-21}$	-
$OH + NH_3 \rightarrow H_2O + NH_2$	3.6×10^{-12}	930 ± 200	1.6×10^{-13}	1.4
$NH_2 + HO_2 \rightarrow products$	-	-	3.4×10^{-11}	2.0
$NH_2 + NO \rightarrow products$	3.8×10^{-12}	$-(450 \pm 150)$	1.7×10^{-11}	2.0
$NH_2 + NO_2 \rightarrow products$	2.1×10^{-12}	$-(650 \pm 250)$	1.9×10^{-11}	3.0
$NH_2 + O_2 \rightarrow products$	-	-	$< 3.0 \times 10^{-18}$	-
$NH_2 + O_3 \rightarrow products$	4.3×10^{-12}	930 ± 500	1.9×10^{-13}	3.0

≠ $OH + HNO_3$ pressure and temperature dependence fit by

$$k(M,T) = k_o + \frac{k_3[M]}{1 + \dfrac{k_3[M]}{k_2}} \text{ with }$$

$k_o = 7.2 \times 10^{-15} \exp(785/T)$
$k_2 = 4.1 \times 10^{-16} \exp(1440/T)$
$k_3 = 1.9 \times 10^{-33} \exp(725/T)$

Table 1. (Continued)

Reaction	A-Factor[a]	E/R±(ΔE/R)	k(298 K)	f(298)[b]

Hydrocarbon Reactions

Reaction	A-Factor[a]	E/R±(ΔE/R)	k(298 K)	f(298)[b]
$OH + CO \rightarrow CO_2 + H$	$1.5 \times 10^{-13}(1+0.6P_{atm})$	0±300	$1.5 \times 10^{-13}(1+0.6P_{atm})$	1.3
$OH + CH_4 \rightarrow CH_3 + H_2O$	2.3×10^{-12}	1700±200	7.7×10^{-15}	1.2
$OH + {}^{13}CH_4 \rightarrow {}^{13}CH_3 + H_2O$				
$OH + C_2H_6 \rightarrow H_2O + C_2H_5$	1.1×10^{-11}	1100±200	2.8×10^{-13}	1.2
$OH + C_3H_8 \rightarrow H_2O + C_3H_7$	1.4×10^{-11}	750±200	1.1×10^{-12}	1.3
$OH + C_2H_4 \rightarrow$ products	(See Table 2)			
$OH + C_2H_2 \rightarrow$ products	(See Table 2)			
$OH + H_2CO \rightarrow H_2O + HCO$	1.0×10^{-11}	0±200	1.0×10^{-11}	1.25
$OH + CH_3OH \rightarrow$ products	6.7×10^{-12}	600±300	8.9×10^{-13}	1.2
$OH + C_2H_5OH \rightarrow$ products	6.8×10^{-12}	225±100	3.2×10^{-12}	1.3
$OH + CH_3CHO \rightarrow CH_3CO + H_2O$	6.0×10^{-12}	-(250±200)	1.4×10^{-11}	1.4
$OH + CH_3OOH \rightarrow$ products	3.8×10^{-12}	-(200±200)	7.4×10^{-12}	1.5
$OH + HCN \rightarrow$ products	1.2×10^{-13}	400±150	3.1×10^{-14}	3.0
$OH + CH_3CN \rightarrow$ products	4.5×10^{-13}	900±400	2.2×10^{-14}	2.0
$O_3 + C_2H_2 \rightarrow$ products	1.0×10^{-14}	4100±500	1.0×10^{-20}	3.0
$O_3 + C_2H_4 \rightarrow$ products	1.2×10^{-14}	2630±100	1.7×10^{-18}	1.25
$O_3 + C_3H_6 \rightarrow$ products	6.5×10^{-15}	1900±200	1.1×10^{-17}	1.2
$HO_2 + CH_2O \rightarrow$ adduct	6.7×10^{-15}	-(600±600)	5.0×10^{-14}	5.0
$O + HCN \rightarrow$ products	1.0×10^{-11}	4000±1000	1.5×10^{-17}	10.0
$O + C_2H_2 \rightarrow$ products	3.0×10^{-11}	1600±250	1.4×10^{-13}	1.3
$O + H_2CO \rightarrow$ products	3.4×10^{-11}	1600±250	1.6×10^{-13}	1.25
$O + CH_3CHO \rightarrow CH_3CO + OH$	1.8×10^{-11}	1100±200	4.5×10^{-13}	1.25
$O + CH_3 \rightarrow$ products	1.1×10^{-10}	0±250	1.1×10^{-10}	1.3
$CH_3 + O_2 \rightarrow$ products	-	-	$<3.0 \times 10^{-16}$	-

Table 1. (Continued)

Reaction	A-Factor[a]	E/R±(ΔE/R)	k(298 K)	f(298)[b]
$CH_3 + O_2 \xrightarrow{M} CH_3O_2$	(See Table 2)			
$C_2H_5 + O_2 \rightarrow C_2H_4 + HO_2$	-	-	$<2.0 \times 10^{-15}$	-
$C_2H_5 + O_2 \xrightarrow{M} C_2H_5O_2$	(See Table 2)			
$CH_2OH + O_2 \rightarrow CH_2O + HO_2$	(See Note)		9.1×10^{-12}	1.3
$CH_3O + O_2 \rightarrow CH_2O + HO_2$	3.9×10^{-14}	900±300	1.9×10^{-15}	1.5
$HCO + O_2 \rightarrow CO + HO_2$	3.5×10^{-12}	-(140±140)	5.5×10^{-12}	1.3
$CH_3 + O_3 \rightarrow products$	5.4×10^{-12}	220±150	2.6×10^{-12}	2.0
$CH_3O_2 + O_3 \rightarrow products$	-	-	$<3.0 \times 10^{-17}$	-
$CH_3O_2 + CH_3O_2 \rightarrow products$	2.2×10^{-13}	-(220±220)	4.6×10^{-13}	1.5
$CH_3O_2 + NO \rightarrow CH_3O + NO_2$	4.2×10^{-12}	-(180±180)	7.6×10^{-12}	1.2
$CH_3O_2 + NO_2 \xrightarrow{M} CH_3O_2NO_2$	(See Table 2)			
$CH_3O_2 + HO_2 \rightarrow products$	3.3×10^{-13}	-(800±400)	4.8×10^{-12}	2.0
$C_2H_5O_2 + C_2H_5O_2 \rightarrow products$	1.6×10^{-13}	300±250	5.8×10^{-14}	2.0
$C_2H_5O_2 + NO \rightarrow products$	8.9×10^{-12}	0±300	8.9×10^{-12}	1.3
$C_2H_5O_2 + HO_2 \rightarrow products$	6.5×10^{-13}	-(650±300	5.8×10^{-12}	2.0
$NO_3 + CO \rightarrow products$	-	-	$<4.0 \times 10^{-19}$	-
$NO_3 + CH_2O \rightarrow products$	-	-	5.8×10^{-16}	1.3
$NO_3 + CH_3CHO \rightarrow products$	1.4×10^{-12}	1900±300	2.4×10^{-15}	1.3
ClO$_x$ Reactions				
$Cl + O_3 \rightarrow ClO + O_2$	2.9×10^{-11}	260±100	1.2×10^{-11}	1.15
$Cl + H_2 \rightarrow HCl + H$	3.7×10^{-11}	2300±200	1.6×10^{-14}	1.25
$Cl + CH_4 \rightarrow HCl + CH_3$	1.1×10^{-11}	1400±150	1.0×10^{-13}	1.1
$Cl + C_2H_6 \rightarrow HCl + C_2H_5$	7.7×10^{-11}	90±90	5.7×10^{-11}	1.1
$Cl + C_3H_8 \rightarrow HCl + C_3H_7$	1.4×10^{-10}	-(40±250)	1.6×10^{-10}	1.5

Table 1. (Continued)

Reaction	A-Factor[a]	E/R±(ΔE/R)	k(298 K)	f(298)[b]
$Cl + C_2H_2 \rightarrow$ products	(See Table 2)			
$Cl + CH_3OH \rightarrow CH_2OH + HCl$	5.7×10^{-11}	0±250	5.7×10^{-11}	1.5
$Cl + CH_3Cl \rightarrow CH_2Cl + HCl$	3.3×10^{-11}	1250±200	4.9×10^{-13}	1.2
$Cl + CH_3CN \rightarrow$ products	-	-	$<2.0 \times 10^{-15}$	-
$Cl + CH_3CCl_3 \rightarrow CH_2CCl_3 + HCl$	-	-	$<4.0 \times 10^{-14}$	-
$Cl + H_2CO \rightarrow HCl + HCO$	8.1×10^{-11}	30±100	7.3×10^{-11}	1.15
$Cl + H_2O_2 \rightarrow HCl + HO_2$	1.1×10^{-11}	980±500	4.1×10^{-13}	1.5
$Cl + HOCl \rightarrow Cl_2 + OH$	3.0×10^{-12}	130±250	1.9×10^{-12}	2.0
$Cl + HNO_3 \rightarrow$ products	-	-	$<2.0 \times 10^{-16}$	-
$Cl + HO_2 \rightarrow HCl + O_2$	1.8×10^{-11}	-(170±200)	3.2×10^{-11}	1.5
$\rightarrow OH + ClO$	4.1×10^{-11}	450±200	9.1×10^{-12}	2.0
$Cl + Cl_2O \rightarrow Cl_2 + ClO$	9.8×10^{-11}	0±250	9.8×10^{-11}	1.2
$Cl + OClO \rightarrow ClO + ClO$	3.4×10^{-11}	-(160±200)	5.8×10^{-11}	1.25
$Cl + ClOO \rightarrow Cl_2 + O_2$	1.4×10^{-10}	0±250	1.4×10^{-10}	3.0
$\rightarrow ClO + ClO$	8.0×10^{-12}	0±250	8.0×10^{-12}	3.0
$Cl + Cl_2O_2 \rightarrow$ products	-	-	1.0×10^{-10}	2.0
$Cl + ClONO_2 \rightarrow$ products	6.8×10^{-12}	-(160±200)	1.2×10^{-11}	1.3
$Cl + NO \xrightarrow{M} NOCl$	(See Table 2)			
$Cl + NO_2 \xrightarrow{M} ClONO (ClNO_2)$	(See Table 2)			
$Cl + NO_3 \rightarrow ClO + NO_2$	2.6×10^{-11}	0±400	2.6×10^{-11}	2.0
$Cl + N_2O \rightarrow ClO + N_2$				
$Cl + ClNO \rightarrow NO + Cl_2$	5.8×10^{-11}	-(100±200)	8.1×10^{-11}	1.5
$Cl + O_2 \xrightarrow{M} ClOO$	(See Table 2)			
$ClO + O \rightarrow Cl + O_2$	3.0×10^{-11}	-(70±70)	3.8×10^{-11}	1.2
$ClO + NO \rightarrow NO_2 + Cl$	6.4×10^{-12}	-(290±100)	1.7×10^{-11}	1.15

94

Table 1. (Continued)

Reaction	A-Factor[a]	E/R±(ΔE/R)	k(298 K)	f(298)[b]
ClO + NO$_2$ $\xrightarrow{M}$ ClONO$_2$	(See Table 2)			
ClO + NO$_3$ → products	4.0×10^{-13}	0±400	4.0×10^{-13}	2.0
ClO + HO$_2$ → HOCl + O$_2$	4.8×10^{-13}	$-(700^{+250}_{-700})$	5.0×10^{-12}	1.4
ClO + H$_2$CO → products	$\sim 1.0 \times 10^{-12}$	>2100	$< 1.0 \times 10^{-15}$	-
ClO + OH → products	1.1×10^{-11}	$-(120 \pm 150)$	1.7×10^{-11}	1.5
ClO + CH$_4$ → products	$\sim 1.0 \times 10^{-12}$	>3700	$< 4.0 \times 10^{-18}$	-
ClO + H$_2$ → products	$\sim 1.0 \times 10^{-12}$	>4800	$< 1.0 \times 10^{-19}$	-
ClO + CO → products	$\sim 1.0 \times 10^{-12}$	>3700	$< 4.0 \times 10^{-18}$	-
ClO + N$_2$O → products	$\sim 1.0 \times 10^{-12}$	>4300	$< 6.0 \times 10^{-19}$	-
ClO + ClO → products	8.0×10^{-13}	1250±500	1.2×10^{-14}	2.0
$\xrightarrow{M}$ Cl$_2$O$_2$	(See Table 2)			
ClO + O$_3$ → ClOO + O$_2$	1.0×10^{-12}	>4000	$< 1.0 \times 10^{-18}$	-
→ OClO + O$_2$	1.0×10^{-12}	>4000	$< 1.0 \times 10^{-18}$	-
ClO + CH$_3$O$_2$ → products	(See Note)			
OH + Cl$_2$ → HOCl + Cl	1.4×10^{-12}	900±400	6.7×10^{-14}	1.2
OH + HCl → H$_2$O + Cl	2.6×10^{-12}	350±100	8.0×10^{-13}	1.3
OH + HOCl → H$_2$O + ClO	3.0×10^{-12}	500±500	5.0×10^{-13}	3.0
OH + CH$_3$Cl → CH$_2$Cl + H$_2$O	2.1×10^{-12}	1150±200	4.4×10^{-14}	1.2
OH + CH$_2$Cl$_2$ → CHCl$_2$ + H$_2$O	5.8×10^{-12}	1100±250	1.4×10^{-13}	1.2
OH + CHCl$_3$ → CCl$_3$ + H$_2$O	4.3×10^{-12}	1100±200	1.1×10^{-13}	1.2
OH + CHFCl$_2$ → CFCl$_2$ + H$_2$O	1.2×10^{-12}	1100±150	3.0×10^{-14}	1.1
OH + CHF$_2$Cl → CF$_2$Cl + H$_2$O	1.2×10^{-12}	1650±150	4.7×10^{-15}	1.1
OH + CH$_2$ClF → CHClF + H$_2$O	3.0×10^{-12}	1250±200	4.5×10^{-14}	1.15
OH + CH$_3$CCl$_3$ → CH$_2$CCl$_3$ + H$_2$O	5.0×10^{-12}	1800±200	1.2×10^{-14}	1.3
OH + CHCl$_2$CF$_3$ → CCl$_2$CF$_3$ + H$_2$O	6.4×10^{-13}	850±250	3.7×10^{-14}	1.2

Table 1. (Continued)

Reaction	A-Factor[a]	E/R±(ΔE/R)	k(298 K)	f(298)[b]
$OH + CHFClCF_3 \rightarrow CFClCF_3 + H_2O$	6.6×10^{-13}	1250 ± 300	1.0×10^{-14}	1.2
$OH + CH_2ClCF_2Cl \rightarrow CHClCF_2Cl + H_2O$	3.6×10^{-12}	1600 ± 400	1.7×10^{-14}	2.0
$OH + CH_2ClCF_3 \rightarrow CHClCF_3 + H_2O$	5.2×10^{-13}	1100 ± 300	1.3×10^{-14}	1.3
$OH + CH_3CFCl_2 \rightarrow CH_2CFCl_2 + H_2O$	4.2×10^{-13}	1200 ± 300	7.5×10^{-15}	1.3
$OH + CH_3CF_2Cl \rightarrow CH_2CF_2Cl + H_2O$	9.6×10^{-13}	1650 ± 250	3.8×10^{-15}	1.2
$OH + C_2Cl_4 \rightarrow products$	9.4×10^{-12}	1200 ± 200	1.7×10^{-13}	1.25
$OH + C_2HCl_3 \rightarrow products$	4.9×10^{-13}	$-(450 \pm 200)$	2.2×10^{-12}	1.25
$OH + CCl_4 \rightarrow products$	$\sim 1.0 \times 10^{-12}$	>2300	$<5.0 \times 10^{-16}$	-
$OH + CFCl_3 \rightarrow products$	$\sim 1.0 \times 10^{-12}$	>3700	$<5.0 \times 10^{-18}$	-
$OH + CF_2Cl_2 \rightarrow products$	$\sim 1.0 \times 10^{-12}$	>3600	$<6.0 \times 10^{-18}$	-
$OH + ClONO_2 \rightarrow products$	1.2×10^{-12}	330 ± 200	3.9×10^{-13}	1.5
$O + HCl \rightarrow OH + Cl$	1.0×10^{-11}	3300 ± 350	1.5×10^{-16}	2.0
$O + HOCl \rightarrow OH + ClO$	1.0×10^{-11}	2200 ± 1000	6.0×10^{-15}	10.0
$O + ClONO_2 \rightarrow products$	2.9×10^{-12}	800 ± 200	2.0×10^{-13}	1.5
$O + Cl_2O \rightarrow ClO + ClO$	2.9×10^{-11}	630 ± 200	3.5×10^{-12}	1.4
$OClO + O \rightarrow ClO + O_2$	2.8×10^{-11}	1200 ± 300	5.0×10^{-13}	2.0
$OClO + O_3 \rightarrow products$	2.1×10^{-12}	4700 ± 1000	3.0×10^{-19}	2.5
$OClO + OH \rightarrow HOCl + O_2$	4.5×10^{-13}	$-(800 \pm 200)$	6.8×10^{-12}	2.0
$OClO + NO \rightarrow NO_2 + ClO$	2.5×10^{-12}	600 ± 300	3.4×10^{-13}	2.0
$Cl_2O_2 + O_3 \rightarrow products$	-	-	$<1.0 \times 10^{-19}$	-
$Cl_2O_2 + NO \rightarrow products$	-	-	$<2.0 \times 10^{-14}$	-
$HCl + NO_3 \rightarrow HNO_3 + Cl$	-	-	$<5.0 \times 10^{-17}$	-
$HCl + ClONO_2 \rightarrow products$	-	-	$<1.0 \times 10^{-20}$	-
$HCl + HO_2NO_2 \rightarrow products$	-	-	$<1.0 \times 10^{-21}$	-
$H_2O + ClONO_2 \rightarrow products$	-	-	$<2.0 \times 10^{-21}$	-

96

Table 1. (Continued)

Reaction	A-Factor[a]	E/R±(ΔE/R)	k(298 K)	f(298)[b]
$CF_2ClO_2 + NO \rightarrow CF_2ClO + NO_2$	3.1×10^{-12}	-(500±200)	1.6×10^{-11}	1.3
$CFCl_2O_2 + NO \rightarrow CFCl_2O + NO_2$	3.5×10^{-12}	-(430±200)	1.5×10^{-11}	1.3
$CCl_3O_2 + NO \rightarrow CCl_3O + NO_2$	5.7×10^{-12}	-(330±200)	1.7×10^{-11}	1.3
		BrO_x Reactions		
$Br + O_3 \rightarrow BrO + O_2$	1.7×10^{-11}	800±200	1.2×10^{-12}	1.2
$Br + H_2O_2 \rightarrow HBr + HO_2$	1.0×10^{-11}	>3000	$<5.0 \times 10^{-16}$	-
$Br + H_2CO \rightarrow HBr + HCO$	1.7×10^{-11}	800±200	1.1×10^{-12}	1.3
$Br + HO_2 \rightarrow HBr + O_2$	1.5×10^{-11}	600±600	2.0×10^{-12}	2.0
$Br + Cl_2O \rightarrow BrCl + ClO$	2.0×10^{-11}	500±300	3.8×10^{-12}	2.0
$Br + OClO \rightarrow BrO + ClO$	2.6×10^{-11}	1300±300	3.4×10^{-13}	2.0
$Br + Cl_2O_2 \rightarrow products$	-	-	3.0×10^{-12}	2.0
$BrO + O \rightarrow Br + O_2$	3.0×10^{-11}	0±250	3.0×10^{-11}	3.0
$BrO + ClO \rightarrow Br + OClO$	1.6×10^{-12}	-(430±200)	6.8×10^{-12}	1.25
$\rightarrow Br + ClOO$	2.9×10^{-12}	-(220±200)	6.1×10^{-12}	1.25
$\rightarrow BrCl + O_2$	5.8×10^{-13}	-(170±200)	1.0×10^{-12}	1.25
$BrO + NO \rightarrow NO_2 + Br$	8.8×10^{-12}	-(260±130)	2.1×10^{-11}	1.15
$BrO + NO_2 \xrightarrow{M} BrONO_2$	(See Table 2)			
$BrO + BrO \rightarrow 2 Br + O_2$	1.4×10^{-12}	-(150±150)	2.3×10^{-12}	1.25
$\rightarrow Br_2 + O_2$	6.0×10^{-14}	-(600±600)	4.4×10^{-13}	1.25
$BrO + O_3 \rightarrow Br + 2O_2$	$\sim 1.0 \times 10^{-12}$	>1600	$<5.0 \times 10^{-15}$	-
$BrO + HO_2 \rightarrow products$	-	-	5.0×10^{-12}	3.0
$BrO + OH \rightarrow products$	-	-	1.0×10^{-11}	5.0
$OH + Br_2 \rightarrow HOBr + Br$	4.2×10^{-11}	0±600	4.2×10^{-11}	1.3
$OH + HBr \rightarrow H_2O + Br$	1.1×10^{-11}	0±250	1.1×10^{-11}	1.2

Table 1. (Continued)

Reaction	A-Factor[a]	E/R±(ΔE/R)	k(298 K)	f(298)[b]
$OH + CH_3Br \rightarrow CH_2Br + H_2O$	6.8×10^{-13}	850±200	3.8×10^{-14}	1.25
$OH + CF_2Br_2 \rightarrow$ products	-	-	$<5.0 \times 10^{-16}$	-
$OH + CF_2ClBr \rightarrow$ products	-	-	$<1.5 \times 10^{-16}$	-
$OH + CF_3Br \rightarrow$ products	-	-	$<1.2 \times 10^{-16}$	-
$OH + CF_2BrCF_2Br \rightarrow$ products	-	-	$<1.5 \times 10^{-16}$	-
$O + HBr \rightarrow OH + Br$	5.8×10^{-12}	1500±200	3.8×10^{-14}	1.3
$NO_3 + Br \rightarrow BrO + NO_2$	-	-	1.6×10^{-11}	2.0
$NO_3 + BrO \rightarrow$ products	-	-	1.0×10^{-12}	3.0
$NO_3 + HBr \rightarrow HNO_3 + Br$	-	-	$<1.0 \times 10^{-16}$	-

FO_x Reactions

Reaction	A-Factor[a]	E/R±(ΔE/R)	k(298 K)	f(298)[b]
$F + O_3 \rightarrow FO + O_2$	2.8×10^{-11}	230±200	1.3×10^{-11}	2.0
$F + H_2 \rightarrow HF + H$	1.4×10^{-10}	500±200	2.6×10^{-11}	1.2
$F + CH_4 \rightarrow HF + CH_3$	3.0×10^{-10}	400±300	8.0×10^{-11}	1.5
$F + H_2O \rightarrow HF + OH$	1.4×10^{-11}	0±200	1.4×10^{-11}	1.3
$F + O_2 \xrightarrow{M} FO_2$	(See Table 2)			
$F + NO \xrightarrow{M} FNO$	(See Table 2)			
$F + NO_2 \xrightarrow{M} FNO_2(FONO)$	(See Table 2)			
$F + HNO_3 \rightarrow HF + NO_3$	6.0×10^{-12}	-(400±200)	2.3×10^{-11}	1.3
$NO + FO \rightarrow NO_2 + F$	2.6×10^{-11}	0±250	2.6×10^{-11}	2.0
$FO + FO \rightarrow 2 F + O_2$	1.5×10^{-11}	0±250	1.5×10^{-11}	3.0
$FO + O_3 \rightarrow F + 2 O_2$				
$\rightarrow FO_2 + O_2$				
$FO + NO_2 \xrightarrow{M} FONO_2$	(See Table 2)			
$O + FO \rightarrow F + O_2$	5.0×10^{-11}	0±250	5.0×10^{-11}	3.0

Table 1. (Continued)

Reaction	A-Factor[a]	E/R±(ΔE/R)	k(298 K)	f(298)[b]
$O + FO_2 \rightarrow FO + O_2$	5.0×10^{-11}	0 ± 250	5.0×10^{-11}	5.0
$OH + CHF_3 \rightarrow CF_3 + H_2O$	1.5×10^{-12}	2650 ± 500	2.1×10^{-16}	1.5
$OH + CH_2F_2 \rightarrow CHF_2 + H_2O$	2.5×10^{-12}	1650 ± 200	1.0×10^{-14}	1.2
$OH + CH_3F \rightarrow CH_2F + H_2O$	5.4×10^{-12}	1700 ± 300	1.8×10^{-14}	1.2
$OH + CHF_2CF_3 \rightarrow CF_2CF_3 + H_2O$	8.9×10^{-13}	1750 ± 500	2.5×10^{-15}	2.0
$OH + CHF_2CHF_2 \rightarrow CF_2CHF_2 + H_2O$	8.7×10^{-13}	1500 ± 500	5.7×10^{-15}	2.0
$OH + CH_2FCF_3 \rightarrow CHFCF_3 + H_2O$	1.7×10^{-12}	1750 ± 300	4.8×10^{-15}	1.2
$OH + CH_2FCHF_2 \rightarrow$ products	2.8×10^{-12}	1500 ± 500	1.8×10^{-14}	2.0
$OH + CH_3CF_3 \rightarrow CH_2CF_3 + H_2O$	6.0×10^{-13}	1750 ± 500	1.7×10^{-15}	2.0
$OH + CH_2FCH_2F \rightarrow CHFCH_2F + H_2O$	1.7×10^{-11}	1500 ± 500	1.1×10^{-13}	2.0
$OH + CH_3CHF_2 \rightarrow$ products	1.5×10^{-12}	1100 ± 200	3.7×10^{-14}	1.1
$OH + CH_3CH_2F \rightarrow$ products	1.3×10^{-11}	1200 ± 300	2.3×10^{-13}	2.0
$CF_3O_2 + NO \rightarrow CF_3O + NO_2$	3.9×10^{-12}	$-(400 \pm 200)$	1.5×10^{-11}	1.3
		SO_x Reactions		
$OH + H_2S \rightarrow SH + H_2O$	6.0×10^{-12}	75 ± 75	4.7×10^{-12}	1.2
$OH + OCS \rightarrow$ products	1.1×10^{-13}	1200 ± 500	1.9×10^{-15}	2.0
$OH + CS_2 \rightarrow$ products	(See Note)	-	-	-
$OH + SO_2 \xrightarrow{M} HOSO_2$	(See Table 2)			
$O + H_2S \rightarrow OH + SH$	9.2×10^{-12}	1800 ± 550	2.2×10^{-14}	1.7
$O + OCS \rightarrow CO + SO$	2.1×10^{-11}	2200 ± 150	1.3×10^{-14}	1.2
$O + CS_2 \rightarrow CS + SO$	3.2×10^{-11}	650 ± 150	3.6×10^{-12}	1.2
$S + O_2 \rightarrow SO + O$	2.3×10^{-12}	0 ± 200	2.3×10^{-12}	1.2
$S + O_3 \rightarrow SO + O_2$	-	-	1.2×10^{-11}	2.0
$S + OH \rightarrow SO + H$	-	-	6.6×10^{-11}	3.0

99

Table 1. (Continued)

Reaction	A-Factor[a]	E/R±(ΔE/R)	k(298 K)	f(298)[b]
SO + O$_2$ → SO$_2$ + O	2.6x10^{-13}	2400±500	8.4x10^{-17}	2.0
SO + O$_3$ → SO$_2$ + O$_2$	3.6x10^{-12}	1100±200	9.0x10^{-14}	1.2
SO + OH → SO$_2$ + H	-	-	8.6x10^{-11}	2.0
SO + NO$_2$ → SO$_2$ + NO	1.4x10^{-11}	0±50	1.4x10^{-11}	1.2
SO + ClO → SO$_2$ + Cl	2.8x10^{-11}	0±50	2.8x10^{-11}	1.3
SO + OClO → SO$_2$ + ClO	-	-	1.9x10^{-12}	3.0
SO + BrO → SO$_2$ + Br	-	-	5.7X10^{-11}	1.4
SO$_2$ + HO$_2$ → products	-	-	<1.0x10^{-18}	-
SO$_2$ + CH$_3$O$_2$ → products	-	-	<5.0x10^{-17}	-
SO$_2$ + NO$_2$ → products	-	-	<2.0x10^{-26}	-
SO$_3$ + NO$_2$ → products	-	-	1.0x10^{-19}	10.0
SO$_2$ + NO$_3$ → products	-	-	<7.0x10^{-21}	-
SO$_2$ + O$_3$ → SO$_3$ + O$_2$	3.0x10^{-12}	>7000	<2.0x10^{-22}	-
SO$_3$ + H$_2$O → H$_2$SO$_4$	-	-	<6.0x10^{-15}	-
Cl + H$_2$S → HCl + SH	5.7x10^{-11}	0±50	5.7x10^{-11}	1.3
Cl + OCS → SCl + CO	-	-	<1.0x10^{-16}	-
ClO + OCS → products	-	-	<2.0x10^{-16}	-
ClO + SO$_2$ → Cl + SO$_3$	-	-	<4.0x10^{-18}	-
SH + H$_2$O$_2$ → products	-	-	<5.0x10^{-15}	-
SH + O → H + SO	-	-	1.6x10^{-10}	5.0
SH + O$_2$ → OH + SO	-	-	<4.0x10^{-19}	-
SH + O$_3$ → HSO + O$_2$	9.0x10^{-12}	280±200	3.5x10^{-12}	1.3
SH + NO$_2$ → HSO + NO	2.9x10^{-11}	-(240±100)	6.5x10^{-11}	1.3
SH + NO $\xrightarrow{M}$ HSNO	(See Table 2)			
HSO + NO → products	-	-	<1.0x10^{-15}	-

Table 1.   (Continued)

Reaction	A-Factor[a]	E/R±(ΔE/R)	k(298 K)	f(298)[b]
HSO + NO$_2$ → HSO$_2$ + NO	-	-	9.6x10^{-12}	2.0
HSO + O$_2$ → products	-	-	<2.0x10^{-17}	-
HSO + O$_3$ → products	-	-	1.0x10^{-13}	5.0
HSO$_2$ + O$_2$ → HO$_2$ + SO$_2$	-	-	3.0x10^{-13}	3.0
HOSO$_2$ + O$_2$ → HO$_2$ + SO$_3$	1.3x10^{-12}	330±200	4.4x10^{-13}	1.2
H$_2$S + NO$_3$ → products	-	-	<8.0x10^{-16}	-
CS + O$_2$ → OCS + O	-	-	2.9x10^{-19}	2.0
CS + O$_3$ → OCS + O$_2$	-	-	3.0x10^{-16}	3.0
CS + NO$_2$ → OCS + NO	-	-	7.6x10^{-17}	3.0
OH + CH$_3$SH → products	9.9x10^{-12}	-(360±100)	3.3x10^{-11}	1.2
OH + CH$_3$SCH$_3$ → H$_2$O + CH$_2$SCH$_3$	1.1x10^{-11}	240±100	4.9x10^{-12}	1.2
OH + CH$_3$SSCH$_3$ → products	5.7x10^{-11}	-(380±300)	2.0x10^{-10}	1.3
NO$_3$ + CH$_3$SH → products	4.4x10^{-13}	-(210±210)	8.9x10^{-13}	1.25
NO$_3$ + CH$_3$SCH$_3$ → products	1.9x10^{-13}	-(500±200)	1.0x10^{-12}	1.2
NO$_3$ + CH$_3$SSCH$_3$ → products	1.3x10^{-12}	270±270	5.3x10^{-13}	1.4
NO$_3$ + CS$_2$ → products	-	-	<4.0x10^{-16}	-
NO$_3$ + OCS → products	-	-	<3.0x10^{-15}	-
CH$_3$S + O$_2$ → products	-	-	<3.0x10^{-18}	-
CH$_3$S + O$_3$ → products	-	-	4.1x10^{-12}	2.0
CH$_3$S + NO$_2$ → products	-	-	5.6x10^{-11}	1.3
CH$_3$SO + O$_3$ → products	-	-	1.0x10^{-12}	3.0
CH$_3$SO + NO$_2$ → CH$_3$SO$_2$ + NO	-	-	1.2x10^{-11}	1.4

Table 1. (Continued)

Reaction	A-Factor[a]	E/R±(ΔE/R)	k(298 K)	f(298)[b]
Metal Reactions				
$Na + O_2 \xrightarrow{M} NaO_2$	(See Table 2)			
$Na + O_3 \rightarrow NaO + O_2$	7.6×10^{-10}	0±400	7.6×10^{-10}	1.2
$\rightarrow NaO_2 + O$	$<4 \times 10^{-11}$	0±400	$<4.0 \times 10^{-11}$	-
$Na + N_2O \rightarrow NaO + N_2$	2.4×10^{-10}	1600±400	1.1×10^{-12}	1.3
$Na + Cl_2 \rightarrow NaCl + Cl$	7.3×10^{-10}	0±200	7.3×10^{-10}	1.3
$NaO + O \rightarrow Na + O_2$	3.7×10^{-10}	0±400	3.7×10^{-10}	3.0
$NaO + O_2 \xrightarrow{M} NaO_3$	(See Table 2)			
$NaO + O_3 \rightarrow NaO_2 + O_2$	1.6×10^{-10}	0±400	1.6×10^{-10}	2.0
$\rightarrow Na + 2O_2$	6×10^{-11}	0±800	6.0×10^{-11}	3.0
$NaO + H_2 \rightarrow NaOH + H$	2.6×10^{-11}	0±600	2.6×10^{-11}	2.0
$NaO + H_2O \rightarrow NaOH + OH$	2.2×10^{-10}	0±400	2.2×10^{-10}	2.0
$NaO + NO \rightarrow Na + NO_2$	1.5×10^{-10}	0±400	1.5×10^{-10}	4.0
$NaO + CO_2 \xrightarrow{M} NaCO_3$	(See Table 2)			
$NaO + HCl \rightarrow products$	2.8×10^{-10}	0±400	2.8×10^{-10}	3.0
$NaO_2 + NO \rightarrow NaO + NO_2$			$<10^{-14}$	
$NaO_2 + HCl \rightarrow products$	2.3×10^{-10}	0±400	2.3×10^{-10}	3.0
$NaOH + HCl \rightarrow NaCl + H_2O$	2.8×10^{-10}	0±400	2.8×10^{-10}	3.0
$NaOH + CO_2 \xrightarrow{M} NaHCO_3$	(See Table 2)			

[a] Units are cm^3 molecules-^{1}sec-^{1}.

[b] f(298) is the uncertainty factor at 298K. To calculate the uncertainty at other temperatures, use the expression: $f(T) = f(298) \exp \left| \frac{\Delta E}{R} \left(\frac{1}{T} - \frac{1}{298}\right)\right|$. Note that the exponent is absolute value.

Table 2. Rate Constants for Three-Body Reactions

Reaction	Low Pressure Limit[a] $k_o(T) = k_o^{300}(T/300)^{-n}$		High Pressure Limit[b] $k_\infty(T) = k_\infty^{300}(T/300)^{-m}$	
	k_o^{300}	n	k_∞^{300}	m
$O + O_2 \xrightarrow{M} O_3$	(6.0±0.5)(-34)	2.3±0.5	-	-
$O(^1D) + N_2 \xrightarrow{M} N_2O$	(3.5±3.0)(-37)	$0.6^{+2.0}_{-0.6}$	-	-
$H + O_2 \xrightarrow{M} HO_2$	(5.7±0.5)(-32)	1.6±0.5	(7.5±4.0)(-11)	0±1
$OH + OH \xrightarrow{M} H_2O_2$	(6.9±3.0)(-31)	$0.8^{+2.0}_{-0.8}$	(1.5±0.5)(-11)	0±0.5
$O + NO \xrightarrow{M} NO_2$	(9.0±2.0)(-32)	1.5±0.3	(3.0±1.0)(-11)	0±1
$O + NO_2 \xrightarrow{M} NO_3$	(9.0±1.0)(-32)	2.0±1.0	(2.2±0.3)(-11)	0±1
$OH + NO \xrightarrow{M} HONO$	(7.0±2.0)(-31)	2.6±1.0	(1.5±1.0)(-11)	0.5±0.5
$OH + NO_2 \xrightarrow{M} HNO_3$	(2.6±0.3)(-30)	3.2±0.7	(2.4±1.2)(-11)	1.3±1.3
$HO_2 + NO_2 \xrightarrow{M} HO_2NO_2$	(1.8±0.3)(-31)	3.2±0.4	(4.7±1.0)(-12)	1.4±1.4
$NO_2 + NO_3 \xrightarrow{M} N_2O_5$	(2.2±0.5)(-30)	4.3±1.3	(1.5±0.8)(-12)	0.5±0.5
$Cl + NO \xrightarrow{M} ClNO$	(9.0±2.0)(-32)	1.6±0.5	-	-
$Cl + NO_2 \xrightarrow{M} ClONO$	(1.3±0.2)(-30)	2.0±1.0	(1.0±0.5)(-10)	1±1
$\xrightarrow{M} ClNO_2$	(1.8±0.3)(-31)	2.0±1.0	(1.0±0.5)(-10)	1±1
$Cl + O_2 \xrightarrow{M} ClOO$	(2.7±1.0)(-33)	1.5±0.5	-	-
$Cl + CO \xrightarrow{M} ClCO$	(1.3±0.5)(-33)	3.8±0.5	-	-
$Cl + C_2H_2 \xrightarrow{M} ClC_2H_2$	(8.0±1.0)(-30)	3.5±0.5	(1.0±0.5)(-10)	2.6±0.5
$ClO + ClO \xrightarrow{M} Cl_2O_2$	(1.8±0.5)(-32)	3.6±1.0	(6.0±2)(-12)	0±1
$ClO + NO_2 \xrightarrow{M} ClONO_2$	(1.8±0.3)(-31)	3.4±1.0	(1.5±0.7)(-11)	1.9±1.9
$BrO + NO_2 \xrightarrow{M} BrONO_2$	(5.2±0.5)(-31)	3.8±1.0	(9.0±1.0)(-12)	2.3±1.0
$F + O_2 \xrightarrow{M} FO_2$	(4.4±0.4)(-33)	1.2±0.5	-	-
$F + NO \xrightarrow{M} FNO$	(5.9±3.0)(-32)	1.7±1.7	-	-
$F + NO_2 \xrightarrow{M} Products$	(1.1±0.6)(-30)	2.0±2.0	(3.0±2.0)(-11)	1±1
$FO + NO_2 \xrightarrow{M} FONO_2$	(2.6±2.0)(-31)	1.3±1.3	(2.0±1.0)(-11)	1.5±1.5

103

Table 2. (Continued)

Reaction	Low Pressure Limit[a] $k_o(T) = k_o^{300}(T/300)^{-n}$		High Pressure Limit[b] $k_\infty(T) = k_\infty^{300}(T/300)^{-m}$	
	k_o^{300}	n	k_∞^{300}	m
$CH_3 + O_2 \xrightarrow{M} CH_3O_2$	$(4.5\pm1.5)(-31)$	2.0 ± 1.0	$(1.8\pm0.2)(-12)$	1.7 ± 1.7
$C_2H_5 + O_2 \xrightarrow{M} C_2H_5O_2$	$(2.0\pm1.5)(-28)$	3.8 ± 1.0	$(5.0\pm3.0)(-12)$	0 ± 1
$CH_3O_2 + NO_2 \xrightarrow{M} CH_3O_2NO_2$	$(1.5\pm0.8)(-30)$	4.0 ± 2.0	$(6.5\pm3.2)(-12)$	2 ± 2
$OH + SO_2 \xrightarrow{M} HOSO_2$	$(3.0\pm1.0)(-31)$	3.3 ± 1.5	$(1.5\pm0.5)(-12)$	$0\pm^0_2$
$OH + C_2H_4 \xrightarrow{M} HOCH_2CH_2$	$(1.5\pm0.6)(-28)$	0.8 ± 2.0	$(8.8\pm0.9)(-12)$	$0\pm^0_2$
$OH + C_2H_2 \xrightarrow{M} HOCHCH$	$(5.5\pm2.0)(-30)$	0.0 ± 0.2	$(8.3\pm1.0)(-13)$	$-2\pm^2_1$
$CF_3 + O_2 \xrightarrow{M} CF_3O_2$	$(1.5\pm0.3)(-29)$	4 ± 2	$(8.5\pm1.0)(-12)$	1 ± 1
$CFCl_2 + O_2 \xrightarrow{M} CFCl_2O_2$	$(5.0\pm0.8)(-30)$	2 ± 2	$(6.0\pm1.0)(-12)$	1 ± 1
$CCl_3 + O_2 \xrightarrow{M} CCl_3O_2$	$(1.0\pm0.7)(-30)$	2 ± 2	$(2.5\pm2)(-12)$	1 ± 1
$CFCl_2O_2 + NO_2 \xrightarrow{M} CFCl_2O_2NO_2$	$(3.5\pm0.5)(-29)$	5 ± 1	$(6.0\pm1.0)(-12)$	2.5 ± 1
$CF_3O_2 + NO_2 \rightarrow CF_3O_2NO_2$	$(2.2\pm0.5)(-29)$	5 ± 1	$(6.0\pm1.0)(-12)$	2.6 ± 1
$CCl_3O_2 + NO_2 \rightarrow CCl_3O_2NO_2$	$(5.0\pm1.0)(-29)$	5 ± 1	$(6.0\pm1.0)(-12)$	2.5 ± 1
$HS + NO \xrightarrow{M} HSNO$	$(2.4\pm0.4)(-31)$	3 ± 1	$(2.7\pm0.5)(-11)$	$0\pm^0_2$
$Na + O_2 \xrightarrow{M} NaO_2$	$(2.4\pm0.5)(-30)$	1.2 ± 0.5	$(4.0\pm2.0)(-10)$	0 ± 1
$NaO + O_2 \xrightarrow{M} NaO_3$	$(3.5\pm0.7)(-30)$	2 ± 2	$(5.7\pm3)(-10)$	0 ± 1
$NaO + CO_2 \xrightarrow{M} NaCO_3$	$(8.7\pm2.6)(-28)$	2 ± 2	$(6.5\pm3)(-10)$	0 ± 1
$NaOH + CO_2 \xrightarrow{M} NaHCO_3$	$(1.3\pm0.3)(-28)$	2 ± 2	$(6.8\pm4)(-10)$	0 ± 1

Note: $k(Z) = k(M,T) = \left(\dfrac{k_o(T)[M]}{1 + k_o(T)[M]/k_\infty(T)}\right) 0.6^{\{1 + [\log_{10}(k_o(T)[M]/k_\infty(T))]^2\}^{-1}}$

The values quoted are suitable for air as the third body, M.

a Units are $cm^6/molecule^2$-sec

b Units are $cm^3/molecule$-sec

6.0 Equilibrium Constants

6.1 Format

Some of the three-body reactions in Table 2 form products which are thermally unstable at atmospheric temperatures. In such cases the thermal decomposition reaction may compete with other loss processes, such as photodissociation or radical attack. Table 3 lists the equilibrium constants, $K(T)$, for eleven reactions which may fall into this category. The table has three column entries, the first two being the parameters A and B which can be used to express $K(T)$:

$$K(T)/cm^3 \text{ molecule}^{-1} = A \exp(B/T), \quad (200 \text{ K} < T < 300 \text{ K})$$

The third column entry in Table 3 is the calculated value of K at 298 K.

The data sources for $K(T)$ are described in the individual notes to Table 3. When values of the heats of formation and entropies of all species are known at the temperature T, we note that:

$$\log(K(T)/cm^3 \text{ molecule}^{-1}) = (\Delta S^o{}_T/2.303R) - (\Delta H^o{}_T/2.303RT) + \log(T) - 21.87$$

where the superscript "o" refers to a standard state of one atmosphere. In some cases K values were calculated from this equation, using thermochemical data. In other cases the K values were calculated directly from kinetic data for the forward and reverse reactions. When available, JANAF values were used for the equilibrium constants. The following equations were then used to calculate the parameters A and B:

$$B/^\circ K = 2.303(\log(K_{200}/K_{300}))(300 \times 200)/(300-200)$$

$$= 1382(\log(K_{200}/K_{300}))$$

$$\log(A) = \log(K(T)) - B/2.303T$$

Table 3. Equilibrium Constants

Reaction	A/cm^3 molecule^{-1}	$B \pm \Delta B/^{\circ}K$	$K_{eq}(298\ K)$	$f(298\ K)^a$
$HO_2 + NO_2 \rightarrow HO_2NO_2$	2.1×10^{-27}	$10,900 \pm 1,000$	1.6×10^{-11}	5
$NO + NO_2 \rightarrow N_2O_3$	3.0×10^{-27}	$4,700 \pm 100$	2.1×10^{-20}	2
$NO_2 + NO_2 \rightarrow N_2O_4$	5.9×10^{-29}	$6,600 \pm 250$	2.4×10^{-19}	2
$NO_2 + NO_3 \rightarrow N_2O_5$	4.0×10^{-27}	$10,930 \pm 500$	3.4×10^{-11}	1.5
$CH_3O_2 + NO_2 \rightarrow CH_3O_2NO_2$	1.3×10^{-28}	$11,200 \pm 1,000$	2.7×10^{-12}	2
$Cl + O_2 \rightarrow ClOO$	5.7×10^{-25}	$2,500 \pm 750$	2.5×10^{-21}	2
$ClO + O_2 \rightarrow ClO \cdot O_2$	$<2.9 \times 10^{-26}$	$<5,000 \pm 1,500$	$<5.6 \times 10^{-19}$	500
$Cl + CO \rightarrow ClCO$	1.6×10^{-25}	$4,000 \pm 500$	1.1×10^{-19}	5
$ClO + ClO \rightarrow Cl_2O_2$	3.0×10^{-27}	$8,450 \pm 850$	6.2×10^{-15}	2
$ClO + OClO \rightarrow Cl_2O_3$	1.6×10^{-27}	$7,200 \pm 1,400$	5.0×10^{-17}	10
$F + O_2 \rightarrow FOO$	3.2×10^{-25}	$6,100 \pm 1,200$	2.5×10^{-16}	10

K_{eq}/cm^3 molecule $^{-1}$ = A exp (B/T) [200 < T/K < 300]

a f(298 K) is the uncertainty factor in K_{eq} at 298 K. To calculate the uncertainty at other temperatures, use the expression: $f(T) = f(298\ K)\ exp\ |\Delta B\ (\frac{1}{T} - \frac{1}{298})|$.

106

7.0 Photochemical Data

7.1 Discussion of Format and Error Estimates

In Table 4 we present a list of photochemical reactions considered to be of stratospheric interest. The absorption cross sections of O_2 and O_3 largely determine the extent of penetration of solar radiation into the stratosphere and troposphere. Some comments and references to these cross sections are presented in the text, but only a sample of the data are listed here. (See, for example, WMO Report #11, 1982; WMO-NASA, 1985.) The photodissociation of NO in the O_2 Schumann-Runge band spectral range is another important process requiring special treatment and is not discussed in this evaluation. (See, for example, Frederick and Hudson, 1979; Allen and Frederick, 1982; and WMO Report #11, 1982.)

For some other species having highly structured spectra, such as CS_2 and SO_2, some comments are given in the text of the complete evaluation, but the photochemical data are not presented. The species CH_2O, NO_2, NO_3, ClO, BrO, and OClO also have complicated spectra but, in view of their importance for atmospheric chemistry, a sample of the data is presented in the evaluation; for more detailed information on their high-resolution spectra and temperature dependence, the reader is referred to the original literature.

Table 5 gives recommended reliability factors for some of the more important photochemical reactions. These factors represent the combined uncertainty in cross sections and quantum yields, taking into consideration the atmospherically important wavelength regions, and they refer to the total dissociation rate regardless of product identity (except in the case of $O(^1D)$ production from photolysis of O_3).

107

Table 4.   Photochemical Reactions of Stratospheric Interest

$O_2 + h\nu \rightarrow O + O$

$O_3 + h\nu \rightarrow O_2 + O$

$O_3 + h\nu \rightarrow O_2 + O(^1D)$

$HO_2 + h\nu \rightarrow products$

$H_2O + h\nu \rightarrow H + OH$

$H_2O_2 + h\nu \rightarrow OH + OH$

$NO + h\nu \rightarrow N + O$

$NO_2 + h\nu \rightarrow NO + O$

$NO_3 + h\nu \rightarrow products$

$N_2O + h\nu \rightarrow N_2 + O(^1D)$

$N_2O_5 + h\nu \rightarrow products$

$NH_3 + h\nu \rightarrow NH_2 + H$

$HNO_2 + h\nu \rightarrow OH + NO$

$HNO_3 + h\nu \rightarrow OH + NO_2$

$HNO_4 + h\nu \rightarrow products$

$Cl_2 + h\nu \rightarrow Cl + Cl$

$ClO + h\nu \rightarrow Cl + O$

$ClOO + h\nu \rightarrow products$

$OClO + h\nu \rightarrow O + ClO$

$ClO_3 + h\nu \rightarrow products$

$Cl_2O_2 + h\nu \rightarrow products$

$HCl + h\nu \rightarrow H + Cl$

$HOCl + h\nu \rightarrow OH + Cl$

$ClNO + h\nu \rightarrow Cl + NO$

$ClNO_2 + h\nu \rightarrow products$

$ClONO + h\nu \rightarrow products$

$ClONO_2 + h\nu \rightarrow products$

$CCl_4 + h\nu \rightarrow products$

$CCl_3F + h\nu \rightarrow products$

$CCl_2F_2 + h\nu \rightarrow products$

$CHClF_2 + h\nu \rightarrow products$

$CH_3Cl + h\nu \rightarrow products$

$CH_3CF_2Cl + h\nu \rightarrow products$

$CF_3CHCl_2 + h\nu \rightarrow products$

$CF_3CHFCl + h\nu \rightarrow products$

$CH_3CFCl_2 + h\nu \rightarrow products$

$CH_3CCl_3 + h\nu \rightarrow products$

$CBrF_3 + h\nu \rightarrow products$

$CF_2Br_2 + h\nu \rightarrow products$

$CBrClF_2 + h\nu \rightarrow products$

$CF_2BrCF_2Br + h\nu \rightarrow products$

$CF_4 + h\nu \rightarrow products$

$C_2F_6 + h\nu \rightarrow products$

$SF_6 + h\nu \rightarrow products$

$CCl_2O + h\nu \rightarrow products$

$CClFO + h\nu \rightarrow products$

$CF_2O + h\nu \rightarrow products$

$BrO + h\nu \rightarrow Br + O$

$BrONO_2 + h\nu \rightarrow products$

$HF + h\nu \rightarrow H + F$

$CO + h\nu \rightarrow C + O$

$CO_2 + h\nu \rightarrow CO + O$

$CH_4 + h\nu \rightarrow products$

$CH_2O + h\nu \rightarrow products$

$CH_3OOH + h\nu \rightarrow products$

$HCN + h\nu \rightarrow products$

$CH_3CN + h\nu \rightarrow products$

$SO_2 + h\nu \rightarrow SO + O$

$OCS + h\nu \rightarrow CO + S$

$H_2S + h\nu \rightarrow HS + H$

$CS_2 + h\nu \rightarrow products$

$NaCl + h\nu \rightarrow Na + Cl$

$NaOH + h\nu \rightarrow Na + OH$

Table 5. Combined Uncertainties for Cross Sections and Quantum Yields

Species	Uncertainty
O_2 (Schumann-Runge bands)	1.4
O_2 (Continua)	1.3
O_3	1.1
$O_3 \to O(^1D)$	1.4
NO_2	1.3
NO_3	2.0
N_2O	1.2
N_2O_5	2.0
H_2O_2	1.4
HNO_3	1.3
HO_2NO_2	2.0
CH_2O	1.4
HCl	1.1
$HOCl$	1.4
$ClONO_2$	1.3
CCl_4	1.1
CCl_3F	1.1
CCl_2F_2	1.1
CH_3Cl	1.1
CF_2O	2.0
CH_3OOH	1.8
$BrONO_2$	1.4
CF_3Br	2.0
CF_2ClBr	3.0
CF_2Br_2	3.0
$C_2F_4Br_2$	3.0

SECTION D

APPENDIX

GAS PHASE ENTHALPY DATA

The following data are adapted mainly from CODATA (1984), although a few entries have been updated.

MOLECULE	$\Delta H_f(298)$ (Kcal/mol)	MOLECULE	$\Delta H_f(298)$ (Kcal/mol)	MOLECULE	$\Delta H_f(298)$ (Kcal/mol)	MOLECULE	$\Delta H_f(298)$ (Kcal/mol)
H	52.1	CH_3OH	-48.2	F_2	0.00	CH_3Cl	-19.6
H_2	0.00	CH_3OOH	-31.3	HF	-65.34	ClCO	-5±1
O	59.57	CH_3ONO	-15.6	HOF	-23.4±1	$COCl_2$	-52.6
$O(^1D)$	104.9	CH_3ONO_2	-28.6	FO	26±5	CHFCl	-14.5±2
O_2	0.00	$CH_3O_2NO_2$	-10.6±2	F_2O	5.9±.4	CH_2FCl	-63±2
$O_2(^1\text{-DELTA})$	22.5	C_2H	135.0	FO_2	6±2	CFCl	7±6
$O_2(^1\text{-SIGMA})$	37.5	C_2H_2	54.35	F_2O_2	5±2	$CFCl_2$	-22±2
O_3	34.1	C_2H_3	68.1	FONO	-15±7	$CFCl_3$	-68.1
HO	9.3	C_2H_4	12.45	FNO	-16±2	CF_2Cl	-64±3
HO_2	3±1	C_2H_5	28.4	FNO_2	-26±2	CF_2Cl_2	-117.9
H_2O	-57.81	C_2H_6	-20.0	$FONO_2$	2.5±7	CF_3Cl	-169.2
H_2O_2	-32.60	CH_2CN	58.6	CF_2	-44±2	$CHFCl_2$	-68.1
N	113.00	CH_3CN	19.1	CF_3	-112±1	CHF_2Cl	-115.6
N_2	0.00	CH_2CO	-14.23	CF_4	-223.0	COFCl	-102±2
NH	82.0	CH_3CO	-5.8	CHF_3	-166.8	CH_2CF_3	-124±2
NH_2	45.3	CH_3CHO	-39.7	CHF_2	-58±2	CH_3CF_2	-72±2
NH_3	-10.98	C_2H_5O	-4.1	CH_2F_2	-107.2	CH_3CF_3	-178
NO	21.57	CH_2CH_2OH	-13±2	CH_2F	-8±2	CF_2CF_3	-213
NO_2	7.9	C_2H_5OH	-56.2	CH_3F	-55.9±1	CHF_2CF_3	-264
NO_3	17±2	CH_3CO_2	-49.6	FCO	-41±14	C_2Cl_4	-3.0
N_2O	19.61	$C_2H_5O_2$	-4±3	COF_2	-151.7	C_2HCl_3	-1.9
N_2O_3	19.8	CH_3OOCH_3	-30.0	Cl	28.9	CH_2CCl_3	11±7
N_2O_4	2.2	C_3H_5	39.4	Cl_2	0.00	CH_3CCl_3	-34.0
N_2O_5	2.7±2	C_3H_6	4.8	HCl	-22.06	CH_2CH_2Cl	19.3±2
HNO	23.8	$n\text{-}C_3H_7$	22.6±2	ClO	24.4	Br	26.7
HONO	-19.0	$i\text{-}C_3H_7$	19±2	ClOO	23±1	Br_2	7.39
HNO_3	-32.3	C_3H_8	-24.8	OClO	23±2	HBr	-8.67
HO_2NO_2	-11±2	C_2H_5CHO	-44.8	$ClOO_2$	>13.4	HOBr	-19±2
C	170.9	CH_3COCH_3	-51.9	ClO_3	37	BrO	30
CH	142.0	S	66.22	Cl_2O	19.5	BrNO	19.7
CH_2	92.3	S_2	30.72	Cl_2O_2	31±3	BrONO	25±7
CH_3	35.1	HS	34±1	Cl_2O_3	33±3	$BrONO_2$	12±5
CH_4	-17.88	H_2S	-4.9	HOCl	-18.6±3	BrCl	3.5
CN	104.0	SO	1.2	ClNO	12.4	CH_2Br	40±2
HCN	32.3	SO_2	-70.96	$ClNO_2$	3.0	$CHBr_2$	45±2
CH_3NH_2	-5.5	SO_3	-94.6	ClONO	20±7	CH_2Br_2	-2.6±2
NCO	38	HSO	1±3	$ClONO_2$	6.3	CH_3Br	-8.5
CO	-26.42	HSO_3	-92±2	FCl	-12.1	I	25.52
CO_2	-94.07	CS	65	CCl	120±5	I_2	14.92
HCO	9.0	CS_2	28.0	CCl_2	57±5	HI	6.3
CH_2O	-26.0	CH_3S	33±2	CCl_3	18±1	CH_3I	3.5
COOH	-50±2	CH_3SH	-5.5	CCl_4	-22.9	CH_2I	54.9±2
HCOOH	-90.5	CH_3SCH_3	-8.9	$CHCl_3$	-24.6	IO	41.1
CH_3O	3.5	CH_3SSCH_3	-5.8	$CHCl_2$	23±2	INO	29.0
CH_3O_2	5±2	OCS	-34	CH_2Cl	29±2	INO_2	14.4
CH_2OH	-6.2	F	18.98	CH_2Cl_2	-22.8		

110

SECTION E

An Assessment of the Impact on Stratospheric Chemistry and Ozone caused by the Launch of the Space Shuttle and Titan IV

Michael J. Prather and Maria M. Garcia
NASA, Goddard Institute for Space Studies, New York, NY

Anne R. Douglass and Charles H. Jackman,
NASA, Goddard Space Flight Center, Greenbelt, MD

Malcolm K. W. Ko and Nien Dak Sze,
Atmospheric and Environmental Research Inc., Cambridge, MA

1.0   INTRODUCTION

The launch of NASA's Space Shuttle and similar rockets injects chlorine compounds directly into the stratosphere, adding to the current burden of stratospheric chlorine. Depletion of the stratospheric ozone layer has been linked to increases in stratospheric chlorine compounds associated predominantly with chlorofluorocarbons (see recent assessments, NASA/WMO, 1986; Watson et al., 1988; UNEP/WMO, 1990). The purpose of this study is to determine the magnitude of the chlorine increases that might be caused by the Space Shuttle and to assess the overall impact on the chemistry and composition of the global stratosphere.

The solid rocket motors on the Space Shuttle and Titan IV launch vehicles use a solid fuel composed of ammonium perchlorate, aluminum and a polymer binder (Peter Evanoff, Thiokol Corp., private communication, 1989). The exhaust consists primarily of gaseous HCl, carbon monoxide, water vapor, molecular nitrogen and aluminum oxide. The last assessment of the Shuttle in terms of stratospheric ozone was more than a decade ago (Potter, 1978), and our understanding of stratospheric chemistry and modelling has evolved much since then.

The launch scenario considered here consists of 9 Shuttles and 6 Titans per year. It is typical of the current schedule, but it may fall short of the frequency needed for major space projects. The chlorine from these launches is used as a stratospheric source of Cl_y (total inorganic chlorine: the sum of HCl, Cl, Cl_2, ClO, $ClONO_2$ and HOCl) in three numerical models of the stratosphere. Calculations have been made with two two-dimensional (latitude by altitude) models with complete chemistry (AER: Ko et al., 1985, 1989; GSFC: Douglass et al., 1989, Jackman et al., 1989a) and a three-dimensional model for chemical tracers (GISS: Prather et al., 1990).

In one numerical simulation, Cl_y enhancements in the middle stratosphere two days after a January launch of the Shuttle are still expected to be clumpy, but the exhaust plume is predicted to have spread over a region about 20° latitude by 30° longitude with an average increase of about 30 ppt (parts per 1012) or 2% above background. One month later the Shuttle plume is well mixed, and increases in Cl_y are less than 4 ppt throughout the stratosphere. The buildup of chlorine from these launches approaches a steady-state limit after several years; on average, Cl_y would increase by about 10 ppt in the middle stratosphere of the northern hemisphere, less than 0.5% above current levels. Corresponding ozone depletions are predicted to be less than 0.2% locally, with smaller perturbations to the ozone column.

The profiles and amounts of chlorine injected from the solid rocket motors are summarized in section 2. The transient response to a single launch is shown in section 3, and model predictions of the steady-state accumulation of Cl_y are described in section 4. The overall impact on stratospheric chemistry and ozone is discussed in section 5.

111

2.0 SOURCE OF CHLORINE FROM ROCKET EXHAUST

Estimates of the amount and distribution of chlorine released from the launch of the NASA Space Shuttle and the Titan IV expendable launch vehicle are available from Thiokol (Peter D. Evanoff, private communication, 1989). In Table 1 we report the kg of chlorine (as Cl) released in 5 km vertical intervals for Shuttle launches from Cape Canaveral, Florida (9 per yr) and for Titan IV launches from both Cape Canaveral (4 per yr) and Vandenberg Air Force Base, California (2 per yr). The chlorine is released as HCl which we treat as Cl_y in the models.

Table 1. Stratospheric Chlorine Released Annually by Shuttle/Titan IV Launches

Altitude	kg of chlorine (Cl)		
	location:		
	29°N 80°W	29°N 80°W	34°N 121°W
15-20 km	176,800	16,800	8,400
20-25 km	136,100	14,700	7,300
25-30 km	109,600	12,600	6,300
30-35 km	87,400	10,600	5,300
35-40 km	69,300	8,900	4,500
40-45 km	25,900	7,300	3,700
45-50 km	4,500	6,000	3,000

The launch scenario assumes 9 Shuttles and 4 Titans from Cape Canaveral, Florida (29°N 80°W) and 2 Titans from Vandenberg AFB, California (34°N 121°W).

The total amount of chlorine released into the stratosphere (above 15 km) by the solid rocket motors is 725,000 kg (0.725 kilotons) per year, and can be compared with that associated with industrial halocarbons. The chemical industry's production of halocarbons exceeds 1,250 kilotons of chlorine per yr (see UNEP/WMO, 1990). The release of chlorine during photochemical destruction of the chlorofluorocarbons (CFCs) occurs predominantly in the stratosphere, but happens slowly, on time scales of order 100 yr, over the lifetime of the gas. The estimated annual source of stratospheric chlorine from the industrial halocarbons is about 300 kilotons of chlorine per yr (AER model); the remainder of the annual emissions goes into the accumulating atmospheric burden of chlorinated halocarbons (about 600 kt/yr) or is destroyed in the troposphere. Thus, the launch schedule in Table 1 would add only about 0.25% to the current stratospheric source of Cl_y.

The release of chlorine from the 15 launches summarized in Table 1 was averaged over the year and put into the models as a continuous source of Cl_y every time step. The vertical distribution specified in Table 1 was used by the models. The latitudinal location of the two launch sites was included in all three models, but the longitudinal location could only be specified in the 3-D simulation.

3.0 TRANSIENT RESPONSE TO A SINGLE SHUTTLE LAUNCH

One launch of the Space Shuttle injects a single, very large pulse of 68,000 kg of chlorine into the stratosphere. Although this amount of chlorine is inconsequential on a globally averaged scale, the greatly enhanced levels of Cl_y in the vicinity of the exhaust plume may lead to large ozone depletions over a spatially limited region. We examined the transient response of stratospheric Cl_y to a single Shuttle launch using the 3-D GISS model. The chlorine is released over Cape Canaveral (29°N, 80°W) by using one-ninth of the annual source given in Table 1 as an instantaneous source.

Simulations were initiated on January 1 and July 1, and continued for one month. Immediately following the launch, the exhaust plume will not be completely mixed over the scales resolved by the model grid, and the calculations are intended to represent the average concentration of the resulting non-uniform distribution. Figures 1 and 2 summarize the instantaneous increase in Cl_y concentrations at 3.4 mbar (about 40 km altitude) as a function of latitude and longitude for days 2(a), 4(b), 8(c) and 30(d) following both the January and July initializations. Other levels in the upper stratosphere show similar effects, but lower altitudes in the stratosphere have smaller absolute enhancements of Cl_y (see Figures 3-5).

After two days (Figures 1a & 2a), the average increase in chlorine in the upper stratosphere, 50 ppt (January) and 70 ppt (July), is localized near the launch site with peak levels not resolved by the model grid (8° latitude by 10° longitude). After eight days (Figures 1c & 2c), the maximum grid-averaged levels have decreased by factors of about four (January) and two (July), have moved away from the launch site in accord with the prevailing winds, and have spread over horizontal scales that are resolved by the model. For the January launch most of the added chlorine (concentrations greater than 1 ppt) resides in the region bounded by 20°N-50°N and 40°W-100°W. The summer stratosphere is less dispersive, and for the July launch most of the Cl_y is contained between 20°N-36°N and 150°E-140°W. Eight days after the January 1 launch (Figure 1c) the largest grid-averaged perturbation to Cl_y (as resolved by the model grid) is less than 10 ppt, about 0.4% above background levels. Eight days after the July launch (Figure 2c) the added Cl_y remains more concentrated, greater than 30 ppt (about 1%) above background over a smaller area.

One month after the Shuttle launch (Figures 1d & 2d), the added chlorine is predicted to have spread over most of the upper stratosphere in the northern hemisphere, and the plume is expected to have mixed thoroughly. The winter stratosphere is dispersive and Cl_y perturbations are less than 1 ppt everywhere. In summer, the exhaust products remain predominantly over midlatitudes (20°N-50°N) with perturbations still as large as 3 ppt. The globally averaged depletion of ozone associated with a single launch should be less than that caused by the steady-state buildup of chlorine, as discussed below. Local destruction of ozone in the immediate vicinity of the rocket plume could be significantly larger and is not explicitly resolved in these global models.

4.0 STEADY-STATE ACCUMULATION OF STRATOSPHERIC CHLORINE

The three models used the continuous source of stratospheric chlorine from the rocket launches as described in section 2. The ultimate removal for the injected stratospheric Cl_y is transport into the lower atmosphere (troposphere) where most inorganic chlorine species are soluble and therefore removed rapidly by rainfall and other processes. In these models, this sink was applied by imposing either rapid loss for Cl_y below 10 km (2-D models) or a negligibly small concentration of Cl_y below 1 km (3-D model). Small differences in the application of this lower boundary condition do not affect the calculated stratospheric Cl_y distribution, because almost all of the chlorine transported into the troposphere is removed and cannot be recirculated back into the stratosphere.
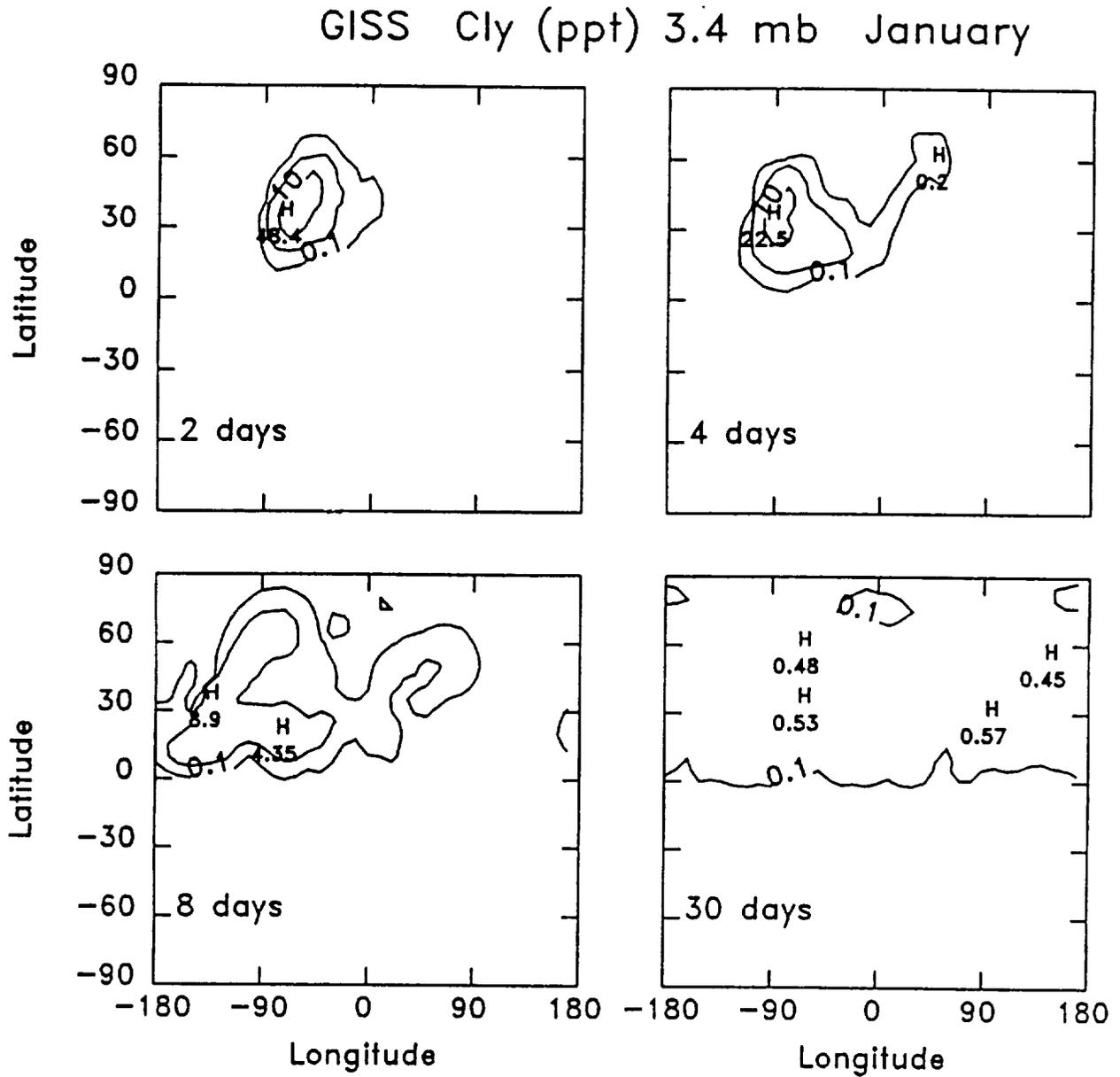
Figure 1. Latitude by longitude contours of chlorine enhancements near 40 km altitude due to a single Shuttle launch on January 1. Results from the GISS model are shown for (a) 2, (b) 4, (c) 8 and (d) 30 days following the launch.

GISS Cly (ppt) 3.4 mb July
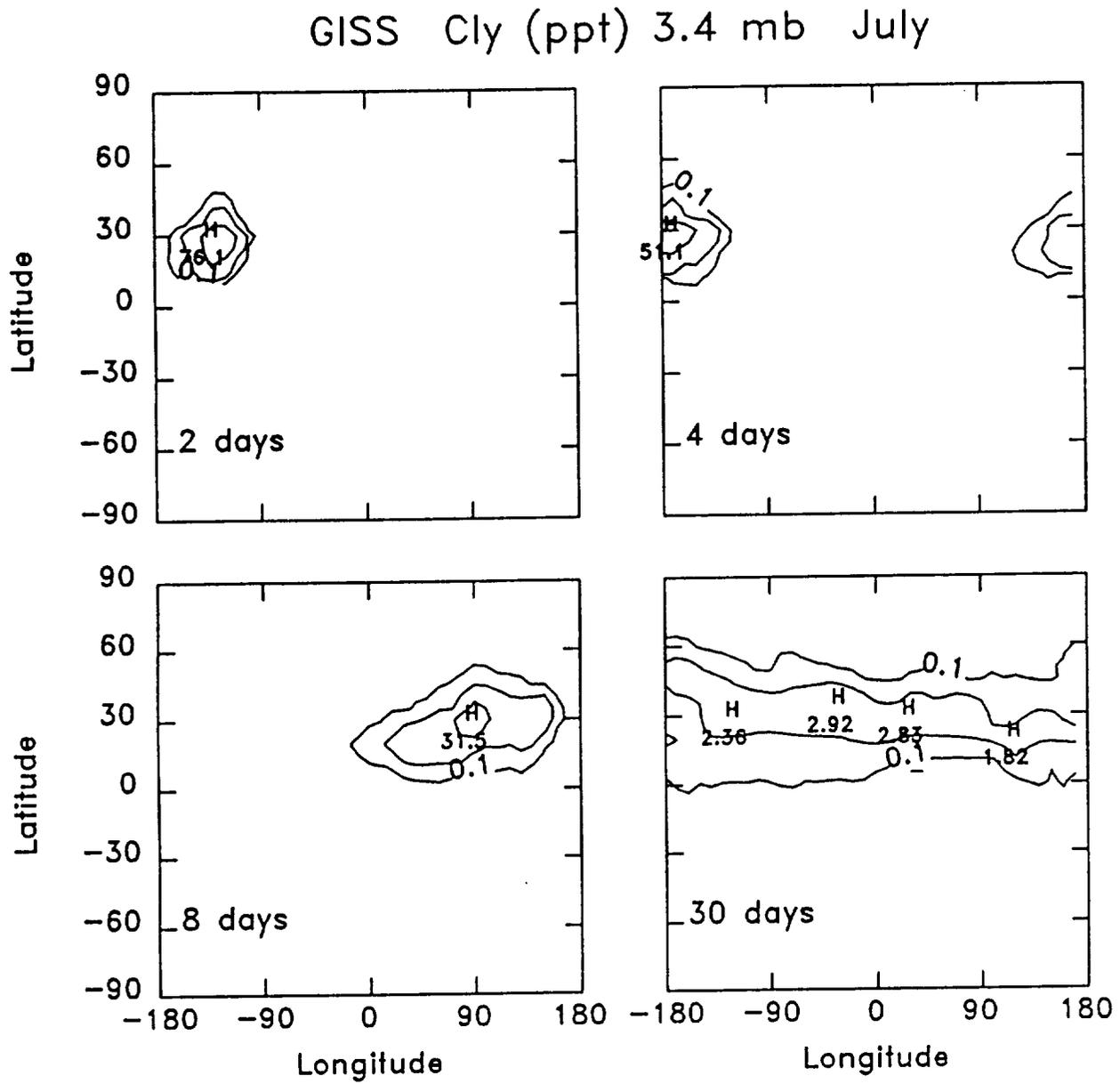
Figure 2. Latitude by longitude contours of chlorine enhancements due to a single Shuttle launch on July 1. See Figure 1.

115

These calculations were initiated and then continued for several model years until a steady-state distribution was reached. In steady state, stratospheric Cl_y additions have built up until the amount of chlorine injected into the stratosphere equals that transported into the lower troposphere.

The computed addition to Cl_y (ppt) associated with the Shuttle/Titan launches is shown as monthly, zonal averages in Figures 3-5 for the GSFC, AER and GISS models, respectively. The magnitudes of the Cl_y increase is largest in northern midlatitudes (30°N-50°N) near the source, and peaks in the upper stratosphere (30-45 km altitude) where the rocket emissions are largest on a molecule per molecule of air basis. Increased concentrations of Cl_y in the northern upper stratosphere range from 6 to 14 ppt in the GSFC model (Figure 3), 4 to 9 ppt in the AER model (Figure 4) and 6 to 12 ppt in the GISS model (Figure 5). The GSFC and GISS models predict a similar buildup of Cl_y; the AER model appears to have a more rapid stratospheric circulation (see Jackman et al., 1989b) that flushes out the chlorine more rapidly. In the lower stratosphere (15-25 km altitude) Cl_y concentrations are less enhanced: about 2 ppt at 15 km increasing to about 6 ppt at 25 km. Several years are required to transport substantial concentrations of the rocket source of Cl_y into the southern hemisphere stratosphere. Enhancements in the southern stratosphere range from less than 1 to as much as 6 ppt, and are generally a factor of 2 or greater below the corresponding enhancements in the northern stratosphere.

During northern winter, all models show rapid northward mixing between 30°N and the Pole, with isolines that slant poleward and downward. This basic pattern shown in Figures 3a-5a is typical of other long-lived stratospheric tracers, both from model calculations (see Jackman et al., 1989b) and observations (see NASA/WMO, 1986). The pattern of Cl_y during northern summer, however, dramatically shows the impact of a localized stratospheric source in a season without substantial latitudinal mixing. The increases in Cl_y concentration in July (Figures 3b-5b) peak strongly at 30°N between 30 and 50 km altitude in all three models, with monthly and zonally averaged maxima of more than 12 ppt in the GSFC and GISS models, and 9 ppt in the AER model.

In order to determine the relative perturbation to Cl_y from the rocket launches, the 2-D models compared the calculated Cl_y enhancements (Figures 3-4) with the Cl_y calculated from all other sources, the CFCs, CCl_4, CHF_2Cl, CH_3CCl_3, CH_3Cl. Air enters the stratosphere containing a mix of these halocarbons representing the bulk tropospheric mixing ratios of these species and with negligible concentrations of the more soluble inorganic chlorine (Cl_y). In the lower stratosphere, Cl_y concentrations are small because only a fraction of the CFCs have been photochemically destroyed, thereby releasing chlorine atoms. In the upper stratosphere where the halocarbon and CFC concentrations are greatly reduced, Cl_y concentrations approach their upper limit, currently about 3 ppb (parts per 10^9). The scenario for rocket launches in Table 1 leads to only modest perturbations in stratospheric Cl_y, as shown in Figures 6 (GSFC) and 7 (AER). The GSFC results predict increases ranging from 0.3 to 0.6% over the northern midlatitudes; while the AER model gives smaller enhancements, 0.2 to 0.3%. In the southern hemisphere, Cl_y increases are less than 0.2% for the GSFC model and 0.1% for the AER model.

Ozone perturbations at steady state associated with the source of Cl_y from rocket launches are shown in Figure 8 for the GSFC model. The largest depletions in ozone concentration, between 0.10% and 0.15%, occur in the upper stratosphere (30-45 km altitude) in the northern midlatitudes. Losses elsewhere are much smaller with the exception of the corresponding locations in the southern hemisphere. The depletion of the total column abundance of ozone is likewise small, less than 0.1%. The photochemical model used here includes only gas-phase, homogeneous chemical reactions; it does not account for the heterogeneous reactions occurring on polar stratospheric clouds that have been shown to be responsible for the chlorine-catalyzed destruction of ozone in the lower stratosphere during polar winter (the Antarctic ozone hole).
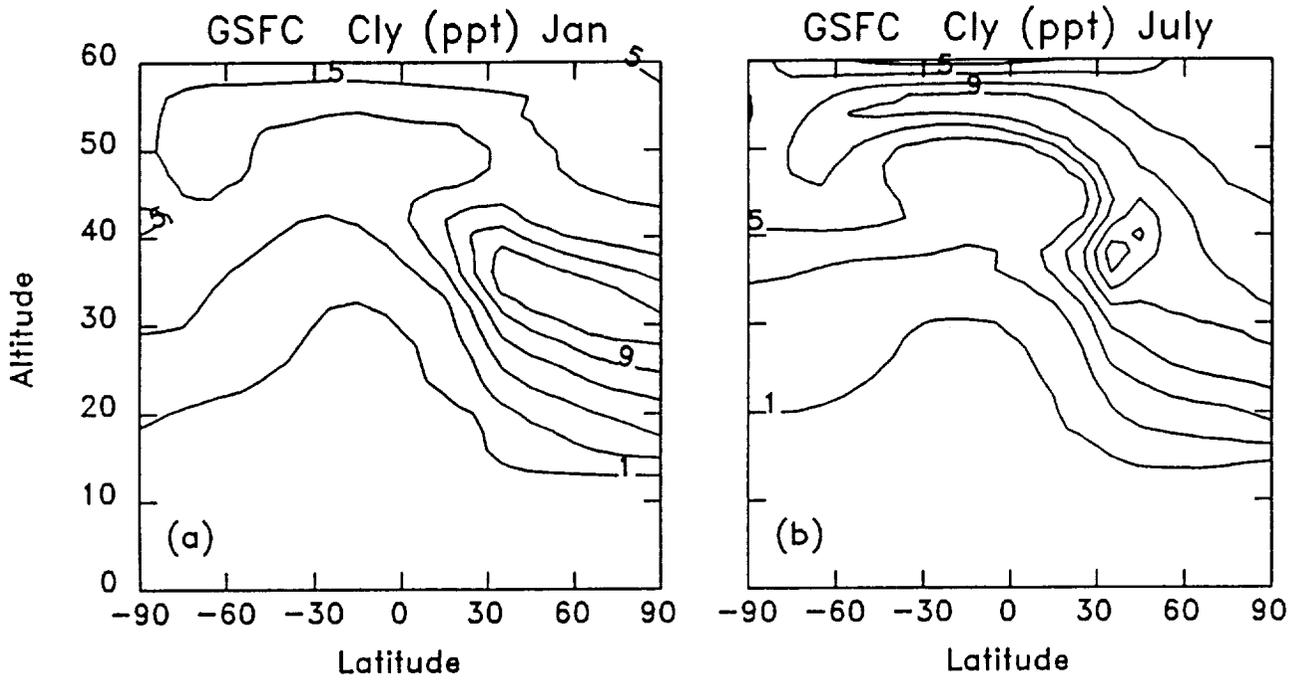
Figure 3. Latitude by altitude (pressure) contours of enhanced chlorine (in ppt) from the GSFC model. The steady-state buildup of chlorine as Cly is caused by the launch of 9 Shuttles and 6 Titan IV vehicles per year. The monthly and zonally averaged concentrations are shown for (a) January and (b) July.
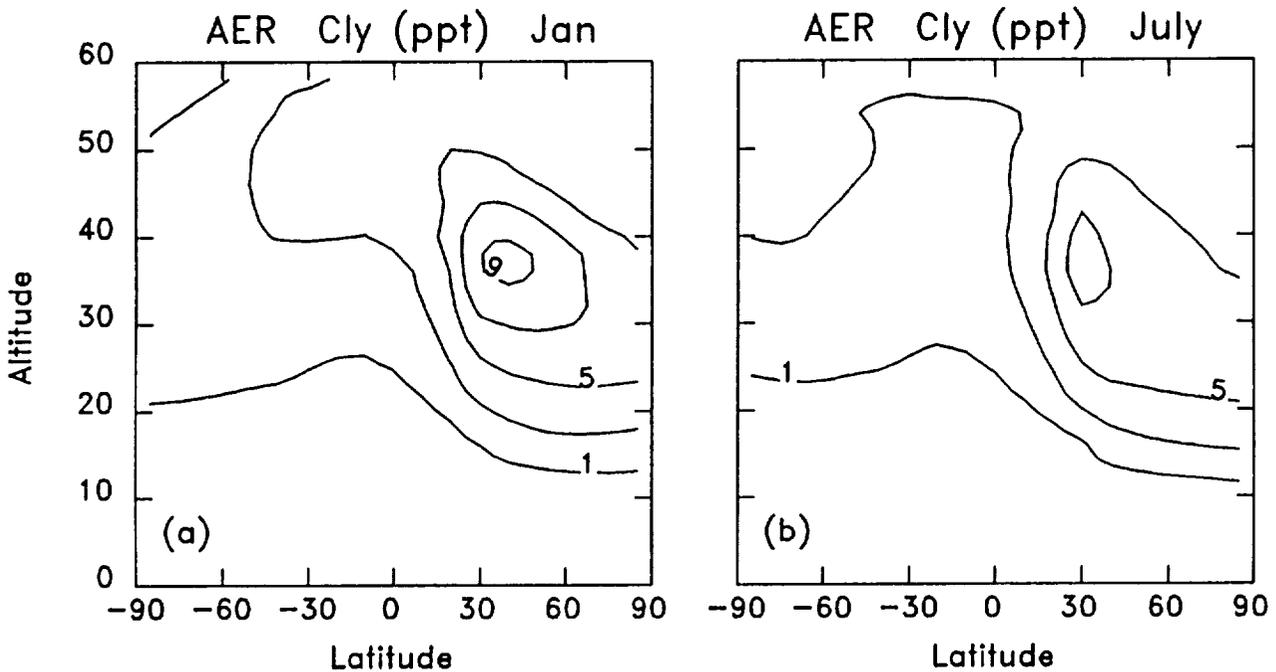

Figure 4. Latitude by altitude (pressure) contours of enhanced chlorine (in ppt) from the AER model. The steady-state buildup of chlorine as Cly is caused by the launch of 9 Shuttles and 6 Titan IV vehicles per year. The monthly and zonally averaged concentrations are shown for (a) January and (b) July.

117

GISS   Cly (ppt)   Jan

GISS   Cly (ppt)   July
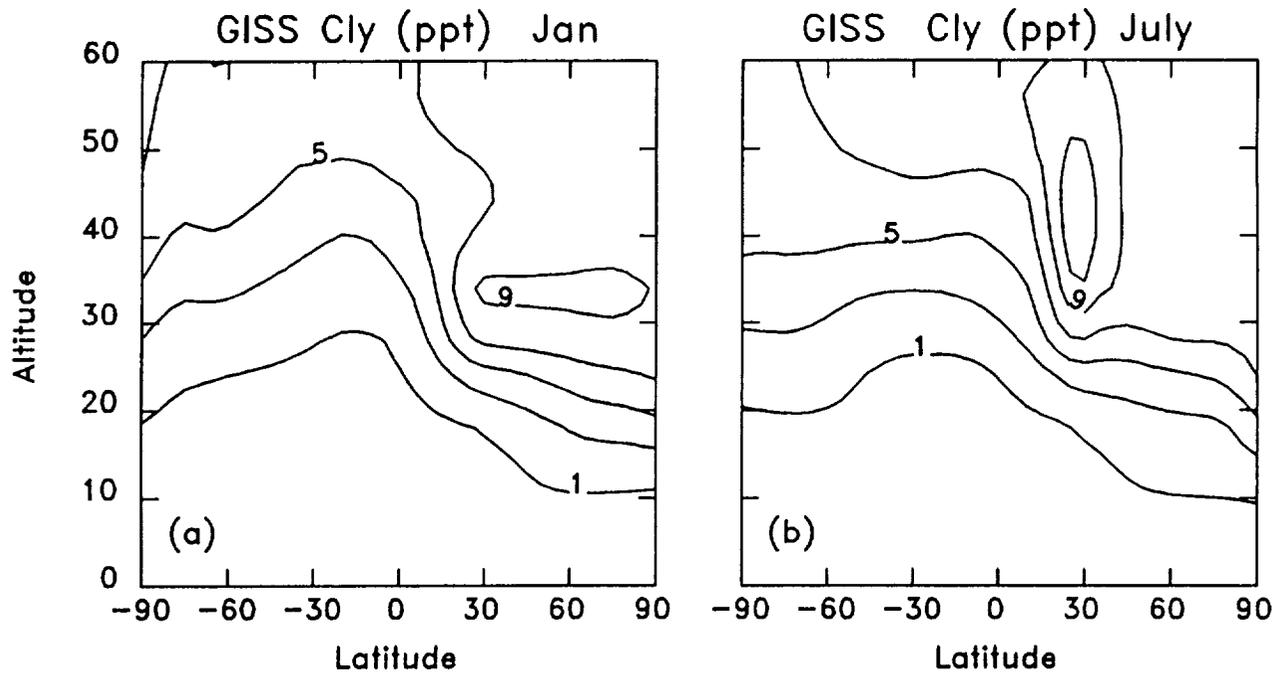
Figure 5. Latitude by altitude (pressure) contours of enhanced chlorine (in ppt) from the GISS model. The steady-state buildup of chlorine as Cl$_y$ is caused by the launch of 9 Shuttles and 6 Titan IV vehicles per year. The monthly and zonally averaged concentrations are shown for (a) January and (b) July.

GSFC   ΔCly (%)   Jan

GSFC   ΔCly (%)   July
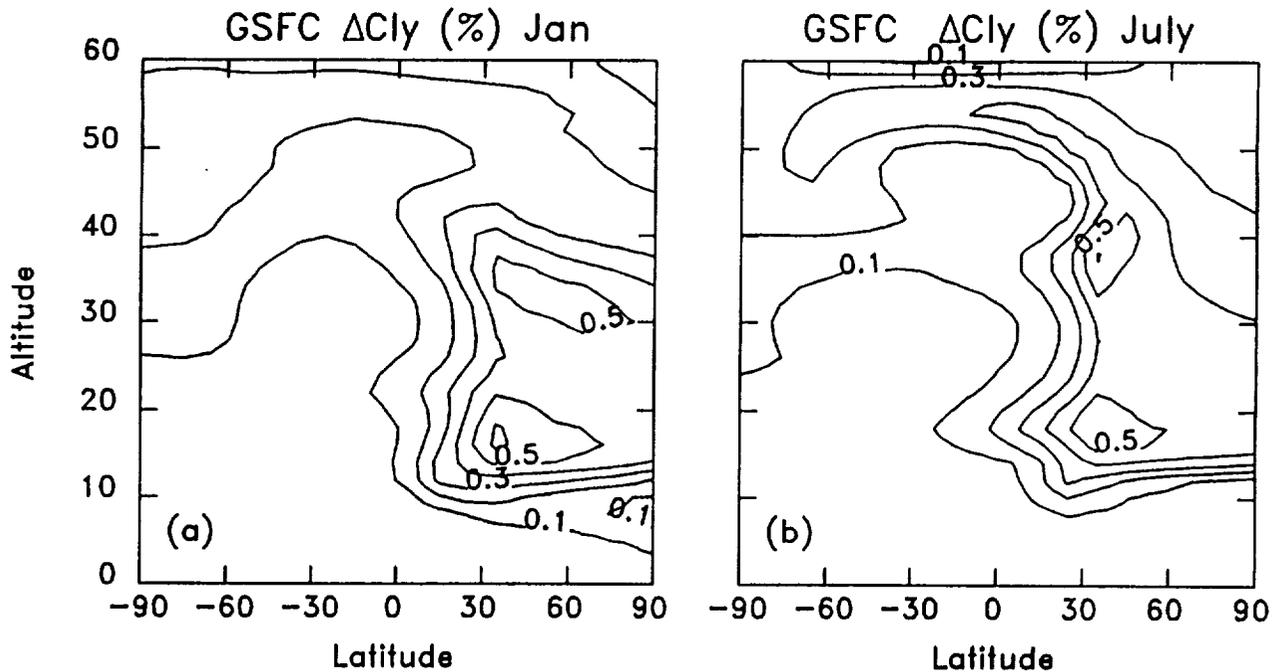
Figure 6. Latitude by altitude (pressure) contours of the perturbation to background Cl$_y$ levels (%) from the GSFC model. The steady-state buildup of chlorine as Cly is caused by the launch of 9 Shuttles and 6 Titan IV vehicles per year. The monthly and zonally averaged concentrations are shown for (a) January and (b) July.
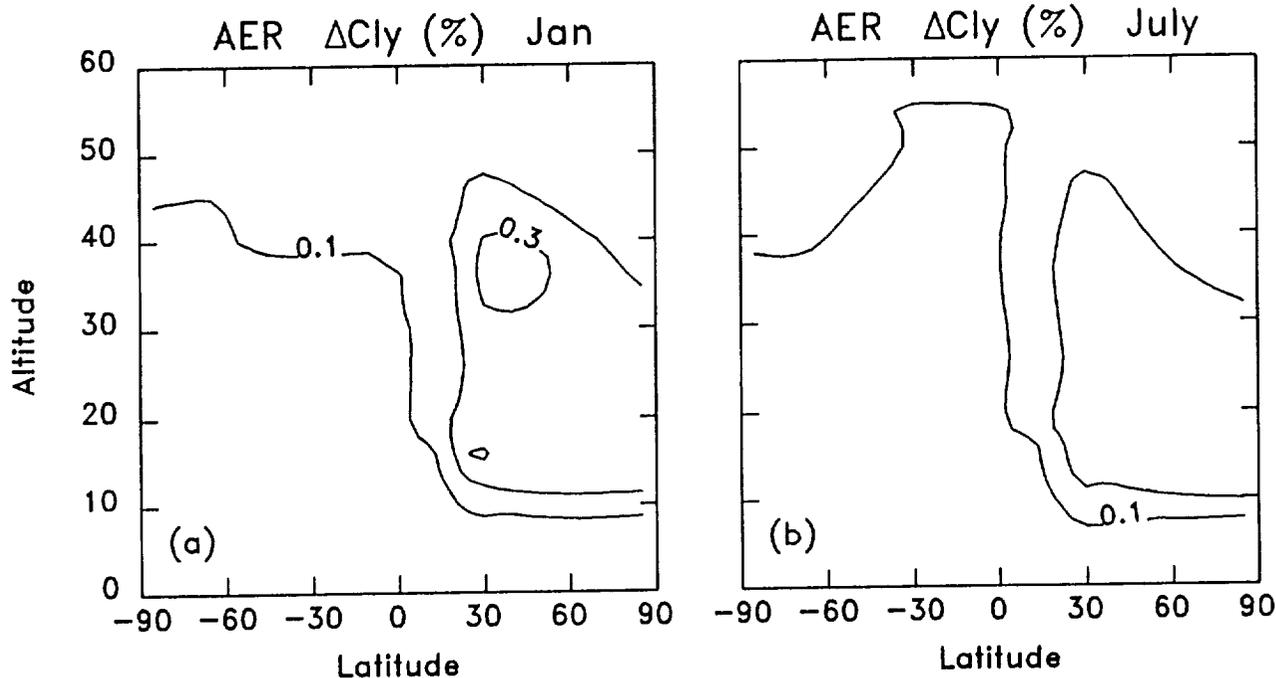
Figure 7. Latitude by altitude (pressure) contours of the perturbation to background Cl_y levels (%) from the AER model. The steady-state buildup of chlorine as Cl_y is caused by the launch of 9 Shuttles and 6 Titan IV vehicles per year. The monthly and zonally averaged concentrations are shown for (a) January and (b) July.
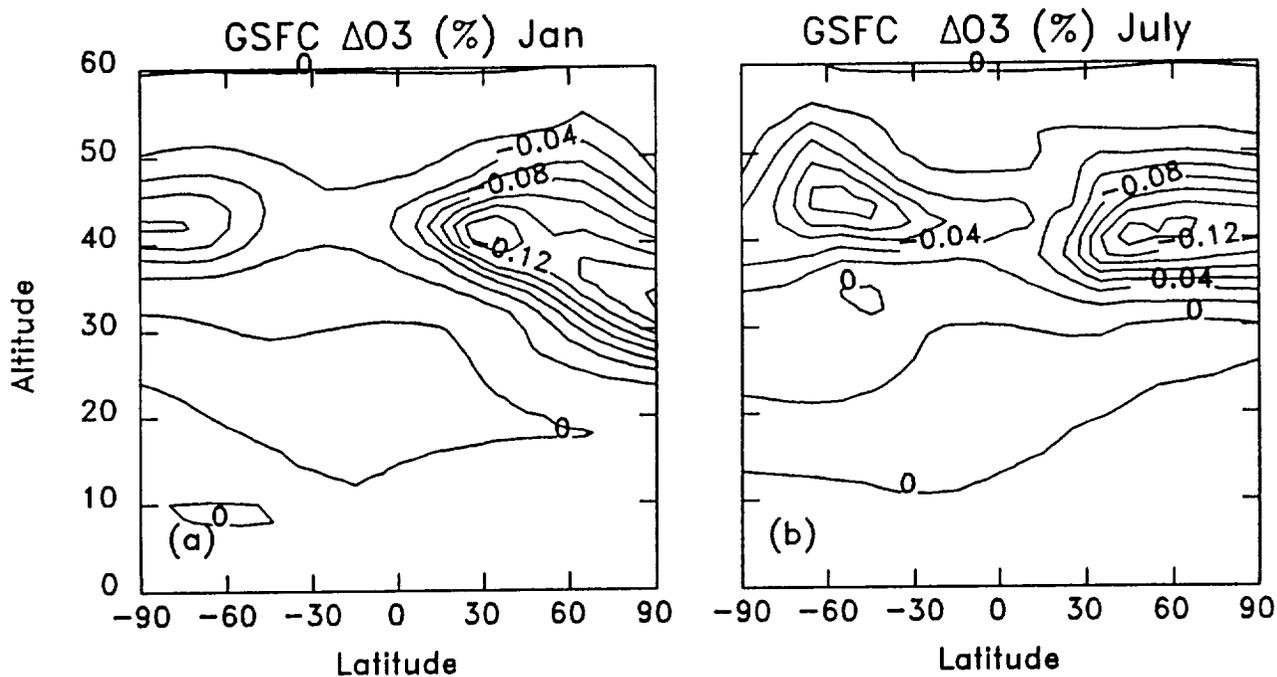

Figure 8. Latitude by altitude (pressure) contours of the perturbation to ozone (%) from the GSFC model. The steady-state buildup of chlorine as Cl_y is caused by the launch of 9 Shuttles and 6 Titan IV vehicles per year. The monthly and zonally averaged concentrations are shown for (a) January and (b) July.

119

Nevertheless, the impact of Shuttle chlorine on further polar ozone loss can probably be constrained since the relative perturbations to Cl_y in the lower stratosphere are less than 0.1% over Antarctica and 0.5% over the Arctic.

5.0 SUMMARY AND CONCLUSIONS: The Potential for Ozone Depletion

Each launch of the Space Shuttle injects about 0.068 kilotons of chlorine into the stratosphere. This amount is small compared to the current background of stratospheric chlorine (3 ppb), which is generated from the photochemical destruction of industrial and natural halocarbons within the stratosphere at a rate of about 300 kilotons per year. Global stratospheric models are used here to assess the impact of the currently modest launch schedule on stratospheric chemistry and ozone depletion.

In the immediate exhaust plume of the Shuttle (about 40 m across in the upper stratosphere), concentrations of HCl are large, about 0.08 by volume. Even if this plume were mixed over a 10 x 10 km area, concentrations would still exceed 1000 ppb. However, a 100 km^2 area comprises less than 1/1,000,000 of the midlatitude stratosphere, and the global or even regional effects of complete ozone destruction within this corridor would be inconsequential. Furthermore, the chlorine is released predominantly as HCl and would need some time to be chemically processed into more catalytically active forms (Cl or ClO). The path of the Shuttle is not vertically aligned, the corridor of exhaust gases is spread over lateral extent of more than a 1000 km in a day, and thus no local hole in column ozone could occur above the launch site.

This early stage following the launch is not adequately modeled in these calculations, but we believe that strict limits can be placed on the potential for global ozone destruction because the amount of chlorine injected is small compared with that contained in a 1000 km by 1000 km region (less than 0.2 ppb out of more than 2 ppb Cl_y). In order to have a significant impact on ozone globally, the plume must mix with the stratospheric environment and lead to significant perturbations over scales of at least 1000 x 1000 km.

In the few days following a launch, stratospheric winds will have stretched and dispersed the exhaust plume to scales greater than 1000 km. The average increase in stratospheric chlorine levels over such an area is modest, at most +5% within a 20° latitude by 20° longitude area. By the end of the month, these perturbations decrease rapidly to less than 0.2% above background levels as the chlorine is mixed laterally throughout the stratosphere.

A continuous series of rocket launches will lead to a buildup of chlorine in the stratosphere whose magnitude is governed by the frequency of launches and the rate of the stratosphere-troposphere circulation. For a scenario of 9 Shuttle and 6 Titan IV launches per year, the accumulation of chlorine in the stratosphere is still modest, ranging from 0.2 to 0.6% over northern midlatitudes and much less in the tropics and southern hemisphere. Corresponding ozone depletions are even smaller, less than 0.25% locally and less than 0.1% in the total column.

The addition of Cl_y to the winter polar stratosphere is of particular interest because of the role that chlorine plays in creating the Antarctic ozone hole, but the expected buildup at the poles represents only a small fractional increase to current levels. In the future, we might hope that stringent controls on industrial production of halocarbons, as envisaged by the Montreal Protocol, would reverse the current trend and lead to lower background levels of Cl_y. Even the most optimistic controls over halocarbons would not lead to Cl_y concentrations less than 2 ppb much before the end of the 21st century.

The Shuttle and Titan IV solid rocket motors comprise the largest source of stratospheric chlorine that is expected from the current space fleet. The major launch vehicles from the U.S. and other space agencies use non-chlorinated (e.g., liquid) fuels or employ much smaller rockets. The U.S. strategic nuclear arsenal uses solid fuel containing chlorine, but in such launches most of the chlorine would be released below 15 km.

The exhaust from the solid rocket motors also contains other possible stratospheric pollutants. The major gaseous components are CO (24% by wt), HCl (21%), H_2O (10%), N_2 (9%), CO_2 (4%) and H_2 (2%). The perturbation to CO should be about the same in mixing ratio as that to Cl_y, and would not significantly affect the background levels of order 100 ppb. Clearly the HCl represents the largest fractional perturbation to the background stratosphere; the remaining effluents should have negligible impact on the stratosphere.

Another principal exhaust product, particulate Al_2O_3 (30%), has the potential to perturb stratospheric chemistry. Most of the alumina is reported to form particles of radii greater than 1 micron; these fall out of the stratosphere more rapidly than the gaseous products which are removed by the circulation exchanging air between the stratosphere and troposphere (modeled here). The abundance of the larger alumina particles appears to be increasing (Zolensky et al., 1989) and has been attributed to solid rocket motors as well as space debris. However, some atmospheric measurements (Cofer et al., 1985) indicate that a significant fraction of the mass is in particles with radii of about 0.1 micron and thus would accumulate in a manner similar to Cl_y in these calculations. Alumina particles may act as ice deposition nuclei in the lower stratosphere (Turco et al., 1982). Observational evidence (Cofer et al., 1984) and laboratory studies suggest that alumina particles react with the HCl in the exhaust to form chlorides and may provide active sites for Cl_y-NO_y heterogeneous reactions in the lower stratosphere. Thus the buildup of small particles in the lower stratosphere may enhance both precipitation (dehydration or denitrification) and ozone destruction in the lower stratosphere. The role of particulates from solid rocket motors in the chemistry of the stratosphere is not well characterized today, and further research will be needed for a reliable assessment of future impacts.

REFERENCES

Cofer, W. R., III, G. L. Pellett, D. I. Sebacher and N. T. Wakelyn, Surface chloride salt formation on Space Shuttle exhaust alumina, J. Geophys. Res., 89, 2535-2540, 1984.

Cofer, W. R., III, et al., Airborne measurements of space shuttle exhaust constituents, AIAA J., 23, 283-287, 1985.

Douglass, A. R., C. H. Jackman and R. S. Stolarski, Comparison of model results transporting the odd nitrogen family with results transporting separate odd nitrogen species, J. Geophys. Res., 94, 9862-9872, 1989.

Jackman, C. H., A. R. Douglass, P. D. Guthrie and R. S. Stolarski, The sensitivity of total ozone and ozone perturbation scenarios in a two-dimensional model due to dynamical inputs, J. Geophys. Res., 94, 9873-9878, 1989a.

Jackman, C. J., R. K. Seals, Jr. and M. J. Prather, Two-dimensional intercomparison of stratospheric models, NASA Conference Publication 3042, 1989b.

Ko, M. K. W., K. K. Tung, D. K. Weisenstein and N. D. Sze, A zonal mean model of stratospheric tracer transport in isentropic coordinates: numerical simulations for nitrous oxide and nitric acid, J. Geophys. Res., 90, 2313-2329, 1985.

Ko, M. K. W., N. D. Sze and D. K. Weisenstein, The roles of dynamics and chemical processes in determining the stratospheric concentration of ozone in 1-D and 2-D models, J. Geophys. Res., 94, 9889-9896, 1989.

NASA/WMO, Atmospheric ozone 1985: Assessment of our understanding of the processes controlling its present distribution and change, Geneva, World Meteorological Organization, Global Ozone Research and Monitoring Project Report No. 16, 1986.

Potter, A. E., Environmental effects of the Space Shuttle, J. Environ. Sci., 21, 15-21, 1978.

Prather, M. J., M. M. Garcia, R. Suozzo and D. Rind, Global impact of the Antarctic ozone hole: Dynamical dilution with a 3-D chemical transport model, J. Geophys. Res., 95, 3449-3471, 1990.

Radke, L. F., P. V. Hobbs and D. A. Hegg, Aerosols and trace gases in the effluents produced by the launch of large liquid- and solid-fueled rockets, J. App. Meteor., 21, 1332-1345, 1982.

Turco, R. P., O. B. Toon, R. C. Whitten and R. J. Cicerone, Space Shuttle ice nuclei, Nature, 298, 830-832, 1982.

Watson, R. T., M. J. Prather and M. J. Kurylo, Present state of knowledge of the upper atmosphere 1988: an assessment report (NASA's Upper Atmosphere Research Program's Report to the Congress), NASA Reference Publication 1208, 208 pp, 1988.

UNEP/WMO, Scientific Assessment of Stratospheric Ozone: 1989, Vol. II, The AFEAS Report, World Meteorological Organization, Global Ozone Research and Monitoring Project, Report No. 20, 1990.

Zolensky, M. E., D. S. McKay and L. A. Kaczor, A tenfold increase in the abundance of large solid particles in the stratosphere, as measured over the period 1976-1984, J. Geophys., Res., 94, 1047-1056, 1989.

SECTION F

The Atmospheric Effects of Stratospheric Aircraft: Modeling and Measurements in Support of the High-Speed Research Program

(Appendix A to NRA-89-OSSA-16)

INTRODUCTION

The growth in commercial aviation is rapid and expected to continue into the next century. The desire for faster civil aircraft has long been recognized, and supersonic transports (SST's) were first proposed and studied more than two decades ago. The emissions from aircraft, both the current subsonic fleet and the projected supersonic fleet, are expected to perturb the chemical and physical environment in which they are emitted. The chemical perturbations expected from aircraft emissions include the enhancement in concentrations of odd-nitrogen compounds (NOx = NO + NO$_2$) and water vapor, and the subsequent photochemical perturbations to ozone. The magnitude of atmospheric effects is uncertain and may range from local impacts in preferred flight corridors to global perturbations through long- range atmospheric transport of emissions.

In order to assess the atmospheric impact of a fleet of commercial supersonic aircraft that cruise predominantly in the stratosphere, it is necessary to develop a scientifically sound understanding of the many perturbations that may result. It has been recognized in previous assessments of stratospheric aircraft (CIAP Report of Findings, A.J. Grobecker et al., eds., Climate Impact Assessment Program, DOT-TST-75-58, December 1974) that emissions of NO$_x$ and H$_2$O in the stratosphere may lead to ozone loss and possibly global climate change. The goal of this research program is not to determine what levels of aircraft emissions and ozone loss are environmentally acceptable, but rather more simply to determine what atmospheric effects may be expected for given levels of engine technology and operations.

In making the assessment of possible atmospheric changes caused by a fleet of stratospheric aircraft, it must be remembered that these perturbations are not occurring in isolation or in a static atmosphere. The atmosphere is currently evolving. Trace gases such as methane, nitrous oxide, and the halocarbons are expected to increase substantially (>20 %) over the next several decades. Furthermore, the proposed development of supersonic aircraft would affect all of civil aviation, including the projected operations of the subsonic fleet. Any assessment of the supersonic aircraft fleet must take into account such interactions in a framework of overall global change.

This assessment of stratospheric aircraft cannot be completed with the current global chemistry models since we recognize many areas of uncertainty in these models. The possible sources of error in the global models make it difficult to quantify accurately the perturbations caused by additional aircraft emissions.

OBJECTIVES

We shall, therefore, sponsor a focussed program of atmospheric research. This research shall be directed toward calculating the global impact of atmospheric emissions, and particularly that of stratospheric aircraft on ozone. A fundamental requirement of the program will be the capability of modeling the global atmospheric chemistry in response to a series of aircraft emission scenarios. These models, designated assessment models here, will be used on a regular basis to compare the relative impact of a set of projected emission scenarios. The assessment models must be improved along with the parallel research in this program, and they must be maintained as

123

among the best scientific models for global atmospheric chemistry. Furthermore, specific research topics involving the modeling and measurement of fundamental chemical and dynamical processes in the stratosphere and troposphere will be supported.

A primary objective of the program is that there be annual progress in improving and validating the chemical transport models (CTM's), and hence, to reduce the uncertainties in current assessments. Based on the model predictions resulting from this program, it may be possible to optimize the emissions and operations of future aircraft fleets in order to minimize, and possibly avoid detrimental impacts on the atmosphere.

PROGRAM ELEMENTS

The following topics of research are important components of the High-Speed Research Program (HSRP), and we invite proposals that address one or more of these components:

1. Global chemical models for stratospheric ozone

The overall assessment of the atmospheric impact of stratospheric aircraft will be made with multidimensional global models of stratospheric chemistry and dynamical transport (CTM's). At present, these CTM's are represented by the basic two-dimensional zonally averaged models that have been used to predict perturbations to stratospheric ozone caused by increasing levels of chlorofluorocarbons (R.T. Watson et al., Present State of Knowledge of the Upper Atmosphere 1988: An Assessment Report, NASA Ref. Pub. 1208, August 1988). The 2-D stratospheric models will provide the basic assessment capability for the High-Speed Research Program in the near future. Within the next five years, it is expected that three-dimensional CTM's, currently supported by the Upper Atmosphere Program, will also be able to contribute to the prediction of stratospheric ozone perturbations. The assessment models are the basic tools with which to evaluate the impact of different scenarios of aircraft emissions; they can be used in sensitivity studies to choose between alternative scenarios for operations or emissions.

Preliminary simulations with the current assessment models using a range of typical aircraft emission scenarios show some interesting features: (1) perturbations are highly seasonal with chemical losses of ozone peaking at mid and high latitudes in summer; (2) the ozone decrease is very sensitive to the altitude of injection, with dramatically larger loss when cruise altitude is raised from 19 to 21 km (maximum impact on column ozone occurs for injections between 23-28 km); and (3) the stratospheric response is sensitive to the amounts of Clx.

It is recognized that the current 2-D models have several known uncertainties associated with these assessments. For example, in these models the transport of emissions injected near the tropopause is not treated as a resolved meteorological process, but instead as a highly parameterized diffusive process that has not been well tested. We need to develop a good observational database of species that are sensitive measures of cross-tropopause transport including chemically important tracers such as ozone and nitric acid. Furthermore, heterogeneous chemistry and tropospheric chemistry are not well developed and tested in the 2-D stratosphere models.

NEEDS: Basic global assessment models are an important and critical component of the High-Speed Research Program. They must be capable of simulating many possible scenarios for aircraft emissions. These models must have current chemistry and be validated and documented in the scientific literature. The models must be committed to continued improvement and testing; they must be prepared to incorporate basic improvements and new parameterizations of key processes (e.g., stratosphere-troposphere exchange, heterogeneous chemistry, the nonlinear effects of plume chemistry) as the Program develops and uncertainties are reduced. These models must be available

124

to make sensitivity studies for the overall assessment as determined by the HSRP and Advisory Committee.

2. Emissions scenarios

Aircraft are known to emit water vapor, carbon dioxide, carbon monoxide, nitric oxide, sulfur dioxide, unburnt hydrocarbons, soot, trace metals, and condensation nuclei. With the currently available models, the emissions of NO_x in particular are predicted to give some reduction in ozone over much of the stratosphere, with possible enhancements in tropospheric ozone. With current models the impact varies critically with the cruise altitude: the higher the altitude for NO injection (over the altitude range 16-30 km), the greater the predicted ozone loss.

Aircraft emissions in the atmosphere are basically bimodal between the subsonic fleet (<12 km) and the supersonic fleet (>18 km, lower over land if subsonic flight is required). Most emissions from supersonic aircraft are expected at cruise altitude; with higher Mach numbers resulting in higher desired cruise altitudes: e.g., 18 km at Mach 2.4, 23 km at Mach 3.2. It is important to consider as wide a range as possible for the aircraft emissions scenarios, including emission indices and operational range. The NO_x emission index (EI) ranges from 30 to 50 $g(NO_2)/kg(fuel)$ for current combustor technology applied to advanced (i.e., year 2000 and beyond operation) cycle engines for supersonic aircraft. It appears that significant effort would be required to reduce the EI to a range 5-20 (i.e., practical demonstrated limit for stationary turbine applications) in a commercial aircraft engine, and innovative technology is needed for reduction below 5.

NEEDS: This is a critical HSRP element. It is expected that the HSRP, through the related System Studies, will provide the necessary emission scenarios from the aircraft industry. We also will consider independent proposals to augment these basic scenarios.

More detailed emissions scenarios are needed both in terms of clearly defined emission indices (g of chemical substance per kg of fuel) and in terms of operational flight patterns. We need to characterize the emissions of NO_x, H_2O, CO, hydrocarbons, SO_2, condensation nuclei, soot, and metals as a function of aircraft and engines, and also in terms of the conditions under which they are emitted (e.g., altitude, temperature, ascent, or descent). The emission indices must be realistic, including values for today's engines and those projected for future development. The operational flight pattern of emissions must be specified as a function of latitude and longitude as well as time of year. It is important to identify preferential flight corridors. Seasonal effects may be important in determining the effective altitude above the tropopause and the removal of pollutants by the general circulation. Future scenarios should consider emissions from the combined subsonic plus supersonic aircraft fleet as well as the changes in atmospheric composition due to other human activities or climate change.

3. 3-D chemical transport models and longitudinal asymmetry

The initial emissions from aircraft will occur preferentially along flight corridors. Following the initial mixing of the exhaust plumes (see section 4 below), the wind shear should mix the emissions into a zonally uniform distribution in approximately 5 to 20 days. When the identity of the plumes is lost (>20 days), an "intelligently" parameterized zonal-mean 2-D model would be able to correctly calculate the chemical perturbations.

Nevertheless, this time scale for zonal mixing is sufficient to accumulate enhanced levels of emissions within the preferred flight corridors. Chemical eddies (i.e., nonlinear effects in zonal averaging of the chemical terms) are probably of second-order importance after 5-10 days, with the possible exception of heavily travelled flight corridors.

Accurate simulation of the dynamical mixing of tracers in the stratosphere and upper troposphere is also critical for this assessment, since much of the aircraft emissions occur so close to the tropopause. The 3-D models should be used for calculating transport and redistribution of emissions near and above the tropopause because such transport in a 3-D framework is not tuned to an eddy diffusion parameter as for 2-D.

NEEDS: Three-dimensional models are needed in the early stages of this program to evaluate the importance of 3-D processes in mixing the aircraft emissions throughout the atmosphere. (In this role the 3-D CTM's need not include complete stratospheric chemistry.) Specifically, we recognize that the accumulation of effluents in flight corridors and the details of stratospheric removal of NO_x and H_2O (to the troposphere) can be best addressed with the 3-D global CTM's. Further work is needed on the intelligent parameterization of 2-D zonal models (i.e., mean advective circulation plus unresolved, diffusive mixing) that is based on a self- consistent 3-D circulation. Later in this program, it is expected that some 3-D CTM's with full chemistry will be used in the overall assessment (as noted in section 1 above).

4. Plume chemistry and dispersion

Initially, the exhaust plume from an aircraft is hot and highly turbulent; it entrains ambient air, rising and expanding to dimensions of order 100 m. Thereafter, a combination of wind shear and diffusion act to mix the plume with the ambient stratosphere on time scales of a few days or less. Before dispersion the concentrations of NOx and other effluents within the plume are highly concentrated. The chemical system may be driven by nonlinear reactions involving NOx species and by heterogeneous chemistry occurring on aerosol particles. Specific examples of questions to be addressed include: Is there rapid ozone loss inside the plume? Do ice particles grow large enough within the plume to fall out, thereby removing H_2O, HNO_3, HCl, and HBr?

NEEDS: Models are needed to simulate the dispersion and mixing of aircraft engine emissions, on scales from the initial exhaust plume up to the several hundred kilometers as resolved in the global models. During this mixing, the net chemical effects (e.g., perturbations to ozone, transformations of NO_x and chlorine compounds) must be modelled and assessed in so far as they have global impact after mixing with the ambient stratosphere. One goal of this research will be to develop parameterizations of this subgrid process, where necessary, for the global assessment models.

5. Gas-phase and aerosol chemistry

The chemistry of the lower stratosphere is expected to be perturbed in regions where aircraft emissions build up. In this region of the atmosphere, important chemical transformations include gas-phase reactions (especially three-body processes) and heterogeneous chemical reactions on particles (shown to play a major role in perturbing the winter stratosphere at both poles). There are uncertainties in our chemical modeling of the lower stratosphere, even under unperturbed conditions.

Do we understand the chemical cycles in the stratosphere sufficiently well to predict chemical perturbations in the presence of increased concentrations of a wide variety of emissions? For NO_x the chemistry is moderately well understood with the exception of heterogeneous reactions and, possibly, organic nitrates. For H_2O the chemical effects are straightforward, but the impacts on aerosol growth on water vapor at the tropopause are not well understood. The chemistry of CO is understood, and that of CO_2 should have minimal effect. There is a need to define the major hydrocarbon components (CH_4, C_xH_y, C_xC_yO) in aircraft emissions. The natural cycle of SO_2 and sulfates in the stratosphere currently has large uncertainty. Metals are predicted to play a role in the ozone budget of the mesosphere and upper stratosphere through their interaction with HCl and formation of metallic chlorides, but this has not been verified under conditions appropriate to the lower stratosphere.

126

Further complications to the current chemical models focus on the role of aircraft emissions in heterogeneous processes. If emissions occur in the middle of the natural sulfate aerosol layer, the chemistry in the plume or of the layer itself may be affected by SO_2 emissions. The expected increases in H_2O, HNO_3 and H_2SO_4 may lead to enhanced formation of stratospheric aerosols, including polar stratospheric clouds. Enhanced particle growth and fallout could remove NO_x. We have difficulty modeling gas-particle chemistry now (e.g., the Antarctic ozone hole), and we can expect an enhanced role for aerosol chemistry given the emission of condensation nuclei and other effluents from stratospheric aircraft.

NEEDS: Laboratory measurements and modeling of the chemical processes occurring on aerosols are needed. Many different chemical surfaces may play a role: sulfuric acid, polar stratospheric clouds (type I & II), condensation nuclei from the aircraft. We also need fundamental kinetics measurements, especially for three-body reactions in the lower stratosphere, and for nonlinear reactions important for high concentrations of NO_x, H_2O hydrocarbons and possibly chlorine compounds (e.g., ClO released by aerosol chemistry).

Laboratory measurements and modeling of the microphysics, the growth, and possible fallout of particles will also be important.

6. Tropospheric chemistry

Increased emission of NO_x from the growth of both supersonic and subsonic fleets will likely result in increases in tropospheric NO_x. Enhanced levels of NO_x and nonmethane hydrocarbons are expected to lead to increased levels of ozone under tropospheric conditions, but we cannot currently assess the impacts of the proposed aircraft fleets on tropospheric ozone, and may require 3-D CTM's to do so.

NEEDS: Tropospheric chemistry, especially that involving NO_x, hydrocarbons, and production of O_3, must be developed and included in the global chemical assessment models, especially the 3-D models. A broad database for NO_x and nonmethane hydrocarbons in the upper troposphere should be developed. Current observations need to be gathered and analyzed, and possibly new measurement campaigns designed (see section 8 below).

7. Climate effects

Changes in surface temperature may be driven by radiative forcing due to perturbations in (1) lower stratospheric H_2O, (2) upper tropospheric ozone, or (3) stratospheric aerosols (scattering as well as absorption by soot). The CO_2 emitted by the proposed supersonic fleet is believed to be inconsequential. Further changes in the climate of the middle atmosphere would occur if there were major perturbations to stratospheric ozone, and hence solar heating.

NEEDS: An assessment of the radiative forcing associated with aircraft emissions is a part of this program.

8. Atmospheric observations and field experiments

NEEDS: There is a clear, immediate need for measurements of NO_x, O_3, H_2O and other chemically active species in the lower stratosphere and upper troposphere (see section 6 above) in order to define a reference chemical climatology for this part of the atmosphere. These measurements are a fundamental part of calibrating and testing the global models used in this assessment; they also provide a reference standard for future changes in the chemical composition of the atmosphere.

127

In the near future there will likely be specific flight campaigns with high-altitude aircraft (probably an ER-2 or similar aircraft) to measure the chemical perturbations and dispersion of aircraft emissions (hopefully from current supersonic aircraft). In this case, we may also consider the feasibility of an atmospheric experiment involving release of an artificial tracer along a flight corridor in the lower stratosphere.

In support of such field experiments, we should begin now to develop the strategy, and hence the instruments, needed to measure the chemical perturbations associated with stratospheric aircraft.

SECTION G

CONTRIBUTORS AND REVIEWERS*

Section B
Scientific Assessment of Stratospheric Ozone: 1989
Volume I

CONTRIBUTORS

1. Steering Committee

Co-Chairs

R. T. Watson	NASA Headquarters	USA
D. L. Albritton	NOAA Aeronomy Laboratory	USA

Members

F. Arnold	Max-Planck-Institut für Kernphysik	FRG
R. D. Bojkov	World Meteorolgical Organization	Switzerland
D. Ehhalt	Kernforschungsanlage Julich	FRG
P. Fraser	CSIRO	Australia
I. Isaksen	University of Oslo	Norway
V. Khattatov	State Committee for Hydrometeorology	USSR
C. Mateer	Atmospheric Environment Service (Retired)	Canada
T. Matsuno	University of Tokyo	Japan
M. Prendez	Universidad de Chile	Chile
J. A. Pyle	University of Cambridge	UK
B. H. Subbaraya	Physical Research Laboratory	India
P. Usher	United Nations Environment Programme	Kenya

2. Authors

Chapter 1. Polar Ozone

Coordinator

S. Solomon	NOAA Aeronomy Laboratory	USA

Principal Authors

W. L. Grose	NASA Langley Research Center	USA
R. L. Jones	Meteorological Office	UK
M. P. McCormick	NASA Langely Research Center	USA
M. J. Molina	Massachusetts Institute of Technology	USA
A. O'Neill	Meteorological Office	UK
L. R. Poole	NASA Langley Research Center	USA
K. P. Shine	University of Reading	UK
S. Solomon	NOAA Aeronomy Laboratory	USA

Other Contributors

R. A. Plumb	Massachusetts Institute of Technology	USA

---

* Affiliations have been updated to 1990 to give the most current information known.

| U. Schmidt | Kernforschungsanlage Julich | FRG |
| V. Pope | Meteorological Office | UK |

Chapter 2. Global Trends

Coordinator

| G. Megie | Service d'Aeronomie du CNRS | France |

Principal Authors

M.-L. Chanin	Service d'Aeronomie du CNRS	France
D. Ehhalt	Kernforschungsanlage Julich	FRG
P. Fraser	CSIRO	Australia
J. F. Frederick	University of Chicago	USA
J. C. Gille	National Center for Atmospheric Research	USA
M. P. McCormick	NASA Langley Research Center	USA
G. Megie	Service d'Aeronomie du CNRS	France
M. Schoeberl	NASA Goddard Space Flight Center	USA

Other Contributors

L. Bishop	Allied-Signal, Inc.	USA
R. D. Bojkov	World Meteorolgical Organization	Switzerland
W. Chu	NASA Langley Research Center	USA
J. J. DeLuisi	NOAA Air Resources Laboratory	USA
J. F. Frederick	University of Chicago	USA
M. Geller	SUNY, Stony Brook	USA
S. Godin	Service d'Aeronomie du CNRS	France
N. R. P. Harris	University of California, Irvine	USA
W. J. Hill	Allied-Signal, Inc.	USA
R. D. Hudson	NASA Goddard Space Flight Center	USA
J. B. Kerr	Atmospheric Environment Service	Canada
W. D. Komhyr	NOAA Air Resources Laboratory	USA
K. Kunzi	University of Bremen	FRG
K. Labitzke	Freie Universitat, Berlin	FRG
C. Mateer	Atmospheric Environment Service (Retired)	Canada
R. D. McPeters	NASA Goddard Space Flight Center	USA
A. J. Miller	NOAA Climate Analysis Center	USA
R. M. Nagatani	NOAA Climate Analysis Center	USA
G. C. Reinsel	University of Wisconsin, Madison	USA
G. C. Tiao	University of Chicago	USA

Chapter 3. Theoretical Predictions

Coordinator

| G. Brasseur | National Center for Atmospheric Research | Belgium |

Principal Authors and Contributors

B. A. Boville	National Center for Atmospheric Research	USA
G. Brasseur	National Center for Atmospheric Research	Belgium
C. Bruhl	Max-Planck-Institut für Chemie	FRG
M. Caldwell	Utah State University	USA
P. Connell	Lawrence Livermore National Laboratory	USA
A. De Rudder	Belgium Institute for Space Aeronomy	Belgium

A. Douglass	NASA Goddard Space Flight Center	USA
I. Dyominov	Novosibirk State University	USSR
D. Fisher	E. I. du Pont de Nemours and Co., Inc.	USA
J. F. Frederick	University of Chicago	USA
R. Garcia	National Center for Atmospheric Research	USA
C. Granier	Service d'Aeronomie du CNRS	France
R. Hennig	Max-Planck-Institut für Chemie	FRG
M. Hitchman	University of Wisconsin	USA
I. Isaksen	University of Oslo	Norway
C. Jackman	NASA Goddard Space Flight Center	USA
M. Ko	Atmospheric and Environmental Research, Inc.	USA
S. Madronich	National Center for Atmospheric Research	USA
M. Prather	NASA Goddard Institute for Space Studies	USA
R. Rood	NASA Goddard Space Flight Center	USA
S. Solomon	NOAA Aeronomy Laboratory	USA
F. Stordal	University of Oslo	Norway
T. Sasaki	Meteorological Research Institute	Japan
G. Visconti	University de L'Aquila	Italy
S. Walters	National Center for Atmospheric Research	USA
D. Wuebbles	Lawrence Livermore National Laboratory	USA
A. Zadarozhny	Novosibirk State University	USSR
E. Zhadin	Central Aerological Observatory	USSR

Chapter 4. Ozone Depletion and Halocarbon Global Warming Potentials

Coordinators

R. A. Cox	Natural Environment Research Council	UK
D. Wuebbles	Lawrence Livermore National Laboratory	USA

Principal Authors and Contributors

R. Atkinson	California Statewide Air Pollution Center	USA
P. Connell	Lawrence Livermore National Laboratory	USA
H. P. Dorn	Kernforschungsanlage Julich	FRG
A. De Rudder	Belgium Institute for Space Aeronomy	Belgium
R. G. Derwent	Harwell Laboratory	UK
F. C. Fehsenfeld	NOAA Aeronomy Laboratory	USA
D. Fisher	E. I. du Pont de Nemours and Co., Inc.	USA
I. Isaksen	University of Oslo	Norway
M. Ko	Atmospheric and Environmental Research, Inc.	USA
R. Lesclaux	Universite de Bordeaux	France
S. C. Liu	NOAA Aeronomy Laboratory	USA
S. A. Penkett	University of East Anglia	UK
V. Ramaswamy	NOAA Geophysical Fluid Dynamics Laboratory	USA
J. Rudolph	Kernforschungsanlage Julich	FRG
H. B. Singh	NASA Ames Research Center	USA
W-.C. Wang	Atmospheric and Environmental Research, Inc.	USA

131

3. Reviewers

Attendees: Review Meeting, 10-14 July 1989, Les Diablerets, Switzerland

D. L. Albritton	NOAA Aeronomy Laboratory	USA
R. D. Bojkov	World Meteorological Organization	Switzerland
G. Brasseur	National Center for Atmospheric Research	USA
D. Cariolle	Meteorologie Nationale EERM/CNRM	France
G. D. Cartwright	NOAA National Weather Service/WMO	USA
M.-L. Chanin	Service d'Aeronomie du CNRS	France
A. Charnikov	Central Aerological Observatory	USSR
R. A. Cox	Natural Environment Research Council	UK
D. H. Ehhalt	Kernforschungsanlage Julich	FRG
J. C. Farman	British Antarctic Survey	UK
D. Fisher	E. I. du Pont de Nemours and Co., Inc.	USA
P. J. Fraser	CSIRO	Australia
J. F. Frederick	University of Chicago	USA
J. C. Gille	National Center for Atmospheric Research	USA
W. J. Hill	Allied-Signal, Inc.	USA
M. Hitchman	University of Wisconsin	USA
A. M. A. Ibrahim	Egyptian Meteorological Authority	Egypt
M. Ilyas	University of Science of Malaysia	Malaysia
J. B. Kerr	Atmospheric Environment Service	Canada
M. J. Kurylo	NASA Hqts/Nat. Instit. Stands. & Technology	USA
C. Mateer	Atmospheric Environment Service (Retired)	Canada
T. Matsuno	University of Tokyo	Japan
M. P. McCormick	NASA Langley Research Center	USA
M. McFarland	E. I. du Pont de Nemours and Co., Inc.	USA
G. Megie	Service d'Aeronomie du CNRS	France
M. J. Molina	Massachusetts Institute of Technology	USA
A. O'Neill	Meteorological Office	UK
A. Owino	Kenya Meteorological Department	Kenya
S. A. Penkett	University of East Anglia	UK
M. J. Prather	NASA Goddard Institute for Space Studies	USA
M. J. Prendez	Universidad de Chile	Chile
J. A. Pyle	University of Cambridge	UK
V. Ramaswamy	NOAA Geophysical Fluid Dynamics Laboratory	USA
J. M. Rodriguez	Atmospheric and Environmental Research, Inc.	USA
J. M. Russell	NASA Langley Research Center	USA
S. Solomon	NOAA Aeronomy Laboratory	USA
R. Stolarski	NASA Goddard Space Flight Center	USA
B. H. Subbaraya	Physical Research Laboratory	India
A. F. Tuck	NOAA Aeronomy Laboratory	USA
P. Usher	United Nations Environment Programme	Kenya
R. T. Watson	NASA Headquarters	USA
D. Wuebbles	Lawrence Livermore National Laboratory	USA

Mail Reviewers

J. G. Anderson	Harvard University	USA
J. K. Angell	NOAA Air Resources Laboratory	USA
R. Atkinson	Bureau of Meteorology	Australia
G. Betteridge	Physics and Engineering Laboratory, DSIR	New Zealand
J. P. Burrows	Max-Planck-Institut für Chemie	FRG

B. Carli	IROF-CNR	Italy
S. Chubachi	Meteorological Research Laboratory	Japan
T. S. Clarkson	Meteorological Service	New Zealand
P. Crutzen	Max-Planck-Institut für Chemie	FRG
D. W. Fahey	NOAA Aeronomy Laboratory	USA
G. Fiocco	University la Sapieuza	Italy
A. Ghazi	Commission of the European Communities	Belgium
L. Gray	Rutherford - Appleton Laboratories	UK
J. S. Hoffman	Environmental Protection Agency	USA
Y. Iwasaka	Nagoya University	Japan
P. Johnson	Physics and Engineering Laboratory, DSIR	New Zealand
P. S. Jovanovic	Association of Scientific Unions	Yugoslavia
J. G. Keys	Physics and Engineering Laboratory, DSIR	New Zealand
V. Kirchoff	INPE	Brazil
D. Kley	Kernforschungsanlage Julich	FRG
Y.-P. Lee	National Tsing Hua University	Taiwan
W. A. Matthews	Physics and Engineering Laboratory, DSIR	New Zealand
R. McKenzie	Physics and Engineering Laboratory, DSIR	New Zealand
A. P. Mitra	Department of Science and Industrial Research	India
J. L. Moyers	National Science Foundation	USA
L. P. Prahm	Danish Meteorological Institute	Denmark
M. H. Proffitt	NOAA Aeronomy Laboratory	USA
L. X. Qui	Academia Sinica	PRC
F. S. Rowland	University of California, Irvine	USA
P. C. Simon	Institut d'Aeronomie Spatiale	Belgium
Y. Sasano	National Institute for Environmental Studies	Japan
J. Swager	Air Directorate	Netherlands
D. W. Wei	Institute of Atmospheric Physics, NEPA	PRC
R. Zellner	University of Hannover	FRG
C. S. Zerefos	University of Thessaloniki	Greece

4. Logistical Support

R. D. Bojkov	World Meteorological Organization	Switzerland
M. -C. Charrierts	World Meteorological Organization	Switzerland
F. M. Ormond	NASA Headquarters/Birch & Davis Associates	USA
J. Waters	NOAA Aeronomy Laboratory	USA

Scientific Assessment of Stratospheric Ozone: 1989
Volume II

EXPERTS AND REVIEWERS INVOLVED IN AFEAS

Experts

R. Atkinson	University of California, Riverside	USA
W. L. Chameides	Georgia Institute of Technology	USA
P. S. Connell	Lawrence Livermore National Laboratory	USA
R. A. Cox	Natural Environment Research Council	UK
R. G. Derwent	Harwell Laboratory	UK
D. L. Filkin	E. I. du Pont de Nemours and Co., Inc.	USA
D. A. Fisher	E. I. du Pont de Nemours and Co., Inc.	USA
J. P. Friend	Drexel University	USA

Contributors

C. H. Hales	E. I. du Pont de Nemours and Co., Inc.	USA
R. F. Hampson	National Institute of Standards and Technology	USA
I. S. A. Isaksen	Oslo University	Norway
L. S. Kaminsky	State University of New York at Albany	USA
M. K. W. Ko	Atmospheric and Environmental Research, Inc.	USA
M. J. Kurylo	National Institute of Standards and Technology	USA
R. Lesclaux	Universite de Bordeaux	France
D. C. McCune	Boyce Thompson Institute for Plant Research	USA
M. O. McLinden	National Institute of Standards and Technology	USA
M. J. Molina	Massachusetts Institute of Technology	USA
H. Niki	York University	Canada
M. J. Prather	NASA Goddard Institute for Space Studies	USA
V. Ramaswamy	Princeton University	USA
S. P. Sander	Jet Propulsion Laboratory	USA
F. Stordal	Oslo University	Norway
N. D. Sze	Atmospheric and Environmental Research, Inc.	USA
A. Volz-Thomas	Kernforschungsanlage, Julich	FRG
W-C Wang	Atmospheric and Environmental Research, Inc.	USA
L. H. Weinstein	Boyce Thompson Institute for Plant Research	USA
P. H. Wine	Georgia Institute of Technology	USA
D. J. Wuebbles	Lawrence Livermore National Laboratory	USA
R. Zellner	University of Hannover	FRG

Reviewers

D. L. Albritton	National Oceanic and Atmospheric Administration	USA
J. G. Anderson	Harvard University	USA
R. E. Banks	Univ. of Manchester Inst. of Science and Tech.	UK
J. J. Bufalini	U.S. Environmental Protection Agency	USA
A. W. Davison	Newcastle University	UK
W. B. DeMore	Jet Propulsion Laboratory	USA
D. D. Des Marteau	Clemson University	USA
R. A. Duce	University of Rhode Island	USA
A. Goldman	University of Denver	USA
M. R. Hoffman	California Institute of Technology	USA
C. J. Howard	National Oceanic and Atmospheric Administration	USA
N. Ishikawa	F&F Research Centre, Tokyo	Japan
J. L. Moyers	National Science Foundation	USA
V. Ramanathan	University of Chicago	USA
A. R. Ravishankara	National Oceanic and Atmospheric Administration	USA
F. S. Rowland	University of California, Irvine	USA
P. Simon	Institut d'Aeronomie Spatiale de Belgique	Belgium
H. O. Spauschus	Georgia Institute of Technology	USA
S. Solomon	National Oceanic and Atmospheric Administration	USA
A. Tuck	National Oceanic and Atmospheric Administration	USA
R. T. Watson	National Aeronautics and Space Administration	USA
S. Wofsy	Harvard University	USA

COMPANIES SPONSORING AFEAS

Akzo Chemicals	The Netherlands
Allied-Signal Corporation	USA
Asahi Glass Co., Ltd.	Japan
Atochem	France
Chemical Industries of Northern Greece, S.A.	Greece
Daikin Industries, Ltd.	Japan
E.I. du Pont de Nemours & Co., Inc.	USA
Hoechst AG	Germany
ICI Chemicals and Polymers Ltd.	UK
ISC Chemicals	UK
Kali-Chemie AG	Germany
LaRoche Chemicals	USA
Montefluos SpA	Italy
Pennwalt Corporation	USA
Racon (Atochem)	USA

Section C

Transient Scenarios for Atmospheric Chlorine and Bromine

M. J. Prather   NASA/Goddard Institute for Space Studies, NY
R. T. Watson   NASA Headquarters, Washington, DC

Section D

Chemical Kinetics and Photochemical Data For Use in Stratospheric Modeling

NASA PANEL FOR DATA EVALUATION

W. B. DeMore, Chairman   Jet Propulsion Laboratory, Pasadena, CA

D. M. Golden   SRI International, Menlo Park, CA
R. F. Hampson   National Institute for Standards and Technology, MD
C. J. Howard   NOAA Environmental Research Laboratory, Boulder, CO
M. J. Kurylo   National Institute for Standards and Technology, MD
M. J. Molina   Massachusetts Institute of Technology, Cambridge, MA
A. R. Ravishankara   NOAA Environmental Research Laboratory, Boulder, CO
S. P. Sander   Jet Propulsion Laboratory, Pasadena, CA

135

Section E

An Assessment of the Impact on Stratospheric Chemistry and Ozone caused by the Launch of the Space Shuttle and Titan IV

A. R. Douglass	NASA/Goddard Space Flight Center, Greenbelt, MD
M. M. Garcia	NASA/Goddard Institute for Space Studies, NY
C. H. Jackman	NASA/Goddard Space Flight Center, Greenbelt, MD
M. K. W. Ko	Atmospheric and Environmental Research, Inc., Cambridge, MA
M. J. Prather	NASA/Goddard Institute for Space Studies, NY
N. D. Sze	Atmospheric and Environmental Research, Inc., Cambridge, MA

Section F

High-Speed Research Program Atmospheric Advisory Committee
(as of August 1989)

R. J. Cicerone	University of California, Irvine
D. H. Ehhalt	Kernforschungsanlage Julich, FRG
J. R. Holton	University of Washington
H. S. Johnston	University of California, Berkeley
J. G. Lawless*	NASA/Ames Research Center, Moffett Field, CA
J. D. Lawrence*	NASA/Langley Research Center, Hampton, VA
J. D. Mahlman	NOAA/Geophysical Fluid Dynamics Lab, Princeton, NJ
T. Matsuno	Geophys.Inst., Tokyo, Japan
M. J. Molina	Massachusetts Institute of Technology, Cambridge, MA
M. Oppenheimer	Environmental Defense Fund, NY
R. A. Plumb	Massachusetts Institute of Technology, Cambridge, MA
M. J. Prather* (Co-Chair)	NASA/Headquarters, Code SEU, /GISS, NY
A. F. Tuck	NOAA/Aeronomy Lab, Boulder, CO
R. T. Watson* (Co-Chair)	NASA/Headquarters, Code SEU, Washington, DC
H. L. Wesoky*	NASA/Headquarters, Code RJ, Washington, DC
R. E. Whitehead* (Exec. Secretary)	NASA/Headquarters, Code RJ, Washington, DC
L. J. Williams*	NASA Headquarters, Code RJ, Washington, DC
S. C. Wofsy	Harvard University, Cambridge, MA
D. J. Wuebbles	Lawrence Livermore National Laboratory, Livermore, CA

New Members:

E. Condon*	NASA/Ames Research Center, Moffett Field, CA
R. A. Cox	Natural Environment Research Council, UK
W. L. Grose*	NASA/Langley Research Center, Hampton, VA
J. Hoffman*	Environmental Protection Agency, Washington, DC
N. P. Krull*	Federal Aviation Administration, Washington, DC
M. J. Kurylo	NASA/Headquarters, Code SEU, Washington, DC&NIST
R. W. Niedzwiecki*	NASA/Lewis Research Center, Cleveland, OH
A. R. Ravishankara	NOAA/Environmental Research Lab, Boulder, CO

* ex officio

16. Abstract

This document is issued in response to the Clean Air Act Amendments of 1977, Public Law 95-95, which mandates that the National Aeronautics and Space Administration (NASA) and other key agencies submit biennial reports to Congress and the Environmental Protection Agency. NASA is charged with the responsibility to report on the state of our knowledge of the Earth's upper atmosphere, particularly the stratosphere. This is the seventh ozone assessment report submitted to Congress and the concerned regulatory agencies. Part I of this report, issued earlier this year, summarized the objectives, status, and accomplishments of the research tasks supported under NASA's Upper Atmosphere Research Program during the last two years.

This report presents new findings since the last report to Congress was issued in 1988. It includes several scientific assessments of our current understanding of the chemical composition and physical structure of the stratosphere, in particular how the abundance and distribution of ozone is predicted to change in the future. These reviews include: (Section B) a summary of the most recent international assessment of stratospheric ozone; (Section C) a study of future chlorine and bromine loading of the atmosphere; (Section D) a review of the photochemical and chemical kinetics data that are used as input parameters for the atmospheric models; (Section E) a new assessment of the impact of Space Shuttle launches on the stratosphere; (Section F) a summary of the environmental issues and needed research to evaluate the impact of the newly re-proposed fleet of stratospheric supersonic civil aircraft; and (Section G) a list of the contributors to this report and the science assessments which have formed our present state of knowledge of the upper atmosphere and ozone depletion.

NASA

POSTAGE